

ABSTRACT

Title of Document: INCREASING EFFICIENCY AND SUSTAINABILITY OF WASTE-TO-ENERGY SYSTEMS USING BIOCHAR FOR HYDROGEN SULFIDE CONTROL AND LIFE CYCLE ASSESSMENT

Abhinav Choudhury, Ph.D., 2019

Directed By: Associate Professor, Stephanie Lansing,
Environmental Science and Technology

The research aim was to increase energy production efficiency and reduce the environmental impacts of waste-to-energy technologies, specifically anaerobic digestion (AD) of dairy manure (DM) and combustion of poultry litter (PL). The first objective was co-digestion of DM with gummy vitamin waste (GVW) to increase methane (CH₄) yield. The GVW co-digestion treatments significantly increased CH₄ yield by 126% - 151% compared to DM-only treatment and significantly decreased the H₂S concentration in the biogas by 66% - 83% compared to DM-only.

The second objective was understanding the effect of hydrogen sulfide (H₂S) scrubber management, operation, and maintenance parameters on H₂S removal efficiency. Even though the capital and operating costs for the two H₂S scrubbing systems in this study were low (< \$1500/year), they showed ineffective performance due to insufficient air injection, substitution of proprietary iron oxide-based H₂S adsorbents for cheaper alternatives, and the lack of dedicated operators.

The third objective was adsorption of H₂S using Fe-impregnated biochar as a substitute for activated carbon (AC). Fe-impregnation of biochar led to a 4.3-fold increase in the H₂S adsorption capacity compared to AC. When compared to unimpregnated biochars, Fe-impregnation led to an average 3.2-fold increase in the H₂S adsorption capacity.

The fourth objective was in-situ use of biochar in AD to remove H₂S. In-situ biochar addition at the highest dose (1.82 g biochar/g manure total solids (TS)) resulted in an average H₂S removal efficiency of 91.2%. Biochar particle size had no significant effect on H₂S reduction. In-situ addition of Fe-impregnated biochar resulted in an average H₂S removal efficiency of 98.5%.

The fifth objective was a life cycle assessment (LCA) of a PL fluidized bed combustion (FBC) system. The LCA assessment showed that heating poultry houses using heat obtained from the combustion of PL in the FBC system had 32% lower climate change potential (CCP) compared to use of propane for heating poultry houses. However, analyzing the FBC system under a net positive electrical output scenario resulted in 66% less impact on CCP and a 48 – 98% reduction in environmental impacts compared to the previous scenario with net electricity input.

INCREASING EFFICIENCY AND SUSTAINABILITY OF WASTE-TO-
ENERGY SYSTEMS USING BIOCHAR FOR HYDROGEN SULFIDE
CONTROL AND LIFE CYCLE ASSESSMENT

By

Abhinav Choudhury

Dissertation submitted to the Faculty of the Graduate School of the
University of Maryland, College Park, in partial fulfillment
of the requirements for the degree of
Doctor of Philosophy
2019

Advisory Committee:

Associate Professor Stephanie Lansing, Chair
Professor Ashwani Gupta
Professor Alba Torrents
Associate Professor Gary Felton
Dr. Walter Mulbry

© Copyright by
Abhinav Choudhury
2019

Dedication

To my Mom, Dad, and sister. Thank you for being the constants in my life throughout my journey!

Acknowledgements

I would like to thank my advisor, Dr. Stephanie Lansing, for her support and guidance throughout the last four years; from accepting me as her student to preparing me for the challenges in the future. I would like to thank Dr. Gary Felton and Dr. Walter Mulbry for letting me work in your labs, and training me on essential engineering skills, practical implications of our research, and for nurturing the skills required to conduct scientific investigations. I would also like to thank Dr. Ashwani Gupta and Dr. Alba Torrents for their constant mentorship and guidance that allowed me to evolve as a scientist during the last four years.

I would like to thank the United States Department of Agriculture (USDA), Northeast Agriculture Research and Education (NESARE), Maryland Department of Agriculture (MDA), Department of Environmental Science and Technology (ENST), College of Agriculture and Natural Resources, Clark School of Engineering, and The Graduate School for providing the resources, assistantship, fellowship, and funding for this research.

I would like to thank Late Dr. Bahram Momen for teaching me that statistics is not scary and actually interesting. Thank you to Gary Seibel and the personnel of the UMD ENST Project Development Center for their assistance in helping me design and maintain my lab and field equipment. To everyone in the Waste to Energy laboratory, the AIMLab and FABLAB in the Maryland NanoCenter, and the X-ray Crystallography Center for training me on the instruments required to analyze my results. A special thanks to all the PhD, master's, undergraduate, and high school students who helped me with my research, from driving me to farms to running samples on the gas chromatograph for

hours: Carlton Poindexter, Danielle Delp, Emily Keller, Casey Moore, Kevin Dominey, Maggie Hines, Derrick Sanders, Jon Shay, Brandon Mediate, and Theo Nimpson. Thank you to Sofia D'Ambrosio for being crazy and amazing. To Amro Hassanein, one of the most wonderful, helpful, and dedicated human beings I have ever met, you are awesome. To Freddy Witarsa, my roommate, my unofficial mentor and brother, thank you for everything. Ayella Maile-Moskowitz, thank you for being one of my best friends, for listening to me, and helping me get through all of this. To Annie Yarberry, thank you for your crazy life lessons, constant laughter, and being like an older sister to me. And to Jenna Schueler, my best friend who has supported me through everything in and out of grad school, I could not have done this without you. Finally, thank you to the Choudhury family and my friends for all your support and love.

Table of Contents

Dedication	ii
Acknowledgements	iii
Table of Contents	v
List of Tables	ix
List of Figures	xi
1 Introduction:.....	1
1.2 Co-digestion of substrates with dairy manure:.....	2
1.3 Hydrogen sulfide and its removal from biogas:	4
1.3.1 Biological Scrubbers:	5
1.3.2 Iron Oxide Scrubbers:.....	6
1.3.3 Microaeration:	7
1.3.4 Activated Carbon Adsorption:.....	8
1.4 Biochar as a substitute H ₂ S adsorbent:.....	9
1.5 Biochar as a digester additive for H ₂ S removal:	13
1.6 Life Cycle Assessment (LCA) of poultry litter fluidized bed combustion:	17
1.7 Objectives:.....	19
2 Methane and hydrogen sulfide production from co-digestion of gummy waste with a food waste, grease waste, and dairy manure mixture	21
2.1 Introduction:	21
2.2 Materials and Methods:.....	24
2.2.1 Sample Collection:	24
2.2.2 Experimental Design:	25
2.2.3 Biochemical Methane Potential (BMP) Test Procedures:	26
2.2.4 Analytical Methods:	27
2.2.5 Statistical Analysis:	28
2.3 Results:	28
2.3.1 Methane (CH ₄) Production:	28
2.3.2 Hydrogen Sulfide (H ₂ S) Production:	32
2.3.3 Effect of retention time and solids degradation:.....	35
2.4 Discussion:	36
2.5 Conclusions:	41

3 Evaluation of hydrogen sulfide scrubbing systems for anaerobic digesters on two U.S. dairy farms	42
3.1 Introduction:	42
3.2 Methods:	46
3.2.1 Farm and H ₂ S Scrubber Information:	46
3.2.2 Performance Monitoring and Cost Information:	48
3.2.3 H ₂ S Removal Calculations:	49
3.2.4 Statistical Analysis:	49
3.3 Results and Discussion.....	50
3.3.1 Iron Oxide Scrubber (S _{IOS}):	50
3.3.2 In-vessel biological desulfurization system using air injection (S _{BDS}):.....	55
3.3.3 Economic Analysis	60
3.4. Scrubber management:	63
3.4 Conclusions:	66
4 Adsorption of hydrogen sulfide (H ₂ S) in biogas on iron-impregnated biochar	67
4.1 Introduction:	68
4.2 Methods:	71
4.2.1 Biochar Characterization:	71
4.2.2 Iron impregnation procedure:	72
4.2.3 Experimental set-up for dynamic breakthrough study:	73
4.3 Results and Discussion:.....	75
4.3.1 Characterization of biochar:	75
4.3.2 H ₂ S adsorption capacity in the dynamic system:.....	81
4.3.3 XRD and SEM Results:	87
4.4 Conclusion:.....	94
5 Impact of biochar addition on H ₂ S production from anaerobic digestion	96
5.1 Introduction:	97
5.2 Materials and Methods:	100
5.2.1 Biochar characterization and properties:	100
5.2.2 Sulfide Removal Tests:.....	101
5.2.3 Effect of biochar concentration (Experiment 1):.....	101
5.2.4 Effect of biochar particle size (Experiment 2):	102
5.2.5 Effect of biochar surface modification (Experiment 3):.....	102

5.2.6 Experimental Design:	103
5.2.7 Analytical Methods:	104
5.2.7.1 Biochar testing:	104
5.2.7.2 Manure sampling:	105
5.2.8 Cost Analysis:.....	106
5.2.9 Statistical Analysis:	106
5.3 Results and Discussion:.....	106
5.3.1 Biochar Characterization:	106
5.3.2 Sulfide Removal Test Results:	111
5.3.3 Effect of biochar concentration (Experiment 1):.....	114
5.3.4 Effect of biochar particle size (Experiment 2):	121
5.3.5 Effect of biochar surface modification (Experiment 3):.....	125
5.3.6 Cost Analysis:.....	129
5.4 Conclusions:	131
6 Fluidized bed combustion of poultry litter at farm-scale: a case study on the environmental impacts using a life cycle approach	132
6.1 Introduction:	133
6.2 Methods:.....	136
6.2.1 System Description:.....	136
6.2.2 Analytical Methods:	138
6.2.3 Impact Assessment Methodology:.....	139
6.2.3.1 Goal and Scope of the study	140
6.2.3.2 LCA inventory:	142
6.2.3.3 Sensitivity Analyses:.....	142
6.3 Results and Discussion:.....	143
6.3.1 Energy production from the FBC system:	143
6.3.2 Poultry Litter and Ash Product Characteristics:	146
6.3.2 Life Cycle Environmental Impacts:.....	149
6.3.2.1 Climate Change potential:.....	149
6.3.2.2 Eutrophication and Terrestrial Acidification potential:	153
6.3.2.3 Other Environmental Impact categories:	154
6.3.3 Sensitivity Analysis:	155
6.4 Land Application Considerations:.....	157

6.5 Limitations of the study:	159
6.6 Conclusions:	160
7 Conclusions.....	162
7.1 Intellectual Merit and Broader Impacts:.....	162
Appendix A: Nutrient Load Reduction and Emissions after combustion.....	167
Appendix B: Life Cycle Assessment Detailed Results.....	169
Appendix C: Calculation of Adsorption capacity.....	176
Bibliography	178

List of Tables

Table 2.1 Total and volatile solids content of the individual substrates (gummy vitamin waste, food waste, grease waste, dairy manure) and digester effluent (inoculum) used for the experiment.....	25
Table 2.2 Experimental design using a 1:1 inoculum to substrate ratio, with the calculated initial total solids (TS) and volatile solids (VS) of the treatment mixtures. The percent of GVW inclusion was based on mass. All treatments were conducted in triplicate.....	26
Table 2.3 Methane (CH ₄) and hydrogen sulfide (H ₂ S) production data from the batch digestion testing.	29
Table 2.4 Average pH and volatile solids (VS) in all treatment mixtures pre-digestion (initial) and post-digestion (final). Initial VS data was calculated theoretically, and final VS data was determined experimentally.....	32
Table 2.5 Normalized methane production (mL CH ₄ /g VS) after 20, 46, and 67 days, with the percentage of the cumulative CH ₄ (Day 67) by Days 20 and 46 shown in parentheses.	35
Table 3.1 Recommended hydrogen sulfide (H ₂ S) concentration limits for biogas utilization technologies [20,85].	44
Table 3.2 Capital and operating cost summary of different scrubbing technologies in Northeast US.	63
Table 3.3 Performance summary of two different scrubbing technologies in Northeast US.	64
Table 4.1 Physical and chemical properties of the two biochar types and AC obtained from Soil Control Lab analysis.	76
Table 4.2 Saturation time and adsorption capacity of the different adsorbents tested	83
Table 5.1 Physical and chemical properties of the two biochar types and AC obtained from Soil Control Lab analysis.	107
Table 5.2 Sulfide adsorption capacity of biochar in a model aqueous solution of sodium sulfide.....	112
Table 5.3 Hydrogen sulfide (H ₂ S) volume reduction and normalized mass removed per gram of biochar added into the reactor, and percent reductions in comparison to dairy manure (DM).	116
Table 5.4 Hydrogen sulfide (H ₂ S) volume reduction and normalized mass removed per gram of biochar added into the reactor, and percent reductions in comparison to dairy manure (DM).	122
Table 5.5 Hydrogen sulfide (H ₂ S) volume reduction and normalized mass removed per gram of biochar added into the reactor, and percent reductions in comparison to dairy manure (DM) digestion.	127
Table 5.6 Cost of hydrogen sulfide (H ₂ S) treatment currently available desulfurization technology compared to results from this study (values obtained from literature data for biogas flow rate of 1,350 m ³ /day with 1000 ppm H ₂ S).	130
Table 6.1 Energy production from the fluidized bed combustion (FBC) system over the six flocks tested.....	144

Table 6.2 Average physical characteristics (wet weight basis) of the poultry litter input to the fluidized bed combustion unit during the sixteen-month study.	147
Table 6.3 Elemental composition of the poultry litter, bed ash, and fly ash, and percent change in the bed ash and fly ash compared to the poultry litter substrate.	147
Table 6.4 Impact on climate change potential from poultry litter combustion, electricity production and liquefied propane (LPG) use for heating based on 1 MJ of energy. A negative value indicates a net positive environmental impact.	149
Table A.1 Overall nutrient load reductions for all flocks and their respective fractions in the bed ash, fly ash, and total ash product.	167
Table A.2 Emission test results for the FBC system with a heat input of 2.7 MMBtu/hr	168
Table B.1 LCA inventory for combustion of poultry litter.....	169
Table B.2 Environmental impacts in the baseline scenario	173
Table B.3 Environmental impacts in the improved operational scenario.....	175
Table C.1 Concentration of H ₂ S in the outlet of the biochar column as a function of time	176
Table C.2 Operational parameters for H ₂ S adsorption using a biochar adsorption column	176

List of Figures

Figure 2.1 Methane (CH ₄) production normalized by gram of substrate (mL CH ₄ /g substrate) (A, top) and by gram of volatile solids (mL CH ₄ /g VS) (B, bottom) in the batch digestion testing of gummy vitamin waste (GVW), grease waste (GW), food waste (FW), dairy manure (DM) digested singularly and as a mixture (DM.FW.GW), with the percent inclusion of GVW shown for the co-digestion mixtures.	30
Figure 2.2 Linear regression of normalized methane (CH ₄) production per gram of added substrate and percent gummy vitamin waste (GVW) within the co-digestion mixture....	31
Figure 2.3 Hydrogen sulfide (H ₂ S) concentration (ppm) in the biogas over time in the batch digestion testing of gummy vitamin waste (GVW), grease waste (GW), food waste (FW), dairy manure (DM) digested singularly and as a mixture, with the GVW inclusion shown for each co-digestion mixture tested.....	33
Figure 2.4 Normalized hydrogen sulfide (H ₂ S) production per kilogram of added substrate and percent gummy vitamin waste (GVW) within the co-digestion mixture....	34
Figure 3.1 Hydrogen sulfide (H ₂ S) concentrations in the biogas from the iron oxide scrubber (S _{IOS}), with scrubber media replacement to steel wool after 105 days (mid-November).	52
Figure 3.2 Average daily biogas production over two month period from June 2016 to May 2017 in the AD system with the iron oxide scrubber (S _{IOS}).	53
Figure 3.3 Daily average pre-scrubbed and post-scrubbed CH ₄ concentration in biogas produced from the AD system with the iron oxide scrubber (S _{IOS}).	54
Figure 3.4 Hourly H ₂ S and O ₂ concentrations in the biogas from the AD system with in-vessel biological desulfurization (S _{BDS}).	56
Figure 3.5 Hourly biogas CH ₄ concentrations from the AD system with in-vessel biological desulfurization (S _{BDS}).	57
Figure 3.6 Daily biogas production (m ³ /day) through the generator, operating on the farm with S _{BDS} , for electricity production.	60
Figure 4.1 Laboratory set up for evaluating the efficiency of H ₂ S adsorption using biochar.....	75
Figure 4.2 SEM image (A) and EDS data (C) of maple wood biochar (MB) and SEM image (B) and EDS data (D) of corn stover biochar (CSB). The EDS data is shown for the red marked points on the SEM images.	79
Figure 4.3 SEM image (A) and EDS data (C) of iron (Fe) impregnated maple biochar (MB-Fe) and SEM image (B) and EDS data (D) of Fe impregnated corn stover biochar (CSB-Fe). The EDS data is shown for the red marked points on the SEM images.....	81
Figure 4.4 Breakthrough curves for H ₂ S adsorption on raw and Fe-impregnated corn stover biochar (CSB and CSB-Fe), maple biochar (MB and MB-Fe) and activated carbon (AC), where C/C ₀ is the ratio of the outlet to the inlet H ₂ S concentration.	83
Figure 4.5 XRD spectra for fresh and H ₂ S saturated corn stover biochar (CSB), where the peaks mainly show the presence of silica (SiO ₂), calcium carbonate (CaCO ₃), and potassium chloride (KCl).	89

Figure 4.6 XRD spectra for fresh and H ₂ S saturated maple biochar (MB), where the peaks mainly show the presence of calcium carbonate (CaCO ₃). Sulfur peaks were not detected.	89
Figure 4.7 XRD spectra for fresh and H ₂ S saturated Fe impregnated corn stover biochar (CSB-Fe), where the peaks mainly show the presence of silica (SiO ₂), and magnetite (Fe ₃ O ₄) in the fresh CSB-Fe. The presence of ferrous sulfate heptahydrate (FeSO ₄ .7H ₂ O) is seen at 2 theta = 18.3° and 23.8° in H ₂ S saturated CSB-Fe.	90
Figure 4.8 XRD spectra for fresh and H ₂ S saturated iron impregnated maple biochar (MB-Fe), where the peaks show the presence of magnetite (Fe ₃ O ₄), and iron oxide-hydroxide (FeO(OH)) in the fresh MB-Fe. The presence of ferrous sulfate heptahydrate (FeSO ₄ .7H ₂ O) is seen at 2 theta = 18.3° and 23.8° in H ₂ S saturated MB-Fe.	90
Figure 4.9 SEM elemental mapping of H ₂ S saturated biochar (A) showing oxygen (B) and sulfur (C) distribution.	94
Figure 5.1 SEM image (A) and EDS data (C) of maple wood biochar (MB) and SEM image (B) and EDS data (D) of corn stover biochar (CSB). The EDS data is shown for the red marked points on the SEM images.	109
Figure 5.2 SEM image (A) and EDS data (C) of iron impregnated maple biochar (MB-Fe) and SEM image (B) and EDS data (D) of iron impregnated corn stover biochar (CSB-Fe). The EDS data is shown for the red marked points on the SEM images.	111
Figure 5.3 SEM image (A) and EDS data (B) of iron impregnated maple biochar (MB-Fe) after sulfide adsorption from model Na ₂ S aqueous solution. The EDS data is shown for the red marked points on the SEM images.	113
Figure 5.4 XRD spectra for H ₂ S saturated iron impregnated maple biochar (MB-Fe). The presence of ferrous sulfate heptahydrate (FeSO ₄ .7H ₂ O) is seen at 2 theta = 18.3° and 23.8°.	114
Figure 5.5 Cumulative hydrogen sulfide (H ₂ S) production normalized by kilograms of volatile solids (VS) with different biochar concentrations, with dairy manure (DM). Corn stover biochar (CSB) and maple biochar (MB) coupled with the different tested concentrations (0.1, 0.5, 1, 1.82 g/g manure TS) are used to differentiate each treatment.	115
Figure 5.6 SEM image of biochar after digestion showing microbial biomass layers on the biochar surface and pores.	117
Figure 5.7 Percent hydrogen sulfide (H ₂ S) removal over the study period with different biochar concentrations, and dairy manure (DM). Corn stover biochar (CSB) and maple biochar (MB) coupled with the different tested concentrations (0.1, 0.5, 1, 1.82 g/g manure TS) are used to differentiate each treatment.	118
Figure 5.8 Cumulative methane (CH ₄) production normalized by grams of volatile solids (VS) with different biochar concentrations, with dairy manure (DM). Corn stover biochar (CSB) and maple biochar (MB) coupled with the different tested concentrations (0.1, 0.5, 1, 1.82 g/g manure TS) are used to differentiate each treatment.	119
Figure 5.9 Cumulative hydrogen sulfide (H ₂ S) production normalized by kilograms of volatile solids (VS) with different biochar particle sizes, with dairy manure (DM). Corn	

stover biochar (CSB) and maple biochar (MB) coupled with the different tested particle sizes (L,M,S) are used to differentiate each treatment.....	121
Figure 5.10 Cumulative methane (CH ₄) production normalized by grams of volatile solids (VS) for different biochar particle sizes, and dairy manure (DM). Corn stover biochar (CSB) and maple biochar (MB) coupled with the different tested particle sizes (L, M, S).	123
Figure 5.11 Cumulative hydrogen sulfide (H ₂ S) production normalized by volatile solids (VS) for dairy manure (DM), unmodified and Fe-impregnated corn stover biochar (CSB, CSB-Fe) and maple biochar (MB, MB-Fe).	126
Figure 5.12 Hydrogen sulfide (H ₂ S) removal effectiveness over time for unmodified and Fe-impregnated corn stover biochar (CSB, CSB-Fe) and maple biochar (MB, MB-Fe).	126
Figure 5.13 Cumulative methane (CH ₄) production normalized by volatile solids (VS) for dairy manure (DM), unmodified and Fe-impregnated corn stover biochar (CSB, CSB-Fe) and maple biochar (MB, MB-Fe).	128
Figure 6.1 System boundary of the combustion of poultry litter for heat and electricity production.	140
Figure 6.2 Daily thermal (A) and electrical (B) energy production from the fluidized bed combustion (FBC) unit used to heat two poultry houses and provide electricity over sixteen months (six flocks) of monitoring.	145
Figure 6.3 Heating value and volatile solids (VS) variation over the 16 months of sampling.	147
Figure 6.4 Environmental impacts of poultry litter combustion in the baseline scenario compared to LPG production and combustion.	150
Figure 6.5 Environmental impacts of poultry litter combustion with renewable energy production in the improved operational scenario compared to LPG production and combustion and replacement of electricity production in Maryland.	151
Figure 6.6 Percent change in impact categories upon 10% change in the five variables tested for the sensitivity analysis.	156
Figure B.1 Distribution of environmental impacts of poultry litter combustion in the baseline scenario.	172
Figure B.2 Distribution of environmental impacts of poultry litter combustion in the improved operational scenario.	174

1 Introduction:

Rapidly increasing costs associated with energy from fossil fuels and waste disposal methods, such as landfilling, along with increasing concerns about rising greenhouse gas emissions has promoted the conversion of wastes into energy as an environmentally friendly and economically attractive solution. Energy consumption has increased from 5.6×10^3 TWh in the beginning of the 20th century to 1.5×10^5 TWh in 2017 due to an explosion of the world's population and industrialization of many countries [1]. Energy production from waste biomass sources, such as agricultural waste, animal waste, and organic waste materials, have an advantage over fossil fuels due to their renewable nature. These energy sources can be replaced annually or over a few years instead of millions of years required to regenerate fossil fuels.

Currently, energy production from biomass is only a small portion of the total energy production. In 2018, energy generation in the United States was derived from 75.5% fossil fuels (oil, natural gas, and coal), 8.4% nuclear energy, 5.3% from biomass sources, and 11.7% in renewable energy [2]. Biogas, generally produced from organic waste materials, such as sewage sludge, agricultural wastes, industrial wastes, and municipal solid wastes, through anaerobic digestion (AD) provides a renewable energy source for electricity generation, heat production, or as a renewable natural gas source. Solid manure residues, such as poultry litter (PL), can also be subjected to anaerobic digestion or direct combustion for heat and electricity production.

The primary goal of this research was to the increase energy production efficiency and understand the environment impacts of waste-to-energy technologies, specifically, anaerobic digestion of dairy manure and thermal combustion of poultry litter. The

research objectives included: 1) evaluation of a gummy vitamin waste (GVW) product as a co-digestion substrate for AD and to quantify its effect on methane (CH₄) and hydrogen sulfide (H₂S) yield, 2) understanding the effect of hydrogen sulfide (H₂S) scrubber management, operation, and maintenance parameters on H₂S removal efficiency, 3) utilization of iron (Fe) as an impregnating agent to modify the surface of a biochar to increase its H₂S adsorption efficiency, 4) understanding the effect of in-situ biochar addition into AD systems on CH₄ and H₂S production, and 5) evaluation of environmental impacts associated with the combustion of poultry litter using data from a pilot scale fluidized bed combustion (FBC) system.

1.2 Co-digestion of substrates with dairy manure:

Anaerobic digestion of organic wastes produces biogas comprised of mainly CH₄ and carbon dioxide (CO₂), with traces amounts of other gases, such as H₂S. Co-digestion of organic substrates with dairy manure can increase CH₄ content in biogas, while also increasing total biogas production [3]. Limitations from mono-digestion of organic materials arise from substrate properties, such as unbalanced C:N ratios, recalcitrance in the feedstock, high concentrations of long chain fatty acids, and deficiency in trace minerals required for the growth of methanogens [4,5]. These limitations can lead to unfavorable economics for dairy farmers using AD to generate energy on-farm [5,6]. Lisboa and Lansing (2013) reported increases in CH₄ production ranging from 67% to 2940% when co-digesting ice cream waste or chicken processing waste with dairy manure [7]. Even with minimal addition of organic co-digestion substrates, large increases in biogas production may be obtained due to the high density of digestible volatile solids (VS) in the substrate. Moody et al. (2011) determined the biochemical

methane potential (BMP) of a wide range of food waste substrates and concluded that co-digestion of manure and organic waste has the potential to increase biogas production, and in turn increase energy generation, from AD [8]. However, often the studies only concentrate on individual substrates due to differences in organic waste composition and collections.

Several authors have conducted research and published review articles on co-digestion of food waste and dairy manure [9–11]. Zhang et al. (2014) reported that food waste by itself prevented efficient long-term operation due to inhibition from nutrient imbalance with undesirable C:N ratios, excessive macronutrients, and insufficient trace nutrients [9]. The authors reported that co-digestion of food wastes with organic substrates, such as sewage sludge and dairy manure, can be implemented to overcome inhibitory effects. Xu et al. (2018) suggested that co-digestion should be integrated into currently existing DM or sewage sludge AD facilities due to the high capital and labor costs associated with the construction of new AD systems [11]. This can also result in significant increases in heat and electricity outputs, with minimal additions to digester volume and costs. The authors also suggested the need for additional research into co-digestion for continued understanding and improvement of the process.

Waste produced from gummy vitamin factories have a gel-like consistency that can be hard to dispose of without preprocessing operations. In addition, because of their sticky nature, they can create handling problems through clogging of pipelines and preprocessing equipment. Anaerobic digestion of gummy waste may be an attractive solution due to the high density of VS in the waste that may be ideal for biogas production.

1.3 Hydrogen sulfide and its removal from biogas:

Hydrogen sulfide is a product of anaerobic digestion of complex organic substrates due to the presence of sulfate reducing bacteria (SRB), that convert sulfate species into sulfide under reducing conditions. The presence of sulfides can be inhibitory/toxic to both CH₄ producing bacteria or methanogens as well as SRBs [12]. Sulfate reducing bacteria primarily use propionate and hydrogen as their electron donors, with acetate being a minor electron donor [13]. The reduction of sulfate to sulfide using hydrogen ($\Delta G = -154$ kJ) or acetate ($\Delta G = -43$ kJ) as the electron donor is more thermodynamically favorable than the reduction of CO₂ ($\Delta G = -135$ kJ) or acetic acid ($\Delta G = -28.5$ kJ) into CH₄. As a result, sulfidogenesis may reduce the rate of methanogenesis in AD.

Hydrogen sulfide is a toxic gas that can result in range of adverse health effects. OSHA mandates that the acceptable H₂S concentrations cannot exceed 20 ppm in the industry due to its toxicity to humans. Concentrations exceeding 500 ppm in a closed environment can lead to death within 30-60 minutes. In addition, H₂S acts as a corrosive agent and can damage equipment (pipelines, compressors, engine generator sets and gas storage tanks) and is a toxic poison for fuel cells and catalysts, adversely affecting their performance [14]. Furthermore, H₂S can react with water vapor present in the biogas producing sulfuric acid, promoting corrosion. Combustion of H₂S leads to sulfur dioxide emissions, which has harmful environmental effects. Due to these problems, it is important to scrub the biogas before electricity generation or other purposes, such as direct use in a boiler.

H₂S scrubbing systems on the market include:

1. Biological scrubbers using sulfur-oxidizing bacteria to oxidize H₂S to elemental sulfur and sulfates,
2. Chemical absorption and oxidation using oxides of iron,
3. Microaeration or injection of air (or oxygen) into the digester headspace/separate vessel for biological conversion of H₂S via the same mechanism as in biological scrubbers,
4. Activated carbon filtration through physical and chemical adsorption.

1.3.1 Biological Scrubbers:

Biological conversion of H₂S occurs only in an aerated environment, so small concentrations of air or oxygen have to be injected into a biological scrubber. These systems have sulfur oxidizing bacteria, such as *Thiobacillus spp*, that use sulfur as their primary energy source, but they also require other nutrients (diluted manure effluent or proprietary nutrient media), neutral pH, and temperatures in the 15-30°C range to reduce H₂S [15]. The microorganisms colonize the packing media inside the scrubber by forming biofilms. The media provides the surface for microbial attachment. Up to 100% H₂S removal efficiency can be obtained through biological scrubbing and some sulfur oxidation bacteria strains can function efficiently at very low pH ranges [14]. Schieder et al. (2003) was able to treat biogas with up to 5000 ppm of H₂S using BIO-Sulfex biofilter modules at flow rates of 10 – 350 m³/hr at 90% removal efficiency [16]. Some of the advantages of this system are that the packing medium is usually inexpensive and may even contain sufficient nutrients to support microbial growth. In addition to H₂S, biological scrubbers have also been used to remove ammonia from biogas [14].

However, one of the major problems encountered in such systems is the acidification of the packing media due to sulfuric acid formation that can lead to disposal issues. It may also lead to lower H₂S removal efficiencies due to elemental sulfur deposition on the media. Special measures to enhance the buffering capacity of the media by adding alkaline compounds or using a carrier medium that has alkaline properties, and/or washing periodically the packing media with water have to be taken to prevent the pH drop [17]. Another problem with biological scrubbers is the clogging of the packing media, resulting in pressure drops. Regular maintenance and expertise are required to keep all these parameters in check, which increases the maintenance costs of these systems.

1.3.2 Iron Oxide Scrubbers:

Iron oxides and hydroxides react with H₂S forming insoluble iron sulfides. Iron oxide pellets or wood chips impregnated with iron oxide are used to provide the reaction surface for H₂S absorption. The wood chip media is packed into the scrubbing unit and the biogas is passed through it for desulfurization. The iron oxide in the media reacts with the H₂S and is converted into iron sulfide. Extending the life of the wood chip media after saturation is possible by aeration, which forms elemental sulfur and regenerated iron oxide [18]. However, the regeneration process is highly exothermic, which is a safety issue. The iron oxide scrubbing system is simple and can be up to 100% efficient [19]. Proprietary iron oxide scrubbing systems like SOXSIA® can remove up to 2000 ppm of H₂S at 40 °C and flow rates of 1000 Nm³/hr [20]. The disadvantages of the process are that it requires the constant addition of fresh media, has high operating costs, and

generates hazardous waste. It can also be difficult to automate the regeneration phase due to the exothermic heat of reaction generated during the regeneration process [20].

The primary drawback of the iron oxide media, which has led to a reduction in its usage in recent years, is the disposal of spent iron sponge. It is difficult to dispose of safely and in some cases, the spent media is a hazardous waste, which requires special disposal procedures. Additionally, the regenerative reaction is exothermic and has resulted in self-ignition of the wood chips when the operating parameters are not carefully controlled [20]. Due to buildup of elemental sulfur and loss of hydration water, iron sponge activity is reduced by 1/3 after each regeneration. Therefore, regeneration is only practical once or twice before new iron sponge is needed.

1.3.3 Microaeration:

The simplest method of desulfurization of biogas is the controlled addition of oxygen or air directly into the digester headspace or in a separate vessel through which the biogas passes to create a microaerobic environment. The bacteria grow on the gas-liquid interface and the walls of the headspace inside the digester. In case of a separate vessel, it is partially filled with the digester effluent, which acts as the microaerophilic surface and the nutrient source for the microorganisms [21]. Based on the temperature, residence time and the percentage of injected air, full scale digesters have claimed 80 – 99% H₂S reduction, down to 20 – 100 ppm H₂S [15]. The oxygen content in the biogas post-treatment usually varies from 0.5 – 1.8 % on a volumetric basis. This is the least expensive and most easily maintained form of scrubbing for on-farm use to prevent corrosion and odor problems.

The major drawback of desulfurization inside the digester is the necessity to supply oxygen (or air) to the AD system, resulting in a dilute biogas stream. This is especially challenging when biogas has a lower concentration of methane (~ 50-55 % or lower) when a dilution of the biogas could create problems for the engine generators [22]. There is the possibility of injecting pure O₂ into the digester to minimize or avoid the dilution with N₂. However, pure O₂ supply can lead to higher operational costs. Moreover, overdosing of air could be a safety issue, as oxygen in biogas can result in an explosive mixture in the range of 6% to 12% O₂, at 60% CH₄ [20].

1.3.4 Activated Carbon Adsorption:

The attachment of one or more components of a liquid or gas (sorbate) on a solid with a high-surface area (sorbent) is known as adsorption. This phenomenon can be used to remove pollutants from a liquid or a gas stream that have an affinity towards the sorbent. Activated carbon (AC) is one of the typical solid surfaces used for the adsorption process. Commercial adsorbents have surface areas ranging from 100 – 1,200 m²/g, resulting in high adsorption capacities in relation to the weight of the sorbent [23].

There are two types of adsorption processes:

- a) physical adsorption, where the sorbate molecules attach to the pores of the sorbent through forces with weak bonding energies, such as van der Waals forces, and
- b) chemical adsorption, where stronger chemical bonding forces with higher bonding energies lead to much stronger attachment.

Activated carbon is the most commonly used adsorbent for H₂S removal in biogas. In addition to the physical adsorption, activated carbon provides a catalytic

surface for oxidation to elemental sulfur and sulfate, which significantly enhances the removal capacity of H₂S [19]. In presence of oxygen, the following reaction takes place:



In large biogas plants in Sweden, H₂S is commonly removed before CO₂ removal using activated carbon [24]. The ideal conditions for the reaction are pressures of 7 to 8 bar and temperatures of 50 to 70 °C, with addition of air that constitutes 4 – 6 % of the biogas [25]. In the absence of O₂, impregnation of oxidizing chemicals such as KI and KMnO₄ can promote partial oxidation of the H₂S into elemental sulfur or sulfates. Impregnation of other alkaline chemicals such as sodium hydroxide, sodium carbonate, potassium hydroxide, sodium bicarbonate, and metal oxides are the most common coatings employed [26]. A major drawback of activated carbon adsorption is the production of a sulfur saturated activated carbon product that requires appropriate disposal methods that can be expensive.

Even though several H₂S scrubbing technologies exist, there is a lack of field-scale data on long-term H₂S removal efficiency, and the costs associated with owning and operating a scrubbing system, especially on rural dairy farms in the United States. Furthermore, there are no observations or data available on how management of the scrubber systems affect its efficiency. Due to all the uncertainties associated with H₂S scrubbers, more research is required to ascertain if there is a ‘best’ solution for AD practitioners.

1.4 Biochar as a substitute H₂S adsorbent:

Biochar is produced by the thermal degradation of biomass under an oxygen-starved environment (pyrolysis) or in a low oxygen environment (gasification) at

temperatures less than 700 °C [27]. Biochar is a carbonaceous solid with energy density (18 MJ/kg) similar to pulverized coal [28]. Differences in biochar and activated carbon arise from their preparation method, the raw material, and the resulting physiochemical properties of the products. Biochar can be regarded as a precursor to activated carbon, which requires a further activation step using either steam or chemicals, such as sodium hydroxide at high temperatures. This process is intended to increase the surface area for use in industrial processes such as filtration/adsorption [29]. Activated carbon is made from char precursors, which are analogous to biochars – hence, the literature on activated carbon is relevant to the study of biochar. Activated carbon has been used as adsorbent for H₂S in biogas after dosage of iron salts into the digester for enhanced desulfurization [20]. Biochar could be a cheaper scrubbing solution, as there are a variety of raw waste materials that could be used, and the production of biochar below 700 °C is more energy-efficient and less cost-intensive than activated carbon production.

The proposed mechanism of H₂S removal using activated carbon involves [30,31]:

1. H₂S adsorption on the activated carbon surface,
2. H₂S dissolution in a water film,
3. Dissociation of H₂S in an adsorbed state in the water film,
4. Surface reaction of adsorbed O₂ with the formation of elemental sulfur or sulfur dioxide,
5. Further oxidation of SO₂ to H₂SO₄ in the presence of water.

A few recent studies have investigated H₂S removal from biogas using biochar [32–35]. Surface properties of the biochar are an important parameter to determine the effectiveness of the biochar in the removal of H₂S. A study conducted by Suliman et al.

(2016) showed that higher pyrolysis temperatures create a gradual increase in the surface area due to the formation of micropores on the biochar surface [36]. In the aforementioned studies, several analytical techniques were used to characterize the biochar. For example, SEM-EDS was used to characterize the surface of the biochar. N₂ adsorption isotherms were used to estimate the surface area of the biochar. Fourier Transform Infrared Spectroscopy (FTIR) was used for a qualitative analysis of the functional groups on the biochar surface. Zeta potential was used as a measure of the surface charge on the biochar in a solution. Suliman et al. (2016) used these procedures to characterize the biochar prepared from Douglas fir wood, Douglas fir bark, and hybrid poplar wood at six temperatures (623, 673, 723, 773, 823 and 873 K) in a lab scale reactor, and evaluated the significance of each characterization method [36].

Shang et al. (2013) prepared biochar from camphor, bamboo, and rice hull and compared them to activated carbon for H₂S removal from biogas [32]. They hypothesized that the biochar pH was the key factor in H₂S adsorption. From the breakthrough curves obtained from the experiments, the results showed a trend of higher adsorption of H₂S on the biochar surface as the pH of the biochar increased. The authors also stated that FTIR spectra provided evidence of basic functional groups on the biochar surface that may have aided in H₂S removal. However, their results were based on 50 µL H₂S/L of biogas or an H₂S concentration of 50 ppm. In most full-scale digesters, the concentration of H₂S can vary from 1,000 ppm – 10,000 ppm.

There is not a consensus in the literature on the mechanism of H₂S removal using biochar. Xu et al. (2014) proposed that the mechanism was similar to the one proposed by Adib et al. (1999, 2000) for AC, which stated that that the first step of adsorption of H₂S

molecules on the biochar surface was an important factor for the process to be efficient [30,31,35]. They also suggested that features of activated carbon surfaces, such as local environment of acidic/basic groups along with the presence of alkali metals, are important to the oxidation process of H₂S. Activated carbon that have a majority of acid groups and low amount of alkaline metals will not favor H₂S dissociation, thereby limiting treatment. While basic groups that result in a higher local pH and a high concentration of alkaline metals should favor the dissociation of H₂S, thereby leading to a more efficient oxidation process.

However, Shang et al. (2013) disputed this mechanism and suggested that mechanism of H₂S removal by biochar likely differs from that of the activated carbon [32]. In their experiment, they compared H₂S removal from biochar and activated carbon and observed a significant decrease in the adsorption capacity of the activated carbon compared to the biochar. They attributed this decrease in the adsorption capacity of AC to exhaustion caused by the formation of sulfuric acid after oxidation based on the mechanism of H₂S adsorption on activated carbon as described above [30,31]. Lehmann et al. (2011) determined SO₄²⁻ was formed on the biochar surface while elemental sulfur was found to be present in the pores of biochar using SEM-EDS [29]. Shang et al. (2013), however, stated that they observed a small decrease in the biochar pH, which regained its basic pH after exhaustion [32]. They hypothesized that the caustics present in the biochar catalyzed the conversion of sulfide to elemental sulfur, instead of sulfuric acid, allowing the biochar to regain a basic pH after exhaustion. In addition, the AC had a much larger surface area compared to biochar but had the lowest removal efficiency. Feng et al. (2005) had shown that raw AC fibers with higher surface area showed greater adsorption

and retention of sulfur when the adsorption was attributed to a physical process [37]. Mochizuki et al. (2016) also confirmed this observation when their experiment was conducted under dry conditions [38]. A wet surface allows dissolution of the H₂S, which leads to chemical adsorption due to the presence of basic functional groups and alkali metals and higher efficiencies. Therefore, it is likely that H₂S adsorption on biochar is highly dependent on the chemical nature of the surface, especially under humid conditions.

Bamdad et al. (2018) stated that since biochar has a heterogeneous surface with many different functional groups, it is complicated to predict a suitable mechanism for the adsorption of acidic gases on the biochar surface [39]. However, it is mentioned that the adsorption of CO₂ is mainly controlled by physical adsorption in contrast to the chemisorption of H₂S on the biochar surface due to the decrease in the amount of CO₂ adsorbed when the temperature was increased, while the opposite was true for H₂S adsorption. In conclusion, they stated that the original mechanism proposed by Adib et al. (1999) for AC is likely the same for adsorption of acidic gases on biochar, with differences created by the presence of alkali metals and basic functional groups in biochar. They also stated that further studies are required in order to better understand differences in the mechanism for biochar.

1.5 Biochar as a digester additive for H₂S removal:

Recent studies have investigated the direct addition of biochar into an AD system [28,40–42]. These studies focused on increasing CH₄ content upon addition of the biochar but did not study the effect of biochar addition on reducing H₂S production. According to Shen et al. (2015), by adding biochar made from corn stover directly to the

AD system, up to 86% of the CO₂ was sequestered, creating a biogas stream that was more than 90% CH₄ and less than 5 parts per billion H₂S, thus reducing the need for upgrading steps [42]. However, the research was focused on digestion of wastewater and not dairy manure. The experiments were conducted at thermophilic conditions with a low concentration of H₂S that is usually not associated with biogas in dairy manure digesters. The authors also stated that the likely mechanisms for H₂S reduction was adsorption to the high concentrations of potassium, calcium, and magnesium in the biochar along with a high starting pH of the reactor, which aided in CO₂ and H₂S absorption in the liquid phase. Shen et al. (2016) conducted similar experiments using biochar prepared from woody substrates, namely pinewood and white oak [28]. The authors added large amounts of biochar (up to 4.8 g biochar/g substrate TS) into their experimental units, which had 1.3% TS. In dairy manure digesters, the TS concentration can vary from 1% to 10%, which would result in large quantities of biochar addition to digesters. A lower biochar concentration that adequately desulfurizes biogas, while also providing a measure of CO₂ sequestration may be ideal for dairy manure digesters.

Biochar is a recalcitrant material with surface areas comparable to AC and a negative surface charge [43]. As a result, it is more capable of removing positively charged pollutants such as cadmium, copper, lead, zinc and polar organic compounds via ion exchange, electrostatic attraction, physical and chemical adsorption and precipitation, but not as effective at removing anionic pollutants [44]. Based on a review of previous research on anionic pollutants by Sizmur et al. (2017), it is likely that removal of dissolved H₂S follows a similar mechanism [43]. The first pK_a of H₂S is 7 and hence at neutral pH, the concentration of H₂S and HS⁻ is roughly equal. As the HS⁻ ions get

adsorbed on the biochar surface, a reduction in the concentration of the dissolved H₂S is likely. Therefore, it is expected that the H₂S in the biogas will decrease for it to be in equilibrium with the dissolved H₂S. Thus, if the biochar is modified to remove anionic pollutants, it may be possible to see a further increase its H₂S removal capacity the when compared to an unmodified biochar.

Surface area and selectivity for cations and anions can be changed by the activation (chemical or physical) or surface modification of biochar, which can result in enhanced sorption for different pollutants. Usually, surface modification techniques are used to increase the anion sorption capacity [43]. The high surface area of biochar can be used to embed a metal oxide with a positive charge and chemical properties that can aid in H₂S sorption. These biochar-based composites have been shown to remove negatively charged anions from aqueous solutions [43,45]. The composites can be prepared by soaking the biochar or their feedstocks in solutions of metal nitrates or chlorides for a duration of 12-24 hours. After the soaking process is completed, the biochar is heated/dried at temperatures ranging from 50 °C to 300 °C to convert the metal ions to metal oxides.

Agrafioti et al. (2014) prepared metal oxide impregnated biochar by soaking rice husk and municipal waste in calcium oxide, iron powder and iron (III) chloride prior to pyrolysis [46]. These modifications increased the arsenic (V) sorption capacity of the biochar from an aqueous solution. These results were supported by Fristak et al. (2017) where a 20-fold increase in the sorption of arsenic (V) was observed when corncob biochar impregnated with ferric nitrate after pyrolysis was used as an adsorbent [47]. In

addition, the modification was shown to have a negligible effect on sorption of the heavy metal cation, europium.

It has been reported that metal oxide modifications result in a reduction in the surface area of the biochar due to clogging of pores with metal oxide precipitates [48]. Micháleková-Richveisová et al. (2017) prepared modified biochars from garden wood waste, wood chips and corncob using the method followed by Fristak et al. (2017), and it resulted in a decrease in the surface area of the biochar due to the filling of micro and mesopores with iron [47,49]. However, the results showed even with a lower surface area, PO_4^{3-} sorption capacity increased by factors of 12 to 50 due to the phosphate ions binding to positively charged functional groups on the biochar surface.

The sorption of anions, such as PO_4^{3-} and arsenic (V), on the surface of modified biochar is attributed to chemical adsorption or electrostatic attraction to the positively charged metal oxide embedded on the surface. On the other hand, sorption of cations is due to chemical adsorption on oxygenated functional groups around the unmodified areas of the biochar, or precipitation within the metal oxide lattice [43,44]. Usually, metal oxide impregnated biochar has been shown to have a high adsorption capacity for both anionic and cationic pollutants compared to unmodified biochar [50].

Biochar can also reduce nitrogen volatilization through adsorption of nitrates, ammonium, in addition to PO_4^{3-} sorption [43,45]. High surface area and the porous microstructure of biochar can be used as slow release fertilizers of N and P. The presence of acidic functional groups, such as phenolic and carboxylic groups, on the biochar surface probably promotes ammonium adsorption while electrostatic interactions are responsible for nitrate adsorption [51]. Biochar prepared from pinewood has also been

utilized to treat fluoride-contaminated ground water. The prepared had a low surface area ($1 - 3 \text{ m}^2/\text{g}$), but it was able to remove similar amounts or more fluoride than activated carbon ($1000 \text{ m}^2/\text{g}$) [52].

It is likely that the mechanism of H_2S removal will be similar to other anionic pollutants, as seen in the aforementioned previous studies. Adding biochar directly into a digester may also aid in N and P removal in addition to the benefits of reduced H_2S concentration in the biogas. This can provide additional incentive to add biochar directly into a digester instead of using it for H_2S removal in a gas adsorption column.

1.6 Life Cycle Assessment (LCA) of poultry litter fluidized bed combustion:

Life cycle assessment (LCA) is an evaluation of environmental impacts through a systematic, inclusive, and analytical approach for any product or service [53]. An LCA quantifies the inputs and outputs of a system, product, service or a process, as defined by a system boundary, and evaluates the environmental impacts for each input and output [54]. LCA is most commonly used in comparing the environmental impact of a product or service with a comparable alternative in order to determine which product has a lower environmental impact [53]. LCA can also be used to estimate the environmental impact of a product at each stage of its life (cradle to grave) in order to possibly minimize the environmental impacts of the stages that have the highest negative impacts.

The LCA process is divided into four main components [54]:

1. Determination of the assessment scope and boundaries: a clear statement of the intended goal and scope of the analysis, including system boundaries definition, selection of different operations or stages in the process that are to be included in the study.

2. Selection of inventory of outputs and inputs: quantification of all inputs and outputs of the system including energy and raw materials consumed or produced, air and water emissions, and waste and any other releases in the entire life cycle of a product. Inventory analysis originates from the raw material extraction to the final disposal stage of a product.

3. Assessment of environmental impact data compiled in the inventory: quantification of the effects that the inputs and outputs listed in the inventory analysis have on the environment, human health, and depletion of natural resources. Some effects, such as noise pollution, that are difficult to quantify can also be part of the impact analysis.

4) Interpretation of results and suggestions for improvement: evaluation of the focus areas within the system that could be improved to minimize the system's or process' negative environmental impacts. This analysis can include both qualitative and quantitative suggestions for improvement.

The Eastern Shore of Maryland is known for intensive poultry production in the United States. The Delmarva Poultry industry estimated a total of 605 million broiler chickens in 2018, that can generate an estimated 1.1 million tons of litter, bedding, and feathers [55]. It is estimated that 750,000 tons of poultry litter have been remediated or managed alternatively based on the new proposed nutrient management strategies for Maryland from 2000 - 2010 [56].

Combustion significantly reduces the nitrogen, carbon, and moisture contents of a substrate, which makes the final product easier to transport to the fields for fertilization. The concentrated ash form has been shown to be an advantageous soil amendment with

positive effects on plant growth compared to standard fertilizer [57]. Direct spreading of poultry litter on agricultural farms in Maryland has resulted in phosphorus-enriched soils leading to an imbalance of nutrients in the soil. In addition, the leaching of N and P from these soils promotes eutrophication of the Chesapeake Bay.

Even though studies have investigated the viability of combusting poultry litter, optimization is required prior to widespread commercialization. Belgiorno et al. (2003) stated that energy generation and ash production made gasification the most economical disposal solution for poultry litter [58]. Marculescu and Stan (2011) concluded that energy recovery from poultry litter was difficult due to relatively high water content (up to 70%, usually 40-50% in MD) when compared to wood chips [59]. Thermal degradation with pyrolysis and gasification was stated to be a more viable solution. Joseph et al. (2012) also stated that gasification was a viable method of chicken litter disposal and some energy recovery was possible from the process [60]. However, their gasification unit had a low energy efficiency (19.6%), which they stated could be improved by changing the operational parameters. Even though these technologies have been shown to be effective in generating renewable energy and an alternative means of poultry litter disposal in land areas with restricted manure application, it is important to assess their environmental impacts in order to quantify their benefits in comparison to conventional energy from fossil fuel sources.

1.7 Objectives:

1. Co-digestion of gummy vitamin waste with dairy manure: Evaluate the effect of a gummy vitamin waste product as a co-digestion substrate for anaerobic digestion of dairy manure.

2. Market available scrubbing solutions and their efficiencies: Quantify the efficacy and economics of two market available H₂S scrubbers, based on real data gathered from two portable gas analyzer systems, from two different scrubbing systems operating on farms in the Northeast US.
3. Biochar as a substitute adsorbent for activated carbon: Determine the effect of iron impregnation on the performance of corn stover biochar and maple wood biochar for H₂S adsorption from biogas compared to activated carbon
4. Biochar for in-situ removal of H₂S in biogas: Determine the effect of biochar as an additive to anaerobic digestion of dairy manure on H₂S production.
5. Life Cycle Assessment (LCA) of poultry litter fluidized bed combustion: Conduct a life cycle assessment of a poultry litter combustion under improved operational conditions and using actual operating data obtained from a full-scale fluidized bed poultry litter combustion system.

2 Methane and hydrogen sulfide production from co-digestion of gummy waste with a food waste, grease waste, and dairy manure mixture

ABSTRACT

Co-digestion of dairy manure with waste organic substrates has been shown to increase the methane (CH₄) yield of farm-scale anaerobic digestion (AD). A gummy vitamin waste (GVW) product was evaluated as an AD co-digestion substrate using batch AD testing. The GVW product was added at four levels (0, 5, 9, and 23%, on a wet mass basis) to a co-digestion substrate mixture of dairy manure (DM), food-waste (FW), and grease-waste (GW) and compared to mono-digestion of the GVW, DM, FW, and GW substrates. All GVW co-digestion treatments significantly increased CH₄ yield by 126% - 151% (336 – 374 mL CH₄/g volatile solids (VS)) compared to DM-only treatment (149 mL CH₄/g VS). The GVW co-digestion treatments also significantly decreased the hydrogen sulfide (H₂S) content in the biogas by 66% - 83% (35.1 – 71.9 mL H₂S/g VS) compared to DM-only (212 mL H₂S/g VS) due to the low sulfur (S) content in GVW waste. The study showed that GVW is a potentially valuable co-digestion substrate for dairy manure. The high density of VS, and low moisture and S content of GVW resulted in higher CH₄ yields and lower H₂S concentrations, which could be economically beneficial for dairy farmers.

2.1 Introduction:

Anaerobic digestion (AD) of organic substrates with dairy manure, also known as co-digestion, can increase biogas production and result in higher return on investment for

dairy farmers [5]. Biogas produced from AD is a combination of 50 – 75 % methane (CH_4) and 25 – 50% carbon dioxide (CO_2), with trace levels (0.01% - 1%) of hydrogen sulfide (H_2S) that can be used as a source of renewable energy for heat and power generation [61]. Limitations from mono-digestion of organic materials arise from substrate properties, such as unbalanced C:N ratios, recalcitrance in the feedstock, high concentrations of long chain fatty acids, and deficiency in trace minerals required for the growth of methanogens [4,5]. These limitations can lead to unfavorable economics for dairy farmers using AD to generate energy on-farm [5,6]. Furthermore, positive synergy from co-digestion of a mixture of substrates can lead to more CH_4 production than the addition of CH_4 produced from mono-digestion of each individual substrate. A review by Mata-Alvarez et al. (2014) reported that co-digestion of carbon (C) rich organic matter with cattle and poultry manure resulted in up to 3.5 times more CH_4 production than the CH_4 potential of the individual substrates [4]. Lisboa and Lansing (2013) reported a maximum of 29.4 times more CH_4 yield when dairy manure was co-digested with chicken processing waste compared to mono-digestion of dairy manure [7]. Moody et al. (2011) determined the biomethane potential of a wide range of food waste substrates and concluded that co-digestion of manure and organic waste has the potential to increase biogas production, and in turn, increase energy generation from AD [62]. However, often studies are often only applied to individual substrates due to differences in organic waste composition and collection.

Previous research on co-digestion of food waste and dairy manure has primarily focused on the CH_4 production potential of co-substrates [9–11], with limited data on the effects of co-digestion substrate selection on the production of H_2S [63]. The production

H₂S in biogas occurs when sulfur-containing compounds, such as sulfates, sulfites, and thiosulfate, in AD substrates are reduced by sulfate reducing bacteria (SRB) under anaerobic conditions [64]. High H₂S concentrations in biogas (0.05% - 1% by vol.) can become a major problem when utilizing the biogas due to health concerns and corrosion of biogas equipment [65]. Combined heat and power (CHP) systems usually require H₂S concentrations to not exceed 500 ppm to prevent reduced performance from corrosion, and H₂S concentrations over 100 ppm can cause severe adverse human health impacts [63]. Most dairy farms use CHP systems to generate energy for on-farm use and lower H₂S concentrations can lead to improved energy generation efficiencies and reduced maintenance. Corro et al. (2013) observed a reduction in H₂S concentrations when coffee waste was co-digested with dairy manure compared to digestion of dairy manure only, but there was no discussion of the cause for the observed H₂S differences [66]. Research has shown that co-digestion of organic matter with higher C:N ratios in manure-based digesters can reduce ammonia inhibition and enhance methane production [4]. Co-digestion of carbon rich organic matter with a low sulfur (S) content may also reduce the H₂S concentration in the biogas when compared to the mono-digestion of dairy manure and prevent sulfide inhibition.

Industrial food waste comprises 5% of the total food waste generated globally [67]. Although the fraction of industrial food waste is significantly less than food waste from other sources, it has logistical and economic advantages due to its high-volume generation at specific points and homogenous nature. Valorization of these industrial food waste streams can help mitigate disposal costs in landfills, while providing a source of tipping fees for dairy farmers with AD systems. The waste produced from gummy

vitamin industries is high in degradable C compared to dairy manure. Gummy vitamin waste (GVW) material can contain up to 70% sugar and gelatin, with starch or pectin-based gels that create the unique structure that is characteristic of gummy candies [68]. Due to its high sugar content, GVW can be a valuable resource for AD, yet the dense jelly-like consistency may lead to issues, such as a slow degradation rate, increased hydraulic retention time, or possible pipe clogging within the AD system. It is also possible that GVW with a high C:S ratio could reduce the H₂S concentration in the biogas when co-digested with dairy manure.

The main goal of the project was to evaluate a GVW product as a co-digestion substrate for AD. The specific objective was to evaluate the CH₄ and H₂S production and VS degradation of a GVW substrate when co-digested with a dairy manure (DM), food waste (FW) and grease waste (GW) mixtures (DM.FW.GW). A co-digestion mixture was used for testing, as many on-farm digesters incorporate multiple waste streams and to highlight the benefits of testing co-substrates as both mixtures and single substrates. Co-digestion of the tested mixtures was expected to produce a significantly higher amount of CH₄ and lower H₂S compared to the mono-digestion of DM.

2.2 Materials and Methods:

2.2.1 Sample Collection:

Anaerobic digester effluent (inoculum source) and the GVW product were collected from a Northeastern US farm. The farm co-digested dairy manure from heifers with gummy vitamin waste, food waste and grease waste (GW) at a 64% DM, 9% GVW, 16% FW, and 11% GW ratio, by mass. The AD effluent sample was utilized as an inoculum source, as it had been pre-acclimated to the GVW material used at the farm.

The GW and FW were collected from a local supermarket. Un-separated dairy manure from the USDA Beltsville Agricultural Research Center (BARC) in Beltsville, MD was utilized as the DM substrate. Field samples were collected and brought back to lab on ice. The mean total solids (TS) and volatile solids (VS) data for the substrates used in the experiment are shown in Table 2.1.

Table 2.1 Total and volatile solids content of the individual substrates (gummy vitamin waste, food waste, grease waste, dairy manure) and digester effluent (inoculum) used for the experiment.

Parameters	Gummy Vitamin Waste	Food Waste	Grease Waste	Dairy Manure	Inoculum
Total Solids (g/kg)	464 ± 2.0	91.0 ± 1.0	673 ± 4.5	94.5 ± 3.6	64.8 ± 0.9
Volatile Solids (g/kg)	463 ± 2.1	83.1 ± 1.1	645 ± 1.5	81.7 ± 3.6	47.5 ± 0.8

2.2.2 Experimental Design:

The GVW product was added to individual batch digesters at four inclusion levels (0, 5, 9, and 23%, on a wet mass basis) to a co-digestion substrate mixture of dairy manure (DM), food-waste (FW), and grease-waste (GW) and compared to mono-digestion of the GVW, DM, FW, and GW substrates, with an inoculum control. The 9% GVW treatment (64% DM, 16% FW, 11% GW, by mass) represented the mixture that was used at the farm during the time of AD effluent collection. An inoculum to substrate ratio (ISR) of 1:1 (VS basis) was used for the experiment. Table 2.2 shows the experimental design and

the descriptions of the treatment levels for the experiment, with each treatment conducted using triplicate AD reactors. All mass data are expressed on a wet mass basis.

Table 2.2 Experimental design using a 1:1 inoculum to substrate ratio, with the calculated initial total solids (TS) and volatile solids (VS) of the treatment mixtures. The percent of GVW inclusion was based on mass. All treatments were conducted in triplicate.

Digestion Substrate and Inoculum	Inoculum (g)	DM (g)	FW (g)	GW (g)	GVW (g)	TS (g/L)	VS (g/L)
Inoculum Control	31.9	-	-	-	-	64.1	47.0
Dairy Manure (DM)	31.9	18.3	-	-	-	71.7	59.5
Food waste (FW)	31.9	-	18.1	-	-	74.2	60.0
Grease waste (GW)	31.9	-	-	2.3	-	105	87.6
Gummy vitamin waste (GVW)	31.9	-	-	-	3.2	101	85.5
DM.FW.GW (0% GVW)	23.9	5.2	1.4	0.9	-	86.3	71.5
GVW.DM.FW.GW (5% GVW)	28.1	5.2	1.4	0.9	0.4	88.2	73.5
GVW.DM.FW.GW (9% GVW)	31.9	5.2	1.4	0.9	0.8	89.5	74.5
GVW.DM.FW.GW (23% GVW)	47.9	5.2	1.4	0.9	2.4	93.1	78.0

2.2.3 Biochemical Methane Potential (BMP) Test Procedures:

The batch laboratory testing followed the biochemical methane potential (BMP) protocol, which is a laboratory batch study used to characterize CH₄ production potential [8]. Substrate and inoculum were added into 300 mL serum bottles, purged with N₂ gas to establish anaerobic conditions, capped, and incubated at 35°C in an environmental chamber. Biogas, CH₄, and H₂S concentrations were monitored at regular intervals for 67

days, when biogas production had largely ceased, and the daily biogas production was less than 1% of the total biogas production for most treatments. The mass of substrate and inoculum in each bottle ranged from 31.4 to 58.8 g (Table 2.2) to keep the ISR at 1:1 for all treatments.

The quantity of biogas produced was measured using a graduated, gas-tight, wet-tipped 50 mL glass syringe inserted through the septa of the digestion reactors and equilibrated to atmospheric pressure. Biogas samples were collected in 0.5 mL syringes and tested on a gas chromatograph (Agilent 7890) using a thermal conductivity detector (TCD) at a detector temperature of 250 °C for CH₄ and H₂S concentration. The average CH₄ and H₂S production in the triplicates from the inoculum control was subtracted from the other treatments to present the total CH₄ production from the waste substrates only.

2.2.4 Analytical Methods:

The treatment mixtures were analyzed for pH before and after digestion using an Accumet AB15 pH meter. Triplicate samples were tested for TS and VS, according to Standard Methods for the Examination of Water and Wastewater (APHA-AWWA-WEF, 2005) within 24 hours of collection. For TS analysis, triplicate 10.0 ml samples were pipetted into pre-weighed porcelain crucibles. The samples were then dried at 105 °C until a constant mass was obtained for the TS concentration. The crucibles were then placed in a furnace at 550 °C until a constant weight was obtained to determine VS concentration. The gummy waste and inoculum (digester effluent) were tested for total metals (iron, zinc), and total sulfur at Agrolabs Inc, Delaware using ICP-MS (Inductively coupled plasma mass spectrometry).

2.2.5 Statistical Analysis:

Collected data were reviewed in accordance with QA/QC procedures, and analyzed for significant differences in biogas quantity, CH₄, H₂S, TS, VS, and pH using ANOVA and Tukey-Kramer post-hoc multiple mean comparison tests of the reviewed data using SAS. Tests of significance were conducted with an alpha value set at 0.05. Values are reported as means with standard errors (SE).

2.3 Results:

2.3.1 Methane (CH₄) Production:

The co-digestion mixtures GVW.DM.FW.GW had a significantly higher percent CH₄ in the biogas compared to the mono-DM digestion (p -value < 0.0001; Table 2.3). However, there were no significant differences in the biogas CH₄ content among the co-digestion treatments (Table 2.3). The cumulative CH₄ production over the 67-day AD period was normalized using two methods: 1) the total mass of the substrate added (mL CH₄/g substrate), as this normalization provides an estimate of CH₄ production that can be readily used by farmers, and 2) the VS of the substrate (mL CH₄/g VS added) for comparison with other studies [7].

As expected, the co-digestion treatments (with and without GVW addition) produced 359% - 524% more CH₄ compared to mono-DM digestion, when normalized by the mass of substrate added (Table 2.3). Normalized CH₄ production in co-digestion without GVW (DM.FW.GW-only) was 11.6% lower than the 5% GVW.DM.FW.GW mixture, 14.5% lower than 9% GVW.DM.FW.GW mixture, and 36.3% lower than the 23% GVW.DM.FW.GW mixture (Table 2.3; Figure 2.1). The CH₄ production in the 23% GVW.DM.FW.GW mixture was the highest among all treatments. The total normalized

volume of CH₄ increased linearly with the mass percent of GVW added ($r^2 = 0.9866$) (Figure 2.2).

Table 2.3 Methane (CH₄) and hydrogen sulfide (H₂S) production data from the batch digestion testing.

Treatment	CH ₄ (%) *	mL CH ₄ / g VS	mL CH ₄ / g substrate	mL H ₂ S/ kg VS	mL H ₂ S/ kg substrate
Dairy manure (DM)	53.7 ± 0.5	149 ± 11	12.2 ± 0.1	212 ± 17	17.4 ± 1.4
Food waste (FW)	14.8 ± 1.1	0 [#]	0 [#]	99.7 ± 8.8	8.3 ± 0.7
Grease waste (GW)	25.7 ± 3.0	10 ± 4.5	6.3 ± 2.9	33.1 ± 30.4	21.4 ± 19.6
Gummy vitamin waste (GVW)	6.98 ± 0.9	0 [#]	0 [#]	7.0 ± 0.1	3.2 ± 0.1
DM.FW.GW (0% GVW)	67.4 ± 0.2	373 ± 6	56.0 ± 0.8	35.1 ± 2.2	5.3 ± 0.3
GVW.DM.FW.GW (5% GVW)	66.6 ± 1.6	374 ± 12	62.5 ± 2	71.9 ± 13.7	12.0 ± 2.3
GVW.DM.FW.GW (9% GVW)	68.3 ± 1.2	355 ± 3	64.1 ± 0.5	70.4 ± 5.2	12.7 ± 0.9
GVW.DM.FW.GW (23% GVW)	71.1 ± 1.0	336 ± 12	76.3 ± 2.7	68.3 ± 16.6	15.5 ± 3.8

* The % CH₄ shown is the average value of the last two weeks of the 67-day experiment.

[#] The CH₄ production from the inoculum was subtracted from all treatments, resulting in zero values when the inoculum outperformed the treatment.

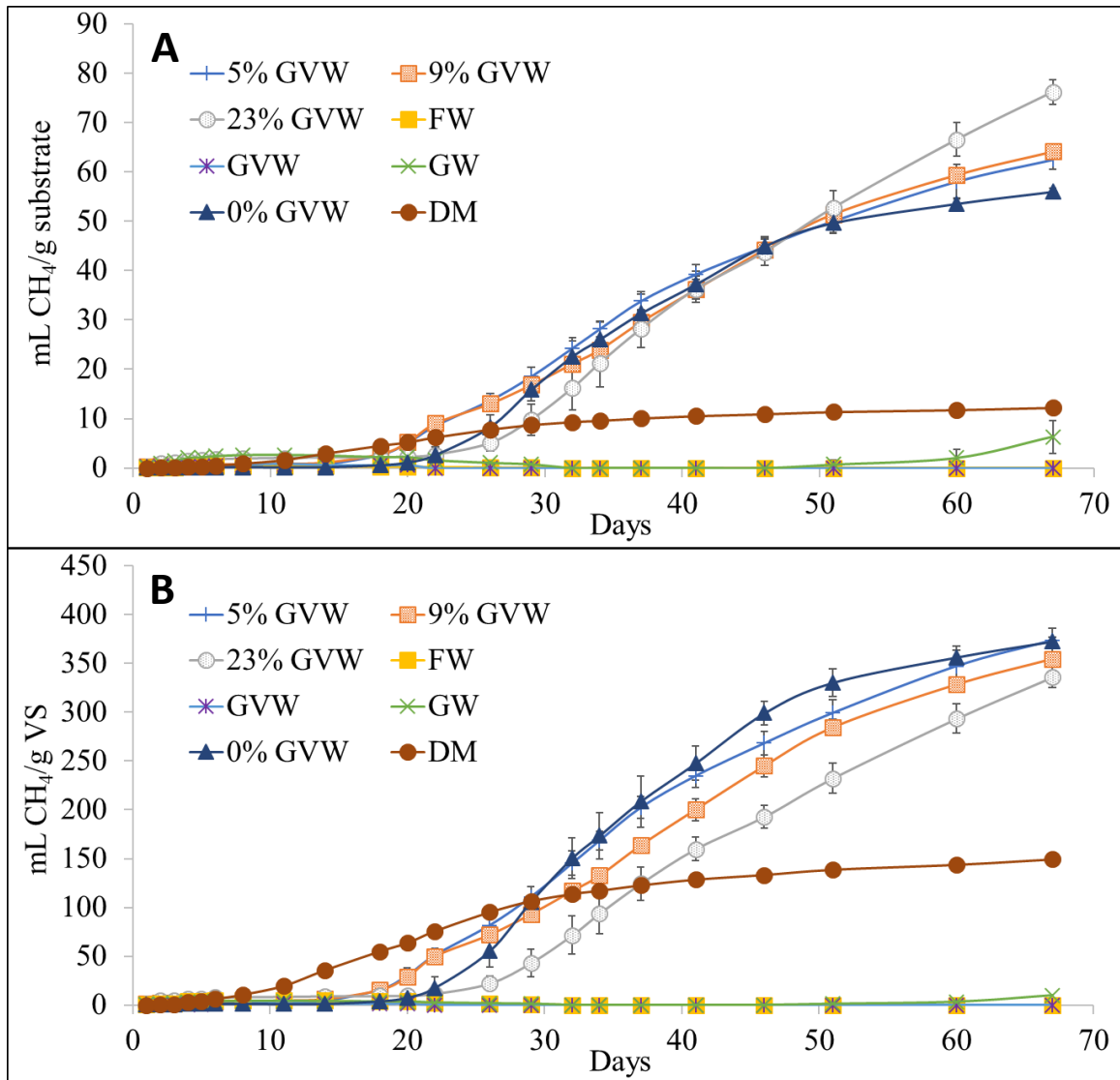


Figure 2.1 Methane (CH₄) production normalized by gram of substrate (mL CH₄/g substrate) (A, top) and by gram of volatile solids (mL CH₄/g VS) (B, bottom) in the batch digestion testing of gummy vitamin waste (GVW), grease waste (GW), food waste (FW), dairy manure (DM) digested singularly and as a mixture (DM.FW.GW), with the percent inclusion of GVW shown for the co-digestion mixtures.

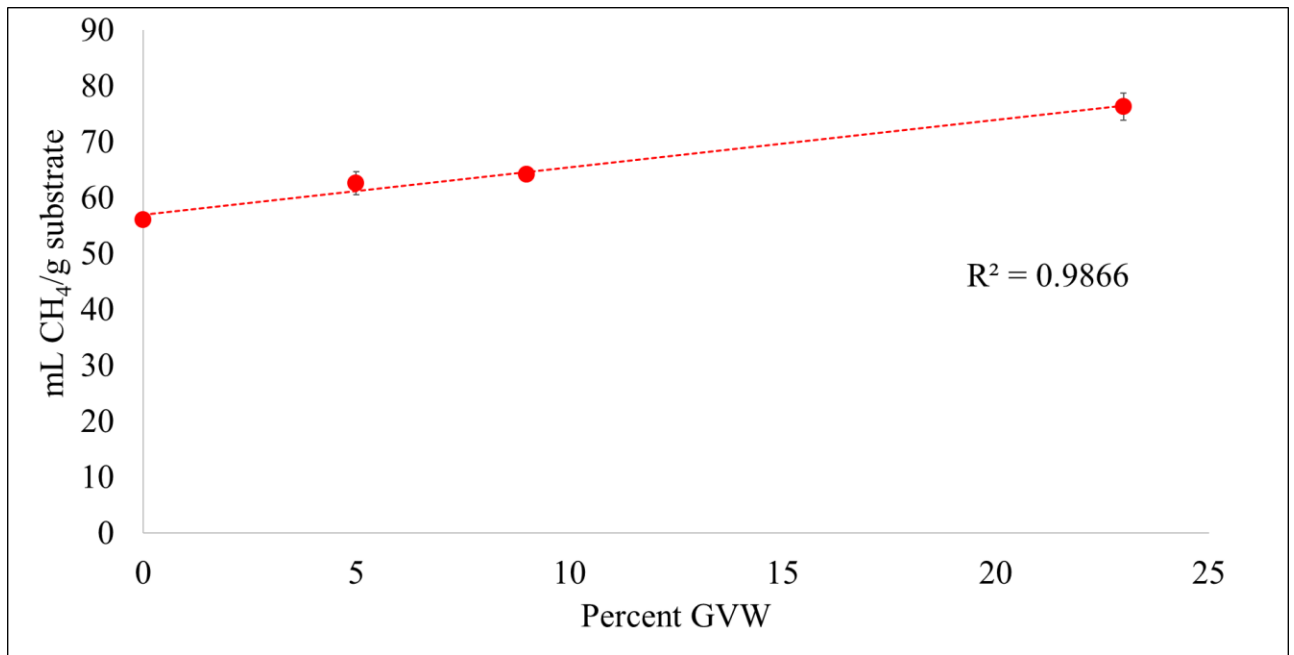


Figure 2.2 Linear regression of normalized methane (CH₄) production per gram of added substrate and percent gummy vitamin waste (GVW) within the co-digestion mixture.

When the total CH₄ produced was normalized by the quantity of organic material added (mL CH₄/g VS), the 23% GVW.DM.FW.GW mixture was significantly lower than the DM.FW.GW mixture with 0% GVW (p -value = 0.0156) and 5% GVW.DM.FW.GW mixtures (p -value = 0.0122) (Table 2.3), with no significant differences between the other co-digestion treatment groups. Mono-GVW digestion resulted in negligible CH₄ production (0 mL CH₄/g VS) over 67 days of digestion due to subtraction of inoculum CH₄ production from each treatment, and higher CH₄ production values in the triplicate inoculum reactors compared to the triplicate GVW-only AD reactors. Both treatments with negligible CH₄ production (Mono-GVW and mono-FW) had low final pH levels in the digestion vessels (under pH 7) (Table 2.4).

Table 2.4 Average pH and volatile solids (VS) in all treatment mixtures pre-digestion (initial) and post-digestion (final). Initial VS data was calculated theoretically, and final VS data was determined experimentally.

Treatment	Initial VS (g/L)	Final VS (g/L)	Decrease in VS (%)	Initial pH	Final pH
Dairy manure (DM)	59.5	48.0 ± 1.8	19.3%	7.64	7.75
Food waste (FW)	60.0	42.0 ± 2.5	30.0%	7.11	6.24
Grease Waste (GW)	87.5	79.5 ± 1.1	9.1%	7.79	7.21
Gummy vitamin waste (GVW)	85.5	53.0 ± 0.5	38.0%	7.75	6.24
DM.FW.GW (0% GVW)	71.5	49.4 ± 0.8	30.9%	7.92	7.97
GVW.DM.FW.GW (5% GVW)	73.5	47.6 ± 3.0	35.2%	7.84	7.95
GVW.DM.FW.GW (9% GVW)	74.5	49.2 ± 1.3	34.0%	7.87	7.95
GVW.DM.FW.GW (23% GVW)	78.0	51.0 ± 2.6	34.6%	7.77	7.88

2.3.2 Hydrogen Sulfide (H₂S) Production:

The DM treatment produced biogas with a peak concentration of 2,145 ppm H₂S after three days of digestion (Figure 2.3). After this time, H₂S levels decreased and no H₂S was detected in the biogas by the 60th day of the experiment. The treatment with the next highest peak H₂S concentration in the biogas was the 9% GVW.DM.FW.GW mixture (804 ppm H₂S), which was 63% less than the DM treatment and 23% greater than the next highest treatment (DM.FW.GW-only mixture with 0% GVW) at 576 ppm H₂S. The peak H₂S concentrations for all treatments were observed within the first 2-3 days before peak CH₄ production. The 23% GVW.DM.FW.GW treatment, DM and FW had detectable H₂S concentrations in the biogas for the longest period (51 days). The mono-GVW treatment did not produce a measurable amount of CH₄, but it had the

shortest period of detectable levels of H₂S (5 days). This is likely due to lowered microbiological activity within the digester due to the low pH levels, which led to low biogas production.

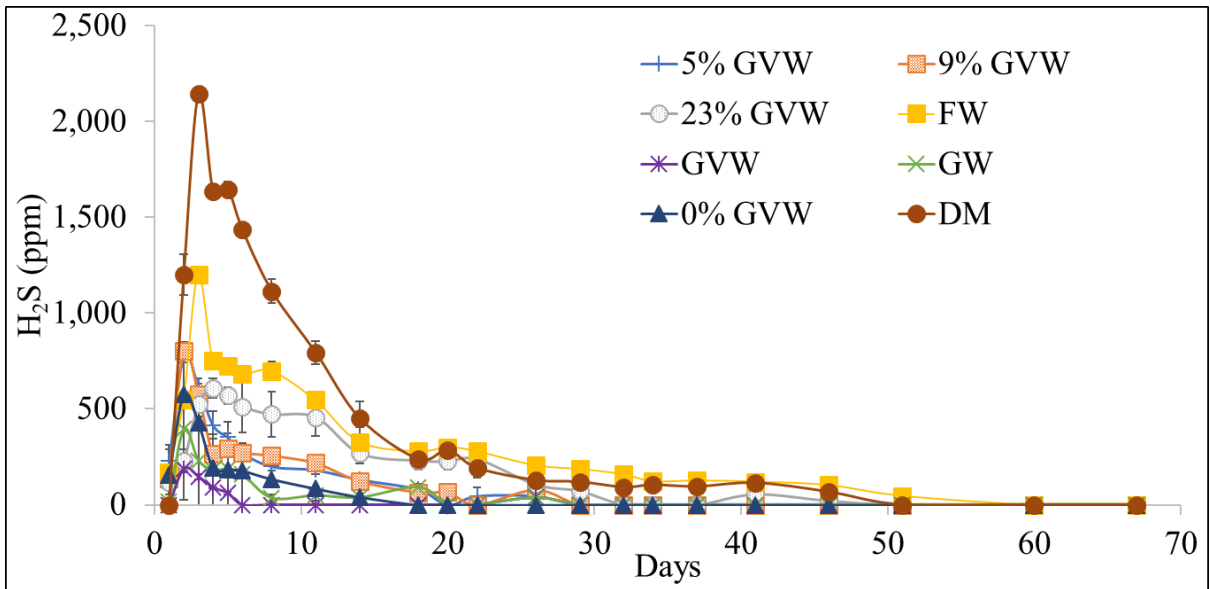


Figure 2.3 Hydrogen sulfide (H₂S) concentration (ppm) in the biogas over time in the batch digestion testing of gummy vitamin waste (GVW), grease waste (GW), food waste (FW), dairy manure (DM) digested singularly and as a mixture, with the GVW inclusion shown for each co-digestion mixture tested.

The quantity of H₂S produced showed an increasing trend with increases in the percent of GVW inclusion (0 – 23%) when normalized by kilograms of substrate addition (5.3 – 15.5 ml H₂S/kg substrate; Table 2.3, Figure 2.4). The H₂S production in the DM treatment (17.4 mL H₂S/kg substrate) was significantly higher than the treatments co-digested with GVW (*p*-value = 0.0046). However, in the DM.FW.GW treatment (0% GVW), the normalized H₂S production was the lowest among the co-digested treatments

(5.3 mL H₂S/kg substrate), and significantly lower than 23% GVW.DM.FW.GW (*p*-value = 0.0106) and DM (*p*-value = 0.0023) treatments. However, there were no significant differences for normalized H₂S production between the 5 – 23% GVW inclusion (*p*-value = 0.633) treatments.

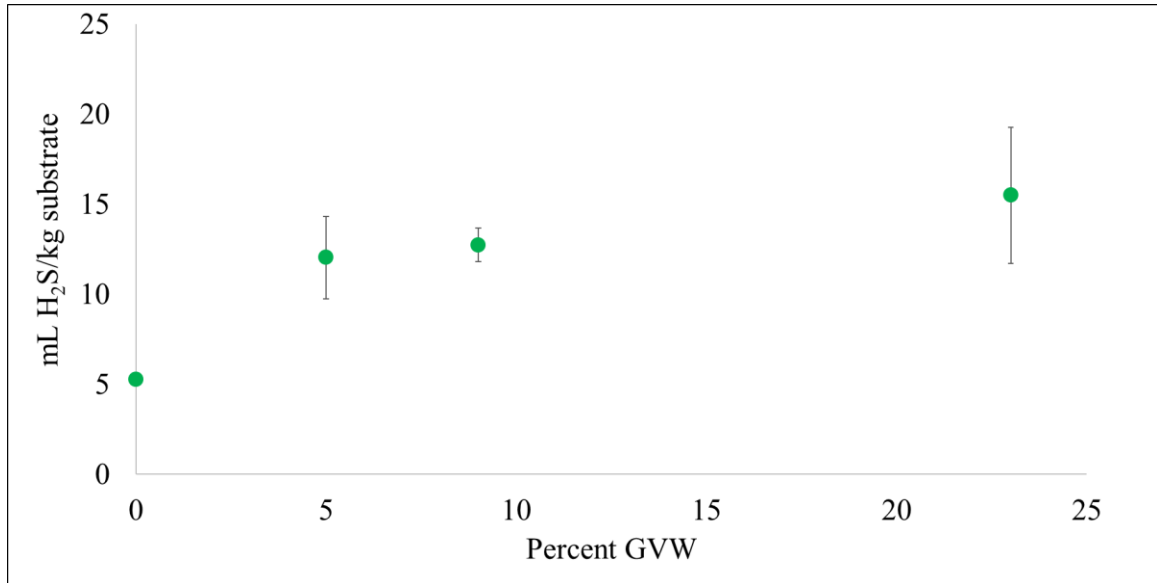


Figure 2.4 Normalized hydrogen sulfide (H₂S) production per kilogram of added substrate and percent gummy vitamin waste (GVW) within the co-digestion mixture.

When the total H₂S was normalized by the amount of VS added, the DM treatment (212 mL H₂S/kg VS) produced a significantly larger amount of H₂S compared to all co-digestion treatments (*p*-value < 0.0001) (Table 2.3). The addition of GVW (68 - 72 mL H₂S/kg VS) showed a significant increase in H₂S production compared to the DM.FW.GW (0% GVW) treatment (35 mL H₂S/kg VS; *p*-value = 0.0003). However, there were no significant differences within the 5 – 23% GVW.DM.FW.GW treatments (*p*-value = 1.000).

2.3.3 Effect of retention time and solids degradation:

The percentage of CH₄ in the biogas of the DM treatments rose above 25% on the 11th day of digestion, while the treatments containing additional substrates (FW, GW and GVW) had a longer lag phase and started producing higher quantities of CH₄ after 20 days of digestion (Figure 2.1), which is a relatively long lag-time for BMP analyses. The DM treatment produced 43% of its total cumulative CH₄ within the first 20 days, while all other treatments had less than 10% of the total cumulative CH₄ production during this time (Table 2.5). By the 41st day of the experiment, 89% of the total cumulative CH₄ from the mono-DM treatment had been produced, but the percent of total cumulative CH₄ from the GVW.DM.FW.GW and DM.FW.GW treatments by Day 41 varied from 57 - 80% of the cumulative CH₄ after 67 days of digestion. The effect of the longer retention times on GVW degradation was seen, as the CH₄ production rate for co-digestion was highest when no GVW was added (DM.FW.GW), with a maximum CH₄ production rate of 16.8 ml CH₄/VS d). The maximum CH₄ production rate decreased with increasing GVW inclusion (10.6 – 11.6 ml CH₄/VS d). The maximum CH₄ production rate was the lowest for DM (6.0 ml CH₄/VS d) for the treatments with CH₄ generation.

Table 2.5 Normalized methane production (mL CH₄/g VS) after 20, 46, and 67 days, with the percentage of the cumulative CH₄ (Day 67) by Days 20 and 46 shown in parentheses.

Treatment	Day 20 (mL CH₄/g VS)	Day 46 (mL CH₄/g VS)	Day 67 (mL CH₄/g VS)
Dairy manure (DM)	64 (43%)	133 (89%)	149
DM.FW.GW (0% GVW)	7 (2%)	299 (80%)	373
GVW.DM.FW.GW (5% GVW)	30 (8%)	268 (72%)	374

GVW.DM.FW.GW (9% GVW)	29 (8%)	245 (69%)	355
GVW.DM.FW.GW (23% GVW)	10 (3%)	193 (57%)	336

The TS and VS concentrations of the GVW showed that the VS comprised 99.7% of the total solids content (46.4% of the wet GVW). While a high percentage of the GVW was degradable, there was only a 34 - 35.2% degradation of VS during digestion (Table 2.4). While there was no CH₄ production from the mono-FW and mono-GW treatments, there was a decrease of >30% of the initial VS content, which can be attributed to the initial breakdown of the organic matter, resulting in CO₂-enriched biogas production. Biogas volume for these treatments was over 200 mL during the first two days, with less than 0.5% CH₄ and over 35% CO₂ for mono-FW and over 50% CO₂ for mono-GVW treatments.

2.4 Discussion:

Increasing the amount of GVW during digestion did increase CH₄ production, as expected. The GVW appeared to completely hydrolyze during digestion, with no visible trace of solid GVW in the post-BMP samples after 67 days of digestion. The GVW accounted for 5 – 23 % of the total mass of substrate added, corresponding to 15 – 50% of the VS inclusion. The GVW product could be beneficial for farmers interested in co-digestion waste substrates that increase CH₄ production, but the longer retention time of the GVW compared to DM digestion should be taken into consideration.

The negligible CH₄ production and low pH values in the mono-GVW, FW and GW treatments compared to the higher CH₄ production (336 – 374 ml CH₄/g VS) and pH range (7.88 – 7.95) in treatments that co-digested GVW, FW, GW and DM showed that the buffering capacity of the added co-substrates is important to mitigate accumulation of

volatile fatty acids (VFA) and lowered pH [4,69]. Carbon rich substrates can have a poor buffering capability, leading to an increased rate of VFA production and methanogenesis inhibition [4]. The mono-GW treatment had an initial pH of 7.79 but did not produce significant amounts of CH₄, possibly due to the slow degradation rate of lipids in the grease waste. Previous studies have also shown that digestion of lipids without co-digestion required the use of lime as a pH stabilizer [70]. The use of a buffer for pH control in the experiment was avoided since the study was originally conducted to emulate the source farm conditions. The AD system on farm did not use any pH stabilizers, as the manure provided sufficient buffering capacity for the digestion process. Generally, the high alkalinity of manure increases digester resistance to acidification for high-fat and sugar content wastes and adds a nitrogen source for micro-organisms [71].

All treatments produced large amounts of biogas during the first two days of digestion (ranging from 39 mL for DM to 379 mL for 23% GVW.DM.FW.GW), mostly composed of CO₂. The biogas volume dropped sharply for all treatments (< 10 mL per day) after Day 2, and the mono-DM treatment recovered the earliest (Day 11) and started producing > 50 mL biogas per day. The reduction in VS in the treatments with negligible CH₄ production for FW, GVW, and GW (Table 2.4) can be attributed to this initial burst of CO₂ enriched biogas production due to the initial breakdown of complex organic molecules. Bujoczek et al. (2000) showed that high organic loading rates may initially lead to large amounts of biogas, composed mainly of CO₂, after which biogas production slows down [72]. In their study, the biogas production recovered after 30 days of digestion with CH₄ as the main component, similar to the results seen in this experiment. The authors also reported that the highest TS content for feasibility of digestion was 10%,

while the shortest lag phase was obtained for 2.7% TS. The TS content in our experiment varied from 7.1% for DM to 11.6% for FW and showed similar CH₄ production trends to their study. The longer lag phase associated with a high TS content could be due to either high VFA concentrations or high ammonia concentrations or a combination of the two factors [72]. The CH₄ production in this study recovered after the lag phase, indicating acclimatization of the methanogenic bacteria to the initial inhibitory conditions, but the quantity of CH₄ generated from the DM treatment (149 ± 11 mL CH₄/g VS) was 38 - 44% lower than the results obtained by Moody et al. (2011) for dairy manure (239 – 264 mL CH₄/g VS) [62]. Witarsa and Lansing (2015) showed that the normalized CH₄ production on a VS basis is often lower for unseparated dairy manure due to the recalcitrant nature of the manure solids, leading to lower VS conversion efficiency [73].

It was expected that CH₄ production normalized by VS in the GVW co-digested treatments would be similar, but a decreasing trend with increasing percent GVW was observed. Normalization by VS illustrates the efficiency of organic material conversion to CH₄. As GVW is a dense substrate in terms of grams of VS per gram of substrate, the increase in GVW inclusion decreased the efficiency and rate of converting the VS to CH₄. The longer lag phase and the larger CH₄ production rates in the GVW treatments compared to DM.FW.GW and DM-only, from Days 41 to 67, suggests that long retention times would be needed to receive the full increase in expected CH₄ production. This effect was also seen by Kaparaju et al. (2002) when black candy, chocolate, and confectionary by-products were digested with dairy manure for 160 days in order to obtain a complete cumulative CH₄ value, with similar normalized CH₄ production for the

confectionary waste (320 – 390 mL CH₄/g VS) compared to the GVW.DM.FW.GW treatments (336 – 374 mL CH₄/g VS) [74].

In all treatments, the VS degradation was low compared to studies conducted by Lisboa and Lansing (2013) and Li et al. (2013), where the VS degradation rates ranged from 48% - 93% [7,75]. Only 19.3% of the initial VS content of the mono-DM treatment was degraded at the end of the experiment, illustrating recalcitrance in the manure feed. The VS degradation was consistent with co-digestion studies of forage radish and dairy manure by Belle et al. (2015b), which used the same manure source as this study with a 21.3% reduction in VS concentration in the mono-DM treatment [76]. The VS degradation of our study (30.9% – 35.2%) was also comparable to the aforementioned study (30.8% – 39.7%), with 50%-80% co-digestion substrate with dairy manure.

In a review conducted by Xie et al. (2018), it was reported that addition of a carbon rich substrate to sewage sludge digestion may lower the H₂S concentration due to a dilution effect [77]. This dilution effect can be attributed to a proportionally higher biogas yield compared to the additional H₂S produced from the co-digested substrates. The S concentration for GVW (212 ppm S) was lower than the inoculum source (368 ppm S), and unseparated dairy manure slurries with a TS content of 7% (~ 1500 ppm S) [78]. The low sulfur concentrations combined with the high VS content (46.3%) of GVW, in comparison to DM (8.2% VS), provide more evidence to the dilution effect observed in the study, as previously hypothesized. Since more biogas was produced in the GVW treatments compared to the DM treatments, the relative percent of the biogas attributed to manure in the mixed substrate treatments was lowered, and thus, the relative contribution of H₂S from the manure substrate also decreased. Furthermore, the

contribution of H₂S from GVW was comparatively lower due to its low sulfur content, leading to the overall decrease in H₂S concentrations in the biogas. However, it should be noted that the GVW addition as a co-digestion substrate increased total normalized H₂S production when compared to co-digestion with 0% GVW addition (DM.FW.GW). A co-digestion substrate with negligible S content could have led to further decreases in H₂S concentrations and total yield. Some gummy vitamins are fortified with Fe, but the concentrations seen in this study (4.3 ppm Fe) was lower than the Fe concentrations in food waste (4800 ppm) and unlikely to have affected H₂S production in our study [79].

The sulfurous compounds in the feedstock were primarily utilized during the initial phase of digestion as most of the H₂S was produced within the first 20 days, after which the CH₄ percentage started rising for all treatments. Similar results were also observed by Belle et al. (2015b) when co-digesting different mass fractions of forage radish with dairy manure in BMP experiments [76]. Forage radish has a high sulfur content and increasing the forage radish percentage led to an expected increase in H₂S production initially, but all the treatments had lowered and similar H₂S production by the end of the study. Belle et al. (2015a) also conducted a pilot-scale study on the same substrates and showed an increased rate of H₂S production during the first two weeks of digestion, after which, the concentration decreased by >75% of the maximum H₂S concentration for the remainder of the digestion period (33 days total) [63]. These observations can be attributed to increased SRB activity during the initial digestion phase, as SRBs can outcompete methanogens when the availability of biodegradable sulfur is higher.

2.5 Conclusions:

Results from the BMP study suggested that gummy waste is a potentially valuable co-digestion substrate with dairy manure. The mixture of substrates containing gummy waste, food waste, grease waste, and dairy manure enhanced CH₄ yields compared to digestion of dairy manure alone. The high density of VS and low moisture content of the gummy waste results in high CH₄ yields per gram of the substrate, but due to the slower degradation rate of the GVW, higher retention times may be needed to yield these higher CH₄ potentials. Co-digestion of GVW with dairy manure lowered the H₂S yield compared to mono-digestion of dairy manure due to its low sulfur content. Co-digestion of industrial byproducts and food waste mixtures in farm-scale biogas digesters could provide economic incentives for farmers through tipping fees and increased biogas production while redirecting valuable waste products from landfills.

3 Evaluation of hydrogen sulfide scrubbing systems for anaerobic digesters on two U.S. dairy farms

Abstract

Hydrogen sulfide (H₂S) is a corrosive trace gas present in biogas produced from anaerobic digestion systems that should be removed to reduce engine generator set maintenance costs. This study was conducted to provide a more complete understanding of two H₂S scrubbers in terms of efficiency, operational and maintenance parameters, capital and operational costs, and the effect of scrubber management on sustained H₂S reduction potential. For this work, biogas H₂S, CO₂, O₂, and CH₄ concentrations were quantified for two existing H₂S scrubbing systems (iron-oxide scrubber, and biological oxidation using air injection) located on two rural dairy farms. In the micro-aerated digester, the variability in biogas H₂S concentration (average: 1,938 ± 65 ppm) correlated with the O₂ concentration (average: 0.030 ± 0.004 %). For the iron-oxide scrubber, there was no significant difference in the H₂S concentrations in the pre-scrubbed (450 ± 42 ppm) and post-scrubbed (430 ± 41 ppm) biogas due to the use of scrap iron and steel wool instead of proprietary iron oxide-based adsorbents often used for biogas desulfurization. Even though the capital and operating costs for the two scrubbing systems were low (< \$1500/year), the lack of dedicated operators led to inefficient performance for the two scrubbing systems.

3.1 Introduction:

Hydrogen sulfide (H₂S) is a corrosive gas that can corrode and damage, even in trace quantities, engine-generator sets (EGS) utilizing biogas from anaerobic digestion (AD) for electricity production. The produced H₂S can react with water vapor present in

the biogas producing sulfuric acid, which can cause corrosion. Hydrogen sulfide gases are also toxic to living organisms under certain concentrations and can result in range of adverse health effects. OSHA mandates that the industry acceptable ceiling concentration for human exposure to H₂S is 20 ppm for an 8-hour duration [80]. In some industrial sectors, the total weighted average exposure limit is 10 ppm over 8 hours. The acceptable peak concentration above the ceiling concentration is 50 ppm, but for a maximum time limit of 10 min. Concentrations exceeding 500 ppm in a closed environment can lead to death within 30-60 minutes, while concentrations exceeding 1000 ppm is instantly fatal [15]. Combustion of H₂S also leads to SO_x emissions, which has harmful environmental effects. Anaerobic digesters, used in conjunction with H₂S scrubbers, are effective at controlling odor problems, which is often perceived as an environmental issue by residents living close to dairy farms [81]. For digestion systems with EGS to operate effectively, it is important to remove H₂S from biogas before utilization.

Corrosion from H₂S has led to interrupted operation of farm-based EGS, resulting in increased maintenance costs and decreased revenues [82]. Biogas is a saturated (4-5% moisture content) mixture of 50-70% methane (CH₄), 30-50% carbon dioxide (CO₂), with traces of H₂S (100 – 10,000 ppm; 0.01 to 1%). The variability of H₂S in biogas production and different efficiencies of scrubbers in reducing H₂S in the biogas over time can also affect EGS downtimes and overall lifetime [83,84]. The recommended upper limits of H₂S concentration for energy conversion technologies that use biogas are outlined in Table 3.1.

Table 3.1 Recommended hydrogen sulfide (H₂S) concentration limits for biogas utilization technologies [20,85].

Technology	H₂S limit (ppmv)
Gas Heating Boilers	< 1,000
Combined Heat and Power (CHP)	< 1,000
Fuel Cells	< 1
Natural Gas Upgrade	< 4 (variations among countries)

The two H₂S scrubbing techniques discussed in this study include: 1) biological desulfurization (BDS) of H₂S using sulfur-oxidizing bacteria (SOB) to oxidize H₂S to elemental sulfur and sulfates, which can occur in a separate bio-trickling filter (BTF) or with air injection into the digester headspace, and 2) physical-chemical adsorption and oxidation using iron oxides.

Biological conversion of H₂S results from microbial oxidation in an oxygenated environment. Small concentrations of air (or oxygen) are injected into a biological scrubbing system, such as a BTF, or into the digester headspace [86]. The oxygen is used by SOB, which use H₂S, sulfur, and thiosulfate as their primary energy sources. Schieder et al. (2003) showed 90% reduction in H₂S concentrations (up to 5000 ppm) using BTF-based biogas scrubbers (BIO-Sulfex[®] biofilter modules), which received the produced biogas at flow rates of 10 – 350 m³/hr [16]. A simpler method of BDS of biogas is the controlled addition of oxygen or air directly into the digester headspace, which creates a micro-aerobic environment for H₂S oxidation. However, air injection needs to be carefully controlled in order to prevent accidental formation of explosive gas mixtures of CH₄ and O₂ [81]. With differences based on the temperature, residence time, and the percentage of injected air, there have been full-scale digesters with micro-aeration that

have observed reductions as high as 80 – 99%, reducing H₂S in the biogas from ~ 500 ppm to 20 – 100 ppm [15].

Iron oxide pellets or wood chips impregnated with iron oxide (also known as ‘iron sponge’) can also be used for biogas desulfurization [87]. The iron oxide in the media reacts with the H₂S and is converted into iron sulfide. Iron sponge is the most recognized iron oxide adsorbent in the industry with H₂S reductions >99.9% (3600 ppm to 1 ppm after scrubbing) reported in the literature [15]. The iron sponge adsorbent can also operate in conjunction with a small air flow into the system, along with the biogas input, to promote continuous regeneration. Sulfide removal rates up to 2.5 kg H₂S/kg Fe₂O₃ have been observed in continuously regenerated systems with <1% oxygen input [19]. Proprietary iron oxide scrubbing systems, such as SOXSIA[®], have been shown to remove up to 2000 ppm of H₂S at 40 °C and biogas flow rates of 1000 Nm³/hr in full-scale AD systems (2 m³/hr or 3 kg/hr H₂S removal rate) [20].

A study conducted by Shelford et al. (2019) investigated the performance and economic benefits of two BTF systems on NY farms and found that the total annual cost to own and operate the scrubbers may not justify the capital and maintenance costs of the scrubber systems compared to increasing the frequency of oil changes [82]. It was suggested that longer monitoring periods may be necessary to understand the benefits of H₂S scrubbing on major generator overhauls. The study also highlighted the importance of a dedicated operator for keeping the systems functioning at peak efficiency. A report published on biomethane production in California estimated the cost of an H₂S scrubbing system to be around 10% of the total capital costs [81]. It was also suggested that the use of H₂S scrubbers was dependent on the end-use of the biogas, as more frequent oil

changes (every 300 hours instead of 600 hours) could be sufficient for maintaining EGS health. Even though several H₂S scrubbing technologies exist, there is only limited field-scale data on long-term H₂S removal efficiency, and the costs associated with operating and maintaining a scrubbing system, especially on rural dairy farms in the United States [15].

The objective of this study was to quantify the efficacy and costs associated with H₂S scrubber systems using units on dairy farms with AD systems. Two different H₂S scrubber systems on rural US dairy farms were evaluated through quantification of scrubbing efficiency, capital costs, maintenance costs, and maintenance practices to determine how scrubber management affected the performance of these systems. The results can be used to understand the costs, maintenance requirements, and variations over time for these two H₂S scrubbing systems.

3.2 Methods:

3.2.1 Farm and H₂S Scrubber Information:

The iron oxide scrubber (IOS) on Farm 1, referred to hereon as S_{IOS}, treated biogas from an ambient temperature anaerobic digester with a capacity of 2,574 m³ receiving food waste and the liquid fraction of dairy manure processed through a solid-liquid separator. The unheated digester was exposed to ambient temperatures, which resulted in lower biogas production during winter months. In addition, there was no mixing of the substrate inside the digester. The farm (750 cows) operated a 110-kW engine-generator set for electricity production, with the produced energy used on-farm.

The vessel for the H₂S scrubber was a 208 L plastic drum. PVC piping was used for the connection from the digester to the scrubber and then to the engine generator. The

iron oxide scrubber was filled with rusted scrap iron and steel scrapings (approximately 50% volume of the scrubber system). New media (approximately 25% of the scrubber volume) was added by the farmer after 45 days of monitoring (without cleaning out used media) to increase the efficiency of the scrubbing unit. After 105 days, the media was changed to fresh grade 000 steel wool (252 pads, 4.4 kg) (Homax, Bellingham, WA) to determine if the increased surface area of this material would affect scrubber performance. The scrubber media covered three-quarter of the entire volume (156 L) of the scrubbing unit in order to enhance the contact time between the untreated biogas and the steel wool.

Biogas flow rate from the digester was measured before the biogas passed through the scrubber. There were no condensation traps before the scrubber. The biogas from the digester entered the scrubber from the bottom and flowed through the barrel, passing through the scrubbing media before exiting from the top of the scrubber vessel. A regenerative blower (Gast Regenair Model - R5325R-50, Benton Harbor, MI) installed at the outlet of the scrubber was used to send biogas to the generator. The generator was operated only during the farm operational hours, which averaged 12 hours per day.

The air injection pump for BDS inside the digester headspace on Farm 2, referred to hereon S_{BDS} , was connected to a commercially designed, mixed anaerobic digester. Raw unseparated dairy manure (650 cows) was mixed with solid food waste (discarded produce) and fed into 1,817 m³ capacity digester. Electricity was generated using a 140-kW generator. The digester was heated to 35 °C using the waste heat from the EGS, with electricity sold to the grid. The generator was operated continuously, with breaks in operation for maintenance and repairs only.

The H₂S scrubber system consisted of an air pump that pumped air into the headspace of the digester. The pump (SST10 Aquatic Ecosystems Inc, Pentair, Apopka, FL) was rated at 223 W, 51 Nm³/hr, and single phase (115/230 V). The air pump was set to inject air at a consistent rate of 2.86 m³/hr. A rotameter attached to the air pump, installed by the farmer, was used to measure the flowrate. The installed air pump did not have an automatic air flow regulator to change the airflow according to the amount of H₂S in the biogas. The pipe from the air pump to the digester headspace required regular maintenance to prevent clogs.

3.2.2 Performance Monitoring and Cost Information:

The CH₄, and H₂S concentration was logged for 179 and 73 days for S_{IOS} and S_{BDS}, respectively, and the AD system and maintenance costs were collected for at least one year from each farm. Untreated and treated biogas were analyzed to detect daily and seasonal differences using two portable continuous biogas testing and monitoring systems (Siemens Model # 7MB2337-3CR13-5DR1, Siemens AG, Munich, Germany) for CH₄ (0 – 100 %), CO₂ (0 – 100 %), O₂ (0 – 100%), and H₂S (0 – 5000 ppm), with a Campbell Scientific CR1000 data logger and acquisition system, and gas meters (Model # 9500, Thermal Instrument Co, Trevose, PA; Model #FT2, Fox Thermal, Marina, CA) and assembled as described in Shelford et al. 2019 [82]. The monitoring system were moved and installed at each farm for the study period (73 and 179 days). The Ultramat 23 was capable of an auto-calibration with air every eight hours, with regular monitoring and calibration of the units were conducted according to manufacturer's standards to maintain the accuracy of the H₂S sensors. The monitoring systems collected data for 15 minutes for each biogas stream (pre and post H₂S scrubbing). Operation and maintenance records

of the AD and scrubbing systems was undertaken by the farmers, with records on the time and costs spent on their AD and scrubber system, including oil change costs, generator repair costs, and electrical energy generated over 12 months, if available.

At the end of December 2016, the gas analyzer system installed for project purposes on Farm 2 (S_{BDS}) started malfunctioning and the system had to be removed for repairs, likely due to H₂S corrosion. The on-farm biogas was then field tested using a Landtec handheld gas meter (Biogas 5000, Landtec, Dexter, MI) during farm visits.

3.2.3 H₂S Removal Calculations:

Hydrogen sulfide removal efficiency (η) was calculated using the formula:

$$\eta = \frac{(C_{in} - C_{out})}{C_{in}} \times 100\%$$

where C_{in} and C_{out} (ppm) are the scrubber inlet and outlet H₂S concentrations. The daily mass (grams/day) of sulfur removed (w) was calculated using the formula:

$$w = \frac{(C_{in} - C_{out}) \times 1.5 \times F}{1000}$$

where C_{in} and C_{out} (ppm) are the scrubber inlet and outlet H₂S concentrations and F is the biogas flow rate (m³/day).

3.2.4 Statistical Analysis:

Significant differences in pre- and post-scrubbed CH₄ and H₂S concentrations over time within each farm was determined using t-tests using SAS, with an alpha value set at 0.05. All values are presented as mean \pm standard error.

3.3 Results and Discussion

3.3.1 Iron Oxide Scrubber (S_{IOS}):

The mean H₂S concentrations in the pre-scrubbed and post-scrubbed biogas of S_{IOS} were 450 ± 42 ppm and 430 ± 41 ppm (n=179), respectively, when averaged over the study period (August 2016 – January 2017) (Figure 3.1). The H₂S concentrations in the pre-scrubbed biogas was 740 ± 53 ppm and post-scrubbed biogas was 719 ± 52 ppm (n=85) prior to the media change from scrap iron to steel wool. After the media change, the pre-scrubbed H₂S concentration (52 ± 9 ppm), which was significantly higher (*p*-value < 0.0001) than the post-scrubbed H₂S concentration (33 ± 6 ppm). This rapid decrease (Days 102 – 120) in H₂S concentration is likely due to the temperature drop in the unheated digester at that time. The temperature of the digester effluent dropped from 28.1 °C in August to 10.5 °C in December, which correspond with the ambient temperatures, which averaged 26.1 °C and 3.5 °C, respectively [88]. Sulfate reducing bacteria (SRB), the primary producers of H₂S in anaerobic digesters, have lowered activities at temperatures below 20 °C [89].

The use of scrap iron and unoxidized steel wool as scrubbing media, instead of iron sponge or proprietary iron-oxide based adsorbents resulted in poor H₂S removal efficiencies for S_{IOS}. Dry iron-oxide based adsorbents are the most commonly used and effective scrubbing technique, but can generate a hazardous waste stream [15]. Commercially available iron sponge media can be up to 100% effective, but the use of scrap iron and steel wool as the adsorption media resulted in low H₂S reduction efficiency (3%) for S_{IOS} [19]. Kohl and Nielsen (1997) also reported that wetted iron-oxide based adsorbents are not as effective as chemically hydrated oxides [90]. The steel

wool media and the scrap iron media were not allowed to oxidize before being used for H₂S scrubbing, which could have contributed to the low scrubbing efficiency.

The media replacement to steel wool and the increased residence time due to the lowered biogas flow rates in the winter season resulted in a decrease in the biogas H₂S content even though the pre-scrubbed H₂S concentration was below 100 ppm. The biogas production varied from 1202 m³/d in the summer (June to September, with an average temperature of 28 °C) to 51 m³/d in the winter (January - February, with an average temperature of 10.9 °C) (Figure 3.2). The average biogas flow rate before the media change was 980 m³/d (n=4), which was reduced to 51 m³/d (n=4) due to the temperature drop that coincided with the media change. The residence time of the biogas in the scrubber increased from 0.25 min to 6 min, as the lower winter temperatures led to a sharp decline in the biogas production from the unheated digester. Commercially available iron oxide media usually require 1 – 15 min residence time and could have been more efficient at removing H₂S for S_{IOs}, especially during the summer months [19]. Zicari (2003) reported that a farm digester (capacity - 554 m³) with an average biogas production of 669 m³/d could reduce H₂S concentrations from 3,600 to <1 ppm, with a 4,200 L iron oxide scrubber with a bed height of 240 cm [15]. The S_{IOs} volume was 208 L with an empty bed height of 88 cm (66 cm media height), with 4.2 kg of steel wool. The low adsorption efficiency seen in this study was affected by the high volume of biogas passing through the scrubber compared to the scrubber size. The total volume of biogas passing through the scrubber from Aug – Nov 2016 was 119,000 m³, with 3.8 kg of H₂S removed from the biogas through the scrubber. After the media replacement with steel wool, a total of 1,800 m³ of biogas flowed through the scrubber in 36 days, with 68

g of H₂S removed. The low sulfur removal was likely due to the low concentrations of H₂S present in the biogas coupled with the comparatively low effectiveness of the fresh steel wool. Iron oxide-based adsorbents have been shown to remove 0.56 kg H₂S/kg adsorbent in a batch system, with a recommended bed height of 120 – 300 cm [90]. Based on the results from the study, the steel wool had an adsorption capacity of 0.016 kg H₂S/kg steel wool, which is an order of magnitude lower than the adsorption capacities of commercially available dry iron oxide-based sorbents.

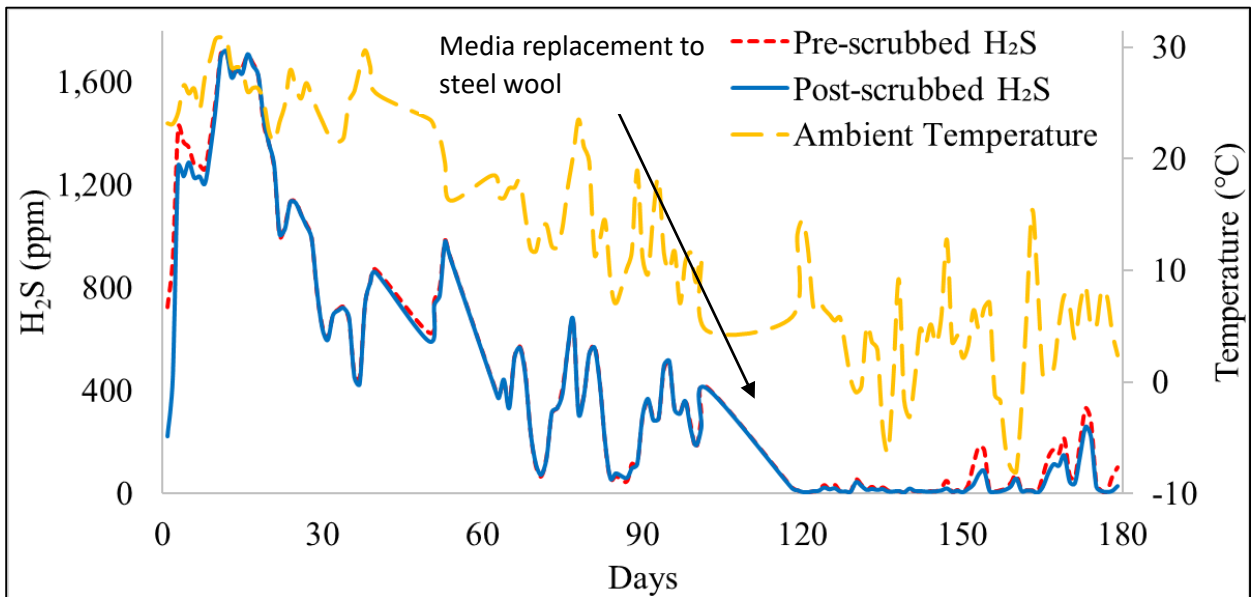


Figure 3.1 Hydrogen sulfide (H₂S) concentrations in the biogas from the iron oxide scrubber (S_{IOS}), with scrubber media replacement to steel wool after 105 days (mid-November).

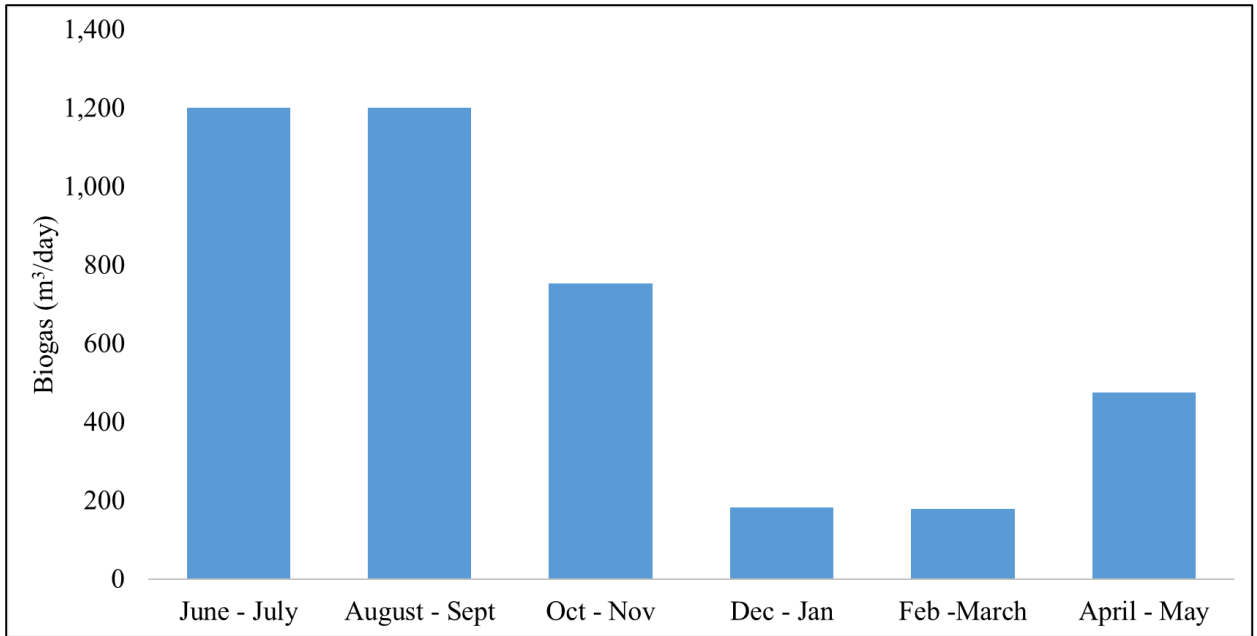


Figure 3.2 Average daily biogas production over two month period from June 2016 to May 2017 in the AD system with the iron oxide scrubber (S_{IOS}).

During the study period, the average CH₄ content in the pre-scrubbed biogas was $64.1 \pm 0.2\%$, with $64.9 \pm 0.2\%$ CH₄ in the post-scrubbed biogas (Figure 3.3). The average CH₄ production rate calculated using the biogas production data over one year (June 2016 to May 2017) was 432 m³/d or 0.58 m³/cow-day. The CH₄ production rate from a mesophilic dairy manure AD system can vary from 1.5 m³/cow-day to 3.9 m³/cow-day [91]. As the AD system in this study was not heated, the average CH₄ yield was below this average range.

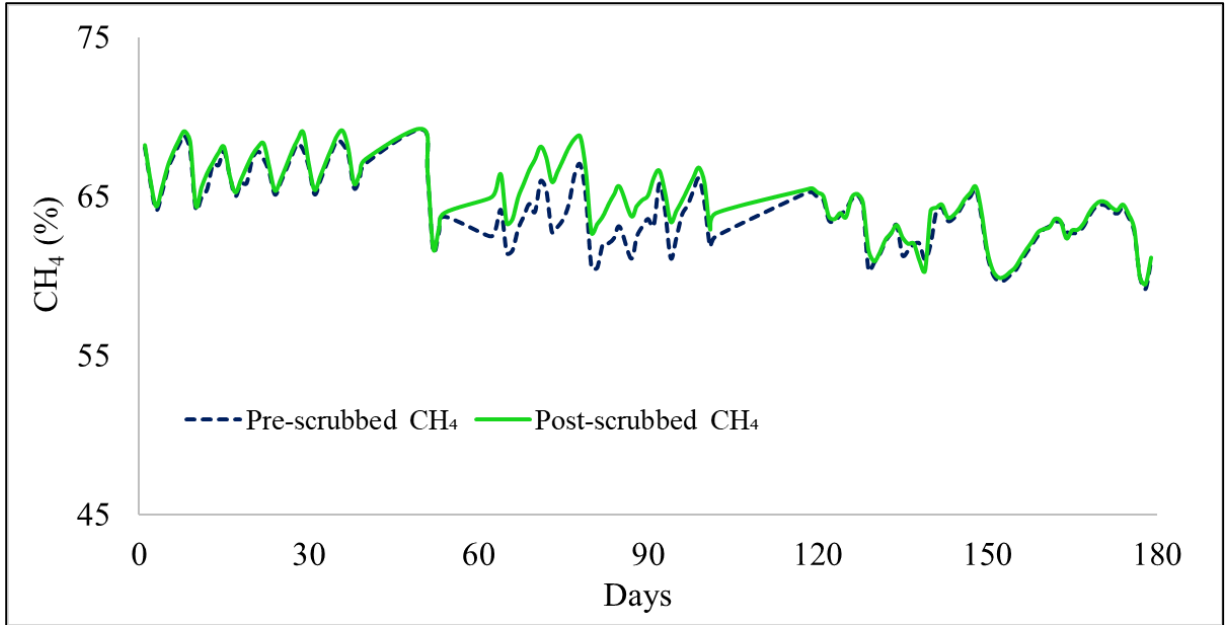


Figure 3.3 Daily average pre-scrubbed and post-scrubbed CH₄ concentration in biogas produced from the AD system with the iron oxide scrubber (S_{IOS}).

The generator produced a total of 47,158 kWh of electrical energy from the produced biogas from August to December 2016 (131 days), resulting in a daily average rate of 380 kWh/d. The engine generator stopped functioning in December 2016, but the exact reason for generator failure was not determined. The generator was not run continuously, and daily runtime varied every day. Typically, it was switched off during the night, and there were additional periods of downtime during the day. On average, it was estimated that the generator operated 12 hr/d. From June to December 2016, the biogas flow rate was continuous during the operational hours, with the regenerative blower supplying the biogas to the generator. The average daily CH₄ production during the monitoring period of generator activity was 542 m³/d. The electricity generated from the

biogas was $0.70 \text{ kWh/m}^3 \text{ CH}_4$, but the flare was not metered, so the actual value may be lower than estimated.

3.3.2 In-vessel biological desulfurization system using air injection (S_{BDS}):

Overall, biogas H₂S concentrations (average: $1,938 \pm 65 \text{ ppm}$; $n=73$) varied considerably during the study period from 171 to 3,327 ppm, but the CH₄ ($56.2 \pm 0.1\%$) and O₂ concentrations ($0.030 \pm 0.004 \%$) were consistent (October to December 2016). Correlations between the H₂S, CH₄, and O₂ were also observed, as expected (Figures 3.4 and 3.5). In mid-October (Day 7), the H₂S concentration decreased to 171 ppm, while the O₂ concentration rose to 0.51%, and the CH₄ concentration dropped to 50%, likely due to nitrogen (N₂) introduced into the biogas stream with air injection. It is likely that once the oxygen was depleted, further oxidation did not take place, and the H₂S concentration increased (after Day 9). Schieder et al. (2003) reported that micro-aeration by itself may not be sufficient to achieve complete desulfurization [16]. They collected data from biogas plants in the state of Baden-Württemberg in Germany and found that 54% of the micro-aerated AD systems had outlet H₂S concentrations $> 500 \text{ ppm}$. They suggested the use of an external biological scrubber to achieve outlet H₂S concentrations of $< 100 \text{ ppm}$ and increase the life of CHP units and decrease the frequency of oil changes. In practice, digester manufacturing companies in the US have recommended limits of 500 ppm H₂S in the biogas [82]. The variable H₂S concentrations during the study period indicated variable treatment efficiency. The O₂ concentration was not always sufficient for adequate H₂S removal ($< 500 \text{ ppm}$) throughout the period after the initial rise to 0.51%

O₂. The O₂ concentrations increased to 0.07% in mid-December for a short duration, which correlated with a decrease in the H₂S concentration from 2,596 to 1,645 ppm.

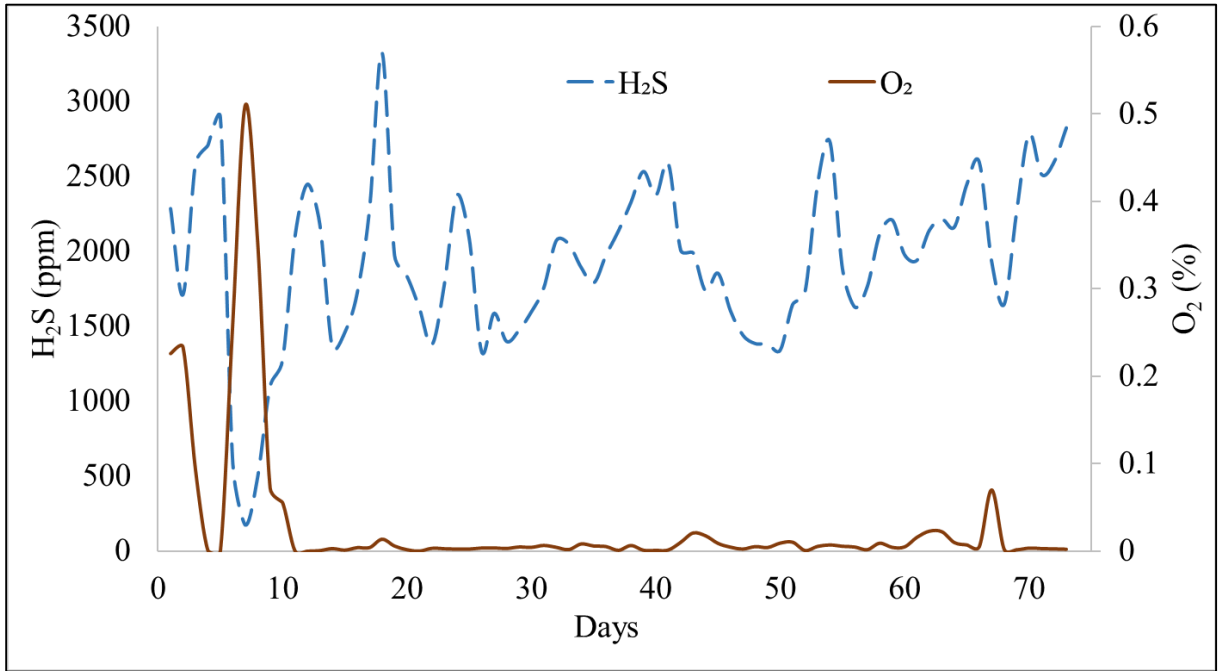


Figure 3.4 Hourly H₂S and O₂ concentrations in the biogas from the AD system with in-vessel biological desulfurization (S_{BDS}).

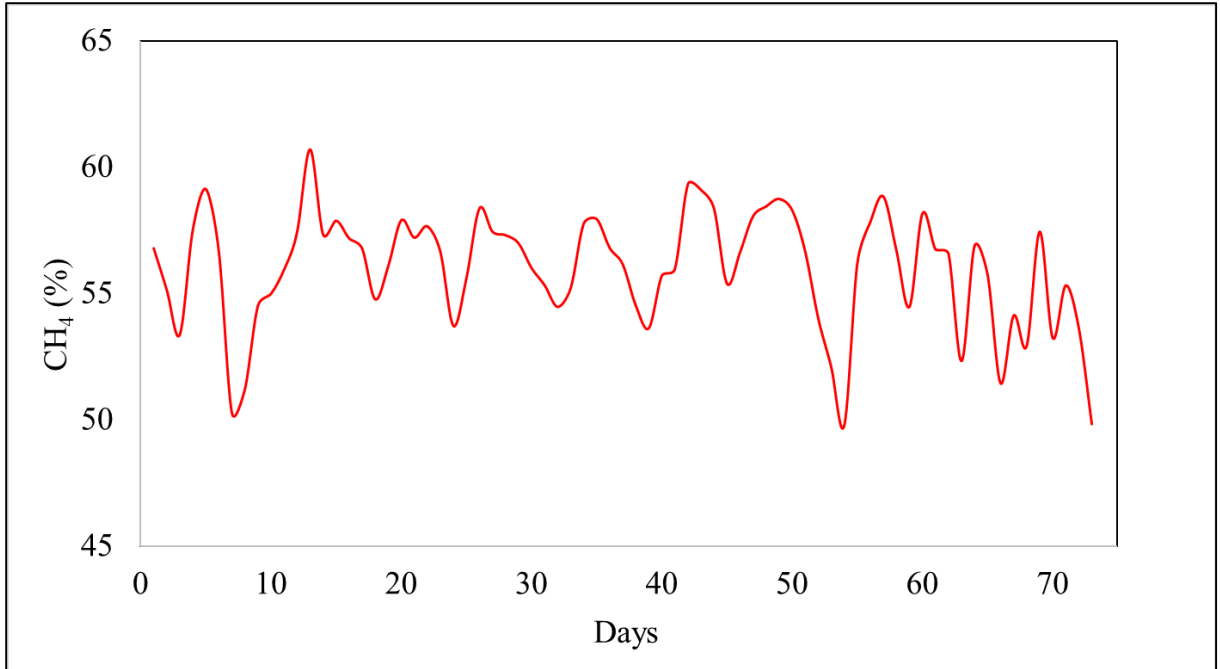


Figure 3.5 Hourly biogas CH₄ concentrations from the AD system with in-vessel biological desulfurization (S_{BDS}).

Ramos et al. (2013) showed that an outlet H₂S concentration of < 200 ppm can be obtained with low O₂ (0.2 – 0.3%) concentrations in the output biogas [21]. The O₂ utilization efficiency for H₂S oxidation by the SOB increased with a decrease in the O_{2input}/H₂S_{initial} ratio. Mulbry et al. (2017) also showed that an outlet H₂S concentration of <100 ppm can be obtained with 0.5% O₂ in the output biogas [92]. In S_{BDS}, the average outlet O₂ concentration was much lower (0.03%), as the air input was set at 2.86 m³/hr (2.75% of the average biogas flow rate), resulting in an average O₂ input of 0.58%. An increase in the air injection rate could have decreased H₂S concentrations further, but at the cost of lowering CH₄ concentration due to N₂ dilution. The AD operator decided against increasing the air injection rate, because the CH₄ concentration fluctuated between 50 – 55%, and generator efficiency can be affected if the CH₄ concentration,

with, a CH₄ concentration of < 50% unsuitable for most CHP generators due to significant decreases in energy production efficiency [15, 16]. In such cases, a pure O₂ input may be desirable over air injection, but at a higher cost.

A constant air flow rate could have reduced the desulfurization efficiency in the digester headspace. A variable air flow rate based on the H₂S production can ensure sufficient desulfurization to meet recommended limits for heating or electricity production while minimizing N₂ dilution [22]. Ramos and Fdz-Polanco (2014) used a PID (proportional-integral-derivative) controller to vary the O₂ flow rate to meet the set output H₂S concentrations. The O₂ input was controlled using two methods: H₂S content in the biogas, and biogas production rate, and in both cases >99% removal of H₂S was obtained [93]. The ORP (oxidation-reduction potential) of the liquid wastewater was used by Khanal and Huang (2006) as a parameter to control the injection rate to prevent underdosing/overdosing of O₂ [94]. However, instead of adding O₂ directly into the headspace, the authors injected it into the outlet of the reactor that contained a mixture of both biogas and the digester effluent. The resulting mixture was then sent to a separate sulfur oxidizing unit to separate the biogas, the effluent, and the elemental sulfur produced by the SOB. The method was able to reduce >99% of the total dissolved and gaseous sulfides for a range of initial dissolved sulfide concentrations (287 mg/L – 1997 mg/L). However, using ORP as a controlling parameter could be unreliable, as each AD system is different and a set standard for an ORP increase may not be appropriate [22]. Addition of O₂/air into the digester liquid could also lead to degradation of organics in the digestate and therefore, a higher dose of air/O₂ may be required for adequate H₂S removal [95].

Another factor that could have affected the desulfurization efficiency is the excess formation of sulfur mats in the digester headspace. The digester headspace was never cleaned, and therefore, large-sized elemental sulfur particles would drop back into the digester, along with the formation of sulfur laden biofilms on the liquid surface [92]. Sulfate reducing bacteria are also known to use elemental sulfur as an energy source for H₂S production [13]. The accumulation of oxidized sulfates and elemental sulfur can be reduced again by SRB and can lead to increased H₂S concentrations in the biogas [96]. External vessels used by Ramos et al. (2013) and Mulbry et al. (2017) that can be cleaned on a regular basis have been suggested as a better alternative to prevent reduction of the accumulated sulfates and sulfur [21,92]., which resulted in a steady CH₄ production rate within the range for mesophilic digesters (1.5 m³/cow-day to 3.9 m³/cow-day) [91]. The farm averaged 2,003 m³/d of biogas flow through the generator (1,125 m³/d or 1.73 m³/cow-day CH₄ yield) and produced 689,656 kWh of electricity in 10 months at a rate of 1.95 kWh/m³ CH₄ combusted. The average rate of electricity production was 2,196 kWh/d. The average biogas flow rate was affected by the generator malfunction during the last 3 weeks of data collection (Figure 3.6).

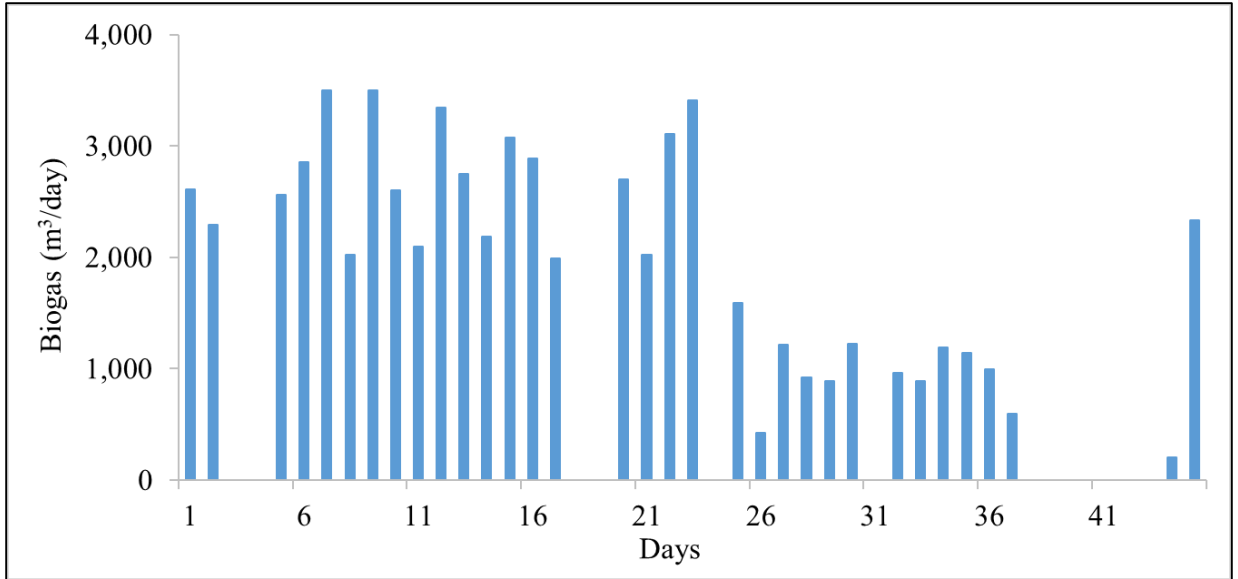


Figure 3.6 Daily biogas production (m³/day) through the generator, operating on the farm with S_{BDS}, for electricity production.

3.3.3 Economic Analysis:

The total cost of the scrubber systems was calculated using data provided by the farm owners. The total capital cost of the iron oxide scrubber system (S_{IOS}) was approximately \$525 based on the reactor vessel and piping costs, as this was a homemade system. All the maintenance was conducted by the farm owner, and the labor costs were considered negligible. Additionally, scrap iron (\$25 cost) was added by the farmer once during the study. Steel wool media cost \$80 to fill the space within the scrubber. The replacement media for the scrubber was calculated to be \$650/year with original iron scrap based on 26 media replacements per year and \$960/year with grade 000 steel wool based on 12 media replacements per year. Approximately, \$450/year was required for oil changes as one liter of oil was added to the generator every other day (183 L/yr). The total cost to own and operate the scrubber was \$1,100 (with iron scrap media) and \$1,410

(with grade 000 steel wool). Generator maintenance and repair can add significant costs as well, but no information was available for generator repair costs.

The total capital cost of S_{BDS} was approximately \$450 for the air pump for air injection into the digester headspace. Scrubber maintenance was carried out by cleaning out the air injection connection into the digester on a weekly basis. This was estimated to take 20 minutes per week and cost the farm \$120/year in labor costs (~\$10/week at \$30/hr.). Oil change costs ranged from \$1,190 to \$1,795 per month and additional costs during a month were for generator repairs. The farm owner spent \$10,798 for oil changes and repairs to the generator engine head in April 2017. One of the primary reasons for the lower costs of oil change for S_{IOS} was the lower average H_2S concentrations (430 ppm) compared to S_{BDS} (1,938 ppm).

Zicari (2003) tabulated data for different proprietary iron-oxide based adsorbents, where the capital costs ranged from \$8,000 - \$43,600 and the operating costs ranged from \$8,290 to \$23,840 for a biogas stream with 4,000 ppm of H_2S and a gas flow rate of $1,350 \text{ m}^3/\text{d}$, which is comparable to the average daily biogas flow rates for both farms in this study [15]. These cited costs were much lower than the costs associated with owning and operating the BTF units in the study conducted by Shelford et al. (2019) [82]. The operational, maintenance and utilities costs for BTF systems in their study ranged from \$17,050 for farm 2 to \$32,563 for Farm 1, which are comparable to the operational costs of iron oxide scrubbers, but the capital costs were at least four times higher. The proprietary iron-oxide scrubbers examined by Zicari (2003) had high H_2S removal efficiencies and low H_2S output concentrations (up to 100% and less than 1 ppm) compared to the lower efficiencies (80.1% and 94.5%) and higher H_2S output

concentrations (450 and 150 ppm) seen in the study by Shelford et al. (2019) [19,82]. However, on larger farms, the operating costs associated with iron oxide scrubbers may be much higher due to the larger volume of biogas to be treated and the higher handling and disposal costs of the spent media [19]. When the costs were normalized on the basis of volume of biogas treated, the costs were comparable, with iron-based adsorbents costs ranging from \$0.024 – 0.046 per m³ of biogas treated and BTF systems costs ranging from \$0.012 – 0.03 per m³ of biogas treated [15,19,82].

Shelford et al. (2019) also calculated the economic benefits of having a BTF scrubbing system by calculating the savings associated with less frequent oil changes after scrubber installation [82]. The farms reported a net annual loss of \$61,593 for BTF 1 and \$30,093 for BTF 2, which may be economically infeasible for smaller farms, especially during low milk price cycles in the US.

The results and observations from this study and Shelford et al. (2019) study showed that even though H₂S scrubbing system existed on all four farms studied, consistent performance was lacking in the inexpensive systems analyzed in our study. Both S_{BDS} and S_{IOS} had significantly lower capital and operating costs than the two BTF systems, but it is unclear if the farmers realized any economic or social benefits from these two H₂S scrubbing systems during the study period. It is also difficult to calculate monetary benefits of having the scrubbing systems, since there was no information available on oil changes prior to scrubber installation and the highly inefficient performance of the scrubbing systems. Table 3.2 shows the cost information of the BTF units from Shelford et al. (2019) in comparison to the scrubbing systems monitored in this study.

Table 3.2 Capital and operating cost summary of different scrubbing technologies in Northeast US.

Scrubber Type	Iron Oxide Scrubber (Sios)	In-vessel biological desulfurization (SBDS)	Bio-trickling filter 1*	Bio-trickling filter 2*
Farm Size	750 cows	650 cows	4,200 cows	1,500 cows
Generator Capacity	110 kW	140 kW	1,000 kW	500 kW
Scrubber System Capital Cost	\$525	\$450	\$342,000	\$185,000
Annual Labor, Cleanout Costs	N/A	\$0	\$10,323	\$4,340
Annual Generator Maintenance Costs	\$450	\$28,708	N/A	N/A
Annual Scrubber Maintenance Costs	\$960 [#]	\$120	\$8,900	\$9,400

*values obtained from [82].

[#]Annual scrubber maintenance costs with steel wool as the scrubbing media

3.3.4 Scrubber management:

An important factor to consider for efficient scrubber operation is scrubber management by farm or AD operators. H₂S management on agricultural digesters has lagged behind municipal and industrial digesters due to limited funding [92]. Hiring full-time operators for ensuring efficient scrubber performance can lead to unaffordable operating and labor costs, especially for farm owners with AD systems.

Changing the iron-oxide media after saturation is a labor-intensive process due to a need for careful handling of the saturated media [19]. Without proper monitoring of biogas quality, it is also impossible for farmers to know when to replace the saturated

media or ascertain if biological conversion of H₂S is occurring in the digester headspace. Portable biogas quality monitoring equipment used in the study cost \$17,000 and required technical expertise for regular calibration and H₂S sensor replacements every 3-6 months for accurate data collection. The farm with in-vessel biological desulfurization (S_{BDS}) had previously installed an external BTF to work in conjunction with the in-vessel micro-aeration. The BTF unit was abandoned for several years after the farmers encountered operational issues that they could not troubleshoot. It is important for manufacturers to provide on-field assistance for the maintenance of these systems for several years after it is purchased. In addition, one of the farms in the Shelford et al. (2019) study had a dedicated operator, and the H₂S scrubbing efficiency was 94.5%, whereas, the other farm had multiple personnel acting as temporary operators for the BTF unit, which contributed to the H₂S scrubbing efficiency dropping to 80.1% (Table 3.3) [82]. S_{IOS} and S_{BDS}, in this study, did not have dedicated operators maintaining the scrubbing systems, and monitoring H₂S concentrations in the scrubbed biogas. As a result, the scrap iron media for S_{IOS} was not replaced upon saturation and it was impossible to determine the effectiveness of the media, leading to poor performance of the system (3% removal efficiency). In the case of S_{BDS}, regular maintenance of the air flow lines to prevent flow obstruction, and appropriate modification of the air flow rates could have resulted in a lower H₂S concentration in the biogas.

Table 3.3 Performance summary of two different scrubbing technologies in Northeast US.

Scrubber Type	Iron Oxide Scrubber (S_{IOS})	In-vessel biological desulfurization (S_{BDS})	Bio-trickling filter 1*	Bio-trickling filter 2*
----------------------	--	---	--------------------------------	--------------------------------

Average Untreated H ₂ S (ppm)	450 ± 42	N/A	2,640 ± 5.85	2,350 ± 5.67
Average Treated H ₂ S (ppm)	430 ± 41	1,938 ± 65	150 ± 1.84	450 ± 3.42
Overall removal Efficiency (%)	3.0	N/A	94.5	80.1
Avg. Mass of H ₂ S removed (kg/hr)	0.0009	N/A	2.37	0.35
Engine-Generator Capacity Factor	N/A	0.76	0.93	0.68

*values obtained from [82].

In a detailed report compiled by Lusk (1998), it was shown that AD operators faced a multitude of problems caused by high H₂S content in biogas [97]. Currently, managing H₂S in biogas is still an issue, as seen from our study results. Based on interaction with the participating farmers operating the AD systems, frequent EGS oil changes to reduce corrosion instead of managing the H₂S scrubbing system was considered to be a more practical solution. Libarle (2014) found that most AD technology adopters encountered operational and maintenance issues due to a lack of training and scientific understanding of the processes involved [98]. Similar issues were observed during this study, as the farm owners of the S_{IOS} and S_{BDS} systems encountered several hurdles while trying to increase the H₂S scrubbing efficiencies of their underperforming systems. In addition, the rural locations of the farms limit access to consultants and AD experts capable of aiding farmers facing challenges from elevated H₂S concentrations in the biogas. There seems to be a need for increased assistance (education and outreach workshops, free biogas monitoring services, etc.) to impart more technical knowledge to the farm owners and offset some of the costs involved in managing and maintaining these systems.

3.4 Conclusions:

The in-vessel air injection system for biological desulfurization had a low capital and time investment, with positive but inconsistent H₂S removal efficiencies. The iron-oxide scrubber also had a low time and labor investment, but little to no H₂S removal efficiencies. The use of the appropriate scrubbing media (commercially available iron oxide or iron sponge) for increased reactivity and contact area, instead of scrap iron and steel wool could have increased the scrubber performance. The study also showed a substantial effect of scrubber operation and management on its performance. H₂S scrubber systems that were better managed with more time and labor investment have shown more efficient and consistent scrubbing performance. Future studies should quantify and incorporate long-term costs (5+ years) associated with engine overhauls, down-times, repairs, etc. undertaken due to H₂S related damage to better understand the economic benefits of H₂S scrubbers.

4 Adsorption of hydrogen sulfide (H₂S) in biogas on iron-impregnated biochar

Abstract:

Hydrogen sulfide (H₂S) in biogas is produced during anaerobic digestion of organic wastes and can lead to corrosion of generators used for energy production. Recently, there has been an interest in utilizing biochar as a substitute for activated carbon to adsorb and remove H₂S from biogas. The effect of iron (Fe)-impregnation in corn stover biochar (CSB) and maple wood biochar (MB) on H₂S adsorption capacity was investigated using dynamic breakthrough experiments to determine the length of time that reduced H₂S concentrations could be sustained with each substrate. Activated carbon (AC) was used as a control treatment to compare its performance to Fe-impregnated and raw CSB and MB. Iron impregnated maple biochar (MB-Fe) had the highest sorption capacity for sulfur (16.8 ± 0.6 mg S/g biochar), and CSB had the lowest (1.67 ± 0.4 mg S/g biochar). Fe-impregnation increased the sorption capacity by a factor of 1.9 for Fe-impregnated corn stover biochar (CSB-Fe) (3.19 ± 0.6 mg S/g biochar) compared to CSB and by a factor of 4.3 for MB-Fe compared to MB (3.93 ± 0.2 mg S/g biochar). Fe-impregnation also led to a higher H₂S adsorption capacity for MB-Fe compared to AC (3.93 ± 0.3 mg S/g biochar) by a factor of 4.3. The presence of iron oxide (Fe₃O₄) observed through X-ray diffraction and scanning electron microscopy in the Fe-impregnated biochars resulted in the formation of ferrous sulfate (FeSO₄) as the major crystalline product on the Fe-impregnated biochar surface.

4.1 Introduction:

Biogas produced from anaerobic digestion (AD) consists of 55 - 70% methane (CH_4), which can be used as a source of renewable energy but also contains carbon dioxide (CO_2) (30 - 45%) and traces of hydrogen sulfide (H_2S) (0.01 – 1%) [99]. H_2S can corrode piping, mixing motors, and electric generator sets that convert CH_4 into electricity. Market available solutions to reduce the high H_2S concentrations in biogas can have high capital costs, operating costs, and/or unpredictable efficiencies [82,100]. A possible alternative could be the use of a carbon-based adsorbent (biochar or activated carbon) to capture H_2S from biogas in an external scrubbing column [100].

Biochar is produced through thermal degradation of biomass under an oxygen-starved environment (pyrolysis) or in a low oxygen environment (gasification) at temperatures less than 700 °C [27]. It is a carbonaceous solid with an energy density (18 MJ/kg) similar to pulverized coal [28]. Biochar can be regarded as a precursor to activated carbon, which requires a further activation step using either steam or chemicals. The activation step is intended to increase the surface area for use in industrial processes, such as filtration/adsorption [29]. In addition to the activation step, differences in biochar and activated carbon arise from the raw material used for preparation and its end use. Biochar is predominantly prepared from biomass sources, while activated carbon can be prepared from both coal and biomass sources [101]. The primary role of activated carbon is adsorption of pollutants and contaminants, while the end use of biochar was primarily envisioned as a soil amendment [29]. However, recent research has focused on the adsorption capabilities of biochar. Activated carbon has been used as an adsorbent for H_2S in biogas after dosage of iron chloride (FeCl_3) into the digester for enhanced

desulfurization (<10 ppm), as only FeCl₃ dosage did not achieve low and stable H₂S concentrations [20]. Biochar could be seen as a cheaper scrubbing solution, as there are a variety of raw waste materials that could be used, and the production of biochar below 700 °C is more energy-efficient and less cost-intensive than activated carbon production [27]. The lower preparation temperatures of biochar in comparison to activated carbon, and no requirement of any activation steps has shown that biochar (\$0.35 - \$1.2/kg) is comparatively cheaper than powdered activated carbon (\$1.1 - \$1.7/kg) [101].

There has been limited investigation into H₂S removal from biogas using biochar, with prior work showing that surface properties of the biochar were an important parameter in the effectiveness of biochar in removing H₂S [32,33,35]. Shang et al. (2013) prepared biochar from camphor, bamboo, and rice hull and compared H₂S removal efficiencies to activated carbon and found higher adsorption of H₂S on the biochar surface compared to activated carbon, with the H₂S removal efficiency increasing as the pH of the biochar increased. The authors hypothesized that the low pH of activated carbon compared to biochar and the formation of sulfuric acid on its surface were the primary reasons for its lower adsorption capacity. However, the study used a H₂S concentration of 50 ppm, while the concentration of H₂S in most dairy manure digesters vary from 600 ppm – 8,000 ppm [82]. Xu et al. (2014) and Kanjanarong et al. (2017) used manure-derived biochar and mixed-wood derived biochar, respectively, for H₂S adsorption and achieved >97% removal efficiencies for concentrations varying from 100 – 10,000 ppm [33,35]. Both studies highlighted that the alkaline nature of the biochar was an important factor for the high removal efficiencies, but they did not specifically

investigate the reaction behavior of H₂S with biochar samples having an acidic surface pH to determine if it is necessary for biochar to be alkaline in nature, for H₂S adsorption.

The catalytic activity and selectivity towards sulfur have been reported to be improved by impregnation of transition metal salts, such as iron (Fe), copper (Cu), and zinc (Zn), in activated carbon, which enhanced H₂S adsorption capacities with only a small additional cost [102,103]. Carbon-based adsorbents impregnated with metal salts from aqueous solutions have been shown to increase selectivity towards acidic gases. Impregnation of activated carbon with FeCl₃ was shown to improve the H₂S adsorption capacity by 14% [104]. However, the authors conducted the experiments at elevated temperatures (400 °C) using H₂S concentrations of 100 ppm. Biochar impregnated with Fe salts has been used to remove toxic heavy metals, such as arsenic and chromium, from aqueous solutions [46,47]. However, to the best of our knowledge, there has not been a study on the use of Fe impregnated biochar for gaseous H₂S adsorption at room temperatures.

The objective of this research was to study the effect of iron impregnation on the performance of corn stover biochar (CSB) and maple wood biochar (MB) for H₂S adsorption from biogas. It was expected that the increase in iron content in the biochar would enhance the adsorption of H₂S through catalytic oxidation [100,105]. The maximum adsorption capacity and breakthrough time were evaluated using a dynamic breakthrough experiment using biochar in a packed column to remove H₂S (1000 ppm) from biogas. Additionally, the biochar was characterized using pH, ash content analysis, X-ray powder diffraction (XRD), N₂ adsorption isotherms for Brunauer–Emmett–Teller (BET) surface area, elemental analysis, and scanning electron microscopy with energy

dispersive X-ray spectrometry (SEM-EDS) to further understand removal mechanisms. Activated carbon (AC) was used as a control treatment to compare its performance to iron-modified and unmodified biochar from CSB and MB.

4.2 Methods:

4.2.1 Biochar Characterization:

The two types of biochar (CSB and MB) were prepared through pyrolysis under an inert O₂-free atmosphere (using N₂ gas) at a final temperature of 500 °C. After the final reactor temperature was attained, the material was held at that temperature for 10 mins (ArtiCHAR, Prairie City, Iowa, USA). The corn stover was obtained from Iowa State University's BioCentury research farm, ground with a hammermill equipped with a 1/2" screen, and dried to less than 15% moisture. The maple wood biochar was prepared from maple sawdust that was previously debarked and ground using a hammermill with a 1/4" screen. Activated carbon was obtained from a commercial supplier (Darco G-60, Fisher Scientific, USA). The corn stover biochar and the maple biochar was chosen to help understand the effect of the differences in the biochar characteristics (surface area, pore volume, mineral content) on H₂S adsorption as CSB was prepared from an herbaceous material and MB was prepared from a woody material.

Nitrogen adsorption isotherms were measured at 77 K (-196.15 °C) using a BET surface area analyzer (ASAP2020 Micromeritics, Norcross, GA, USA) for the biochar samples. The samples were heated to 150 °C and degassed under a vacuum of <5 µm Hg for six hours. The adsorption isotherms were used to calculate the specific surface area, S_{BET} (BET method) in the range of 0.1 < p/p₀ < 0.55, and micropore volume S_{micro} (t-plot Method). The topographic analysis and qualitative elemental composition of the biochar

surface before and after Fe-modification, and before and after H₂S saturation, were conducted using SEM-EDS with a magnification range between 2000x and 10000x using a XEIA3 FIB-SEM (Tescan, Czech Republic). The powder XRD patterns of the raw, Fe-impregnated and H₂S saturated biochar were recorded using Bruker D8 Advance Powder X-ray Diffractometer (Billerica, MA, USA), over a scanning interval (2θ) from 5° to 90° with CuK α radiation ($\lambda = 1.54 \text{ \AA}$). The carbon (C), hydrogen (H), nitrogen content (N), and metal analysis (including heavy metals) of the raw and Fe-impregnated biochar were conducted at Soil Control Labs Inc, California, using dry combustion for C, H, N, and EPA methods (EPA3050B/EPA 6010, 6020) for metals. Biochar pH was measured as described by Rajkovich et al. (2011) [106]. Briefly, 10 g of biochar was mixed with 200 mL (1:20 ratio) of deionized water and the solution pH was measured after the slurry was mixed for 90 mins. The ash content was measured by drying 25.0 g of biochar at 105 °C and combusting the dried sample at 550 °C and weighing the ash product.

4.2.2 Iron impregnation procedure:

For impregnation, 10.0 g of biochar was mixed with a solution containing 0.97 grams of hydrated iron chloride (FeCl₃.6H₂O) in 200 mL deionized water. The slurry was mixed using a magnetic stirrer for 48 hours and then dried in an oven for 24 hours at 105 °C. The dried composites were rinsed three times with deionized water to remove contaminants that can easily leach out and then dried overnight at 105 °C [47]. The Fe-impregnated corn stover and maple biochars were abbreviated as CSB-Fe and MB-Fe, respectively.

4.2.3 Experimental set-up for dynamic breakthrough study:

The experimental set-up is shown in Figure 4.1. In order to promote chemical adsorption along with physical adsorption, the moisture content of the biochar and activated carbon samples were increased to 25% by adding deionized water [33,35]. The samples were packed into a vinyl tube (25.4 mm internal diameter, 200 mm height) strapped to steel rods using zip ties to keep it vertically oriented and plugged using rubber stoppers at the top. An air diffuser was connected to the bottom of the tube to ensure uniform distribution of biogas. The experiment was conducted at room temperature (25 °C) in triplicate where 3 g of each adsorbent was packed up to a height of 75 mm in each column. Each triplicate run tested one of five adsorbents used in the study (CSB, MB, CSB-Fe, MB-Fe and AC). Prior to entering the column, the biogas passed through a biogas humidification system to ensure a low, constant moisture in the biogas tested (25% relative humidity). Although biogas from an AD system is usually fully saturated with moisture, the 25% relative humidity of the biogas maintained the biochar moisture content at 25% over the study period. Sampling points near the inlet and outlet of the column were added to measure the H₂S concentrations before and after treatment. The biogas flow rate was kept constant at 100 mL/min using mass flow controllers (MCS-1SLPM-D/5M, Alicat, USA). The outlet H₂S concentrations were tested hourly, and the adsorption capacities were calculated from the data obtained when the outlet concentration of each reactor exceeded 500 ppm, as most biogas operated engine generator sets have an upper H₂S tolerance limit of 500 ppm [82]. In order to keep the influent H₂S concentrations constant, synthetic biogas containing 1000 ppm H₂S, 40% CO₂, and 59.9% CH₄ (Airgas, Air Liquide, France) was used for the experiment. Biogas

samples at the inlet and outlet sampling ports were collected in 500 μL syringes and tested on an Agilent 7890 gas chromatograph (Agilent, Santa Clara, USA) using a thermal conductivity detector (TCD) at a detector temperature of 250 $^{\circ}\text{C}$ and the oven temperature at 60 $^{\circ}\text{C}$ with helium as the carrier gas. The adsorption capacity was calculated using the formula [107]:

$$\frac{x}{M} = \frac{QM_w}{\omega V_m} (C_i \cdot t_s - \int_0^{t_s} C(t) dt) \quad (4.1)$$

In equation 4.1, x/M is the adsorption capacity (mg/g of sorbent), Q is the inlet flow rate (m^3/s), M_w is the molecular weight of H_2S (g/mol), ω is the weight of biochar in the column (g), V_m is the ideal gas molar volume (L/mol), C_i is the inlet concentration (ppm), t_s is the saturation time (s), and $C(t)$ is the outlet H_2S concentration at time = t . The integral was calculated using experimental data and numerical methods and input into the equation to find the adsorption capacity.

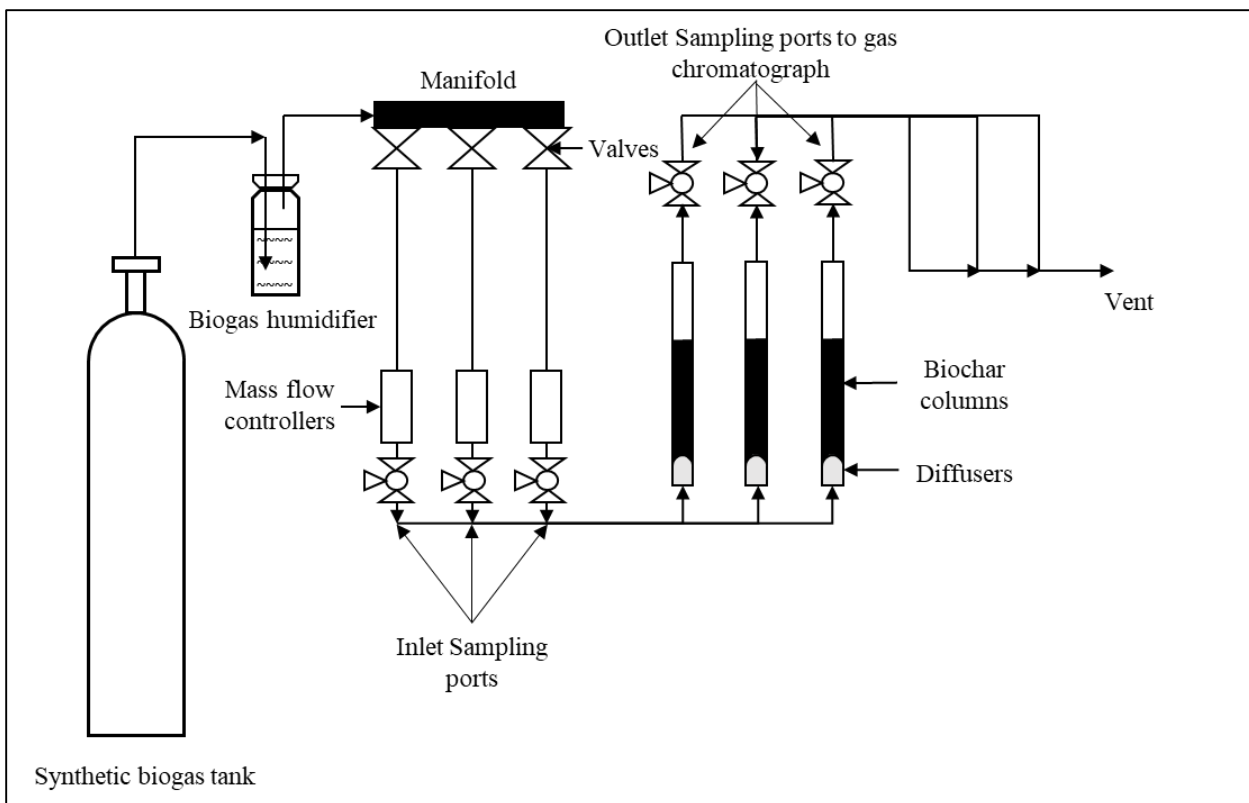


Figure 4.1 Laboratory set up for evaluating the efficiency of H₂S adsorption using biochar

4.3 Results and Discussion:

4.3.1 Characterization of biochar:

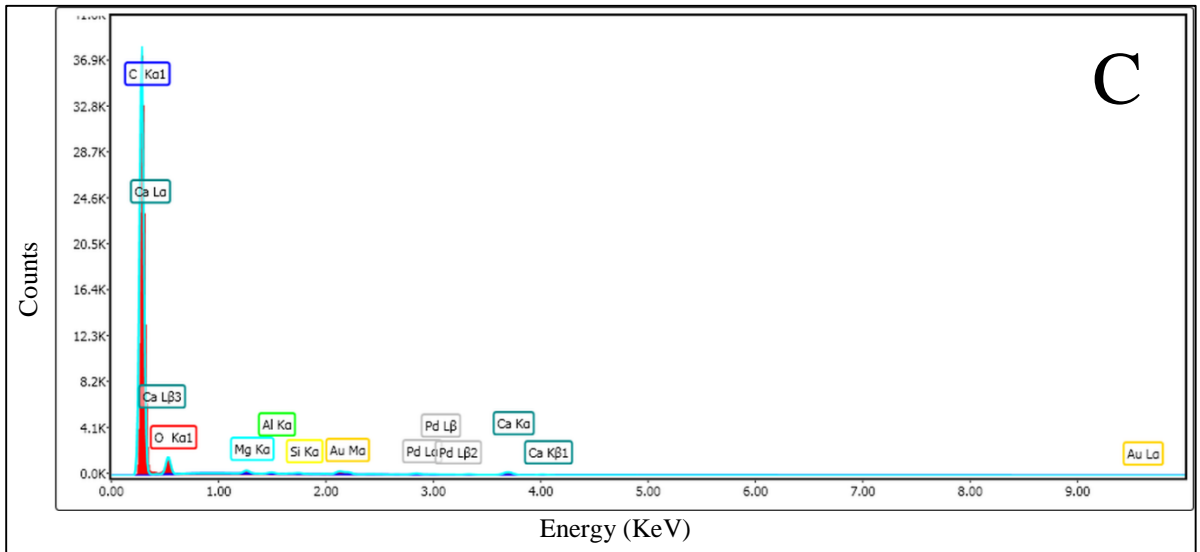
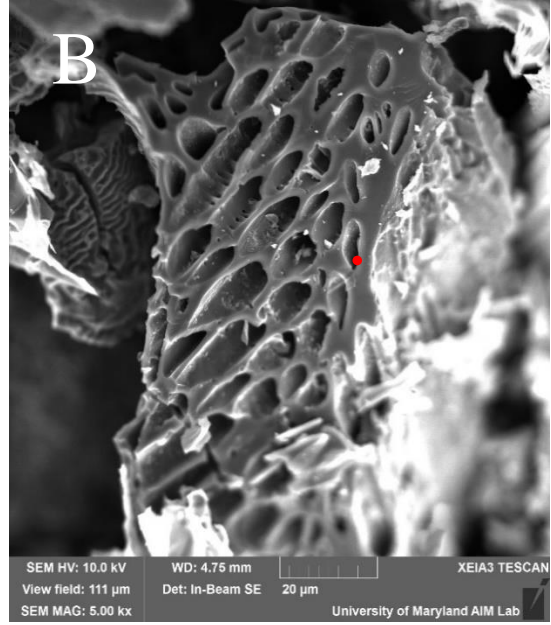
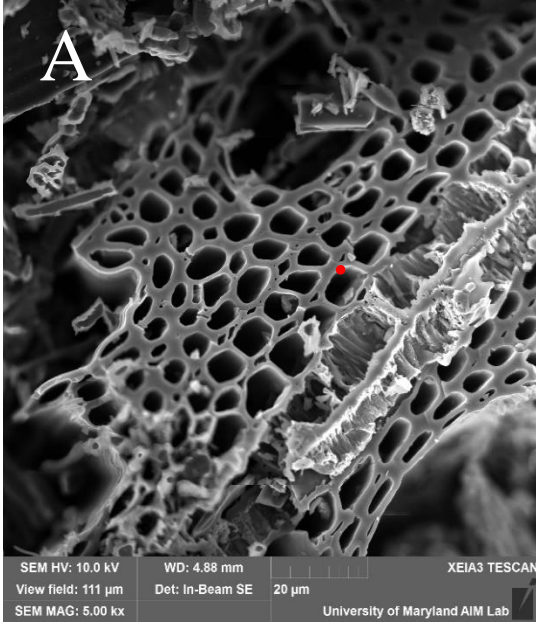
The physical and chemical characteristics of CSB and MB are shown in Table 4.1. MB had lower Fe, magnesium (Mg), potassium (K), N, and phosphorus (P) concentrations than CSB, but a higher C and H concentrations. CSB and MB had a BET surface area of 23.5 and 161 m²/g respectively, which were within the ranges seen for biochar prepared at 500 °C (2 – 400 m²/g), but lower than the surface area of activated carbon (>1000 m²/g) [108,109]. The micropore volume followed a similar trend, with MB (0.095 cm³/g; 3.5 nm) having a higher pore volume and lower average micropore width than CSB (0.011 cm³/g; 6.0 nm). Previous research on activated carbon based

adsorbents for H₂S adsorption have suggested that carbons which had high pore volumes, not high surface areas, achieved higher rates of H₂S oxidation [105,110]. Both the biochars were alkaline in nature due to the high preparation temperature (500 °C), with the pH of CSB higher than MB (10.2 and 9.1, respectively) due to the higher metal concentrations and ash content [111]. Recent studies conducted on biochars prepared from sewage sludge, anaerobically digested fibers, and agricultural waste have highlighted the importance of the alkaline surface as it aids in the dissociation of H₂S for further oxidation reactions [32,112]. Even though these studies attributed a higher H₂S adsorption capacity to the biochar pH, the sample size of tested biochars from different agricultural biomasses was small (2 – 3).

Table 4.1 Physical and chemical properties of the two biochar types and AC obtained from Soil Control Lab analysis.

Parameter	Corn Stover Biochar (CSB)	Maple Biochar (MB)	Activated Carbon (AC)
C (%)	62.9	81.5	N/A
H (%)	3.1	3.4	N/A
N (%)	0.95	0.55	0.91
P (%)	0.21	0.05	0.14
K (%)	2.34	0.49	0.15
S (%)	0.04	0.02	0.12
Ca (%)	1.45	0.96	0.49
Mg (%)	0.31	0.09	0.11
Zn (ppm)	56	43	14
Fe (ppm)	5500	1100	423
Cu (ppm)	12	9.2	8
pH	10.2	9.10	8.3
Ash (%)	29.6	5.8	3.5
Moisture (%)	1.3	0.8	6.4

The carbon content of both biochars were >50%, with MB (81.5%) having a higher C content than CSB (62.9%). The higher ash content in CSB (29.6%) was composed mostly of silica, as previously reported by Shen et al. (2015) and validated by the intense peaks associated with silica in the SEM-EDS and XRD data (Figure 4.2) [42]. Zhao et al. (2018) prepared biochar from corn straw at 500 °C with similar physicochemical parameters (61.8% C, 20.7% ash, and a surface area of 7.7 m²/g) [113]. Similarly, maple biochar prepared by Wang et al. (2015) at 500 °C with a residence time of 30 mins had a carbon content of 78.9%, 1.4% ash content, and a surface area of 257 m²/g [114]. The EDS data verified that the biochar was primarily composed of carbon with smaller amounts of calcium (Ca), magnesium (Mg) and oxygen (O) in MB compared to CSB. The high Ca content in both biochars was mostly in the form of CaCO₃, with intense peaks at $2\theta = 28.3^\circ$ and 29.4° . Mineral content (from EDS analysis) and speciation (from XRD analysis) are important factors to consider since oxides of metals such as Fe, Mg, Ca, and K, can enhance the catalytic oxidation properties of a carbonaceous material for converting H₂S into elemental sulfur and sulfates [100].



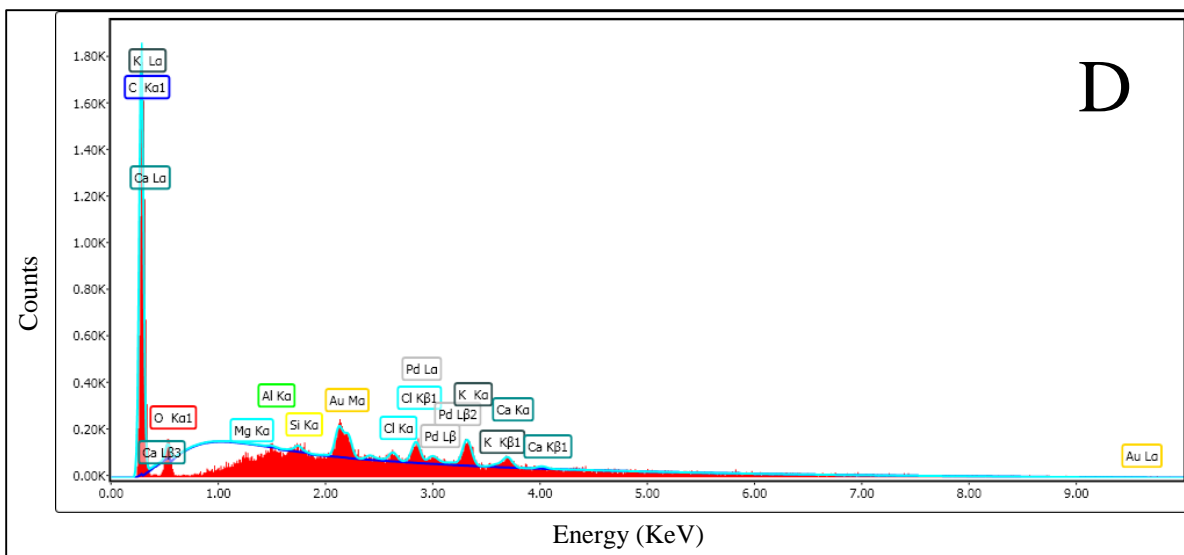
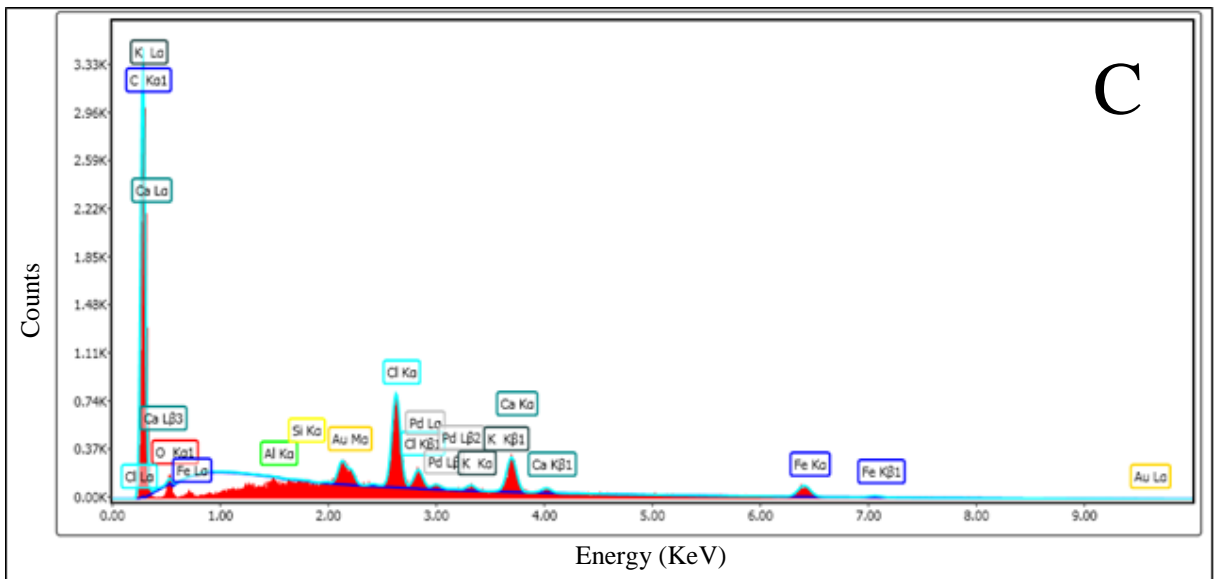
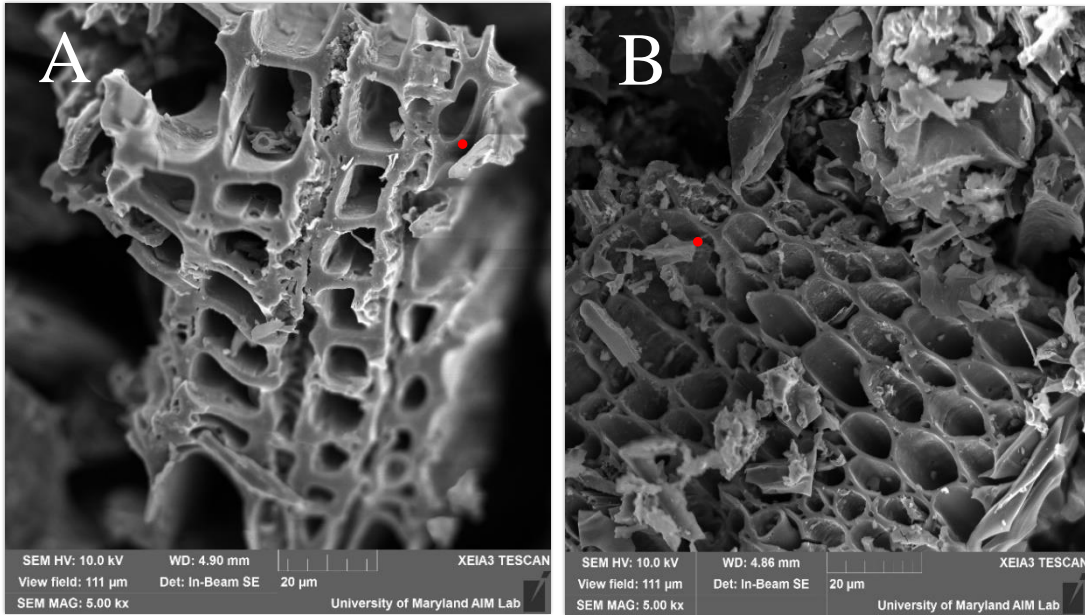


Figure 4.2 SEM image (A) and EDS data (C) of maple wood biochar (MB) and SEM image (B) and EDS data (D) of corn stover biochar (CSB). The EDS data is shown for the red marked points on the SEM images.

The SEM images and EDS data for impregnated CSB-Fe and MB-Fe shown in Figure 4.3 highlight the higher Fe concentrations compared to the unmodified CSB and MB. Due to the acidic nature of FeCl_3 , the pH decreased with the increasing Fe concentrations to 2.8 for CSB-Fe and 6.97 for MB-Fe. The Fe concentrations increased from 5,500 (CSB) to 17,700 ppm in CSB-Fe, and from 11,000 (MB) to 29,700 ppm in MB-Fe. The impregnation process also changed the micropore volumes of the biochars. MB-Fe had a 58% lower micropore volume ($0.04 \text{ cm}^3/\text{g}$) compared to MB, while CSB-Fe had a 64% lower micropore volume ($0.004 \text{ cm}^3/\text{g}$) compared to CSB. Micropore volume decreases in biochar due to impregnation can be attributed to the blockage of micropores by the impregnating agent and a change in the pore size distribution [115]. The surface area of MB-Fe was reduced by 63%, but the surface area of CSB-Fe increased by 48%.

The contrasting effect could be due to the difference in distribution of the resulting Fe-composites on the biochar surface and pores of CSB-Fe and MB-Fe. The XRD spectra showed the formation of Fe_3O_4 crystals on both CSB-Fe and MB-Fe, but MB-Fe had additional crystals of $\text{FeO}(\text{OH})$ that may have lowered the surface area since they are known to agglomerate (see Section 4.3.3 for more information) [116].



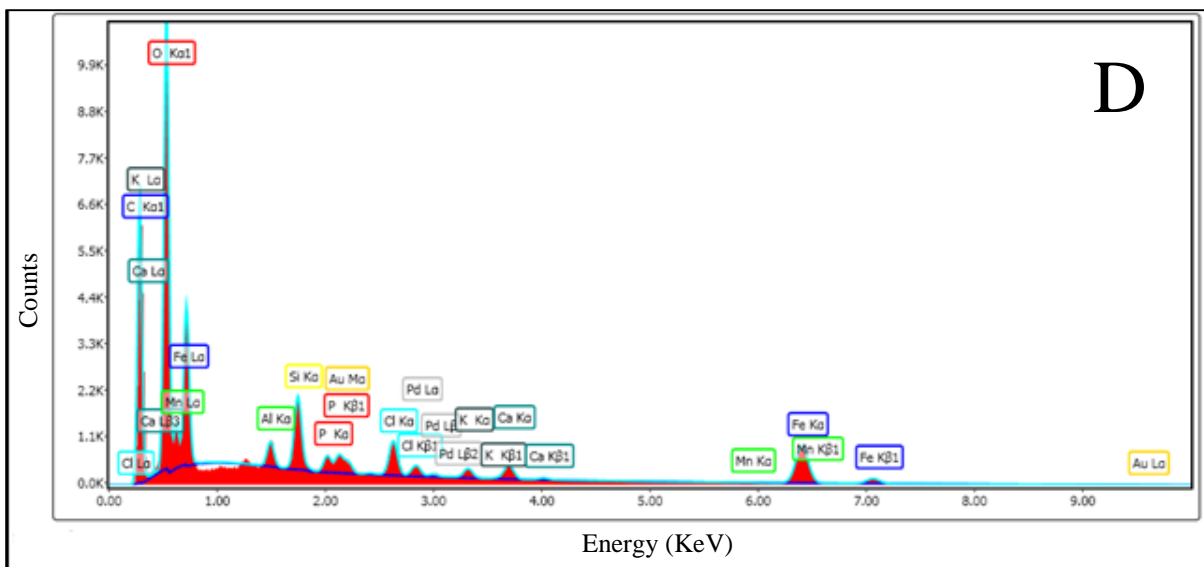


Figure 4.3 SEM image (A) and EDS data (C) of iron (Fe) impregnated maple biochar (MB-Fe) and SEM image (B) and EDS data (D) of Fe impregnated corn stover biochar (CSB-Fe). The EDS data is shown for the red marked points on the SEM images.

4.3.2 H₂S adsorption capacity in the dynamic system:

The breakthrough time (the time when the first non-zero H₂S concentration was detected in the outlet) was the longest for MB-Fe (300 mins), and shortest for CSB, with a breakthrough time of 10 mins (Figure 4.4; Table 4.2). As a result, the breakthrough capacity was the highest for MB-Fe (15.2 mg ± 0.0 S/g biochar), and the lowest for CSB (0.51 ± 0.0 mg S/g biochar). The final adsorption capacity also followed a similar pattern (Table 4.2), with MB-Fe having the highest sorption capacity for sulfur (16.8 ± 0.6 mg S/g biochar), and CSB having the lowest (1.7 ± 0.4 mg S/g biochar). Iron impregnation increased the sorption capacity by a factor of 1.9 for CSB-Fe (3.2 ± 0.4 mg S/g biochar) compared to CSB and by a factor of 4.3 for MB-Fe compared to MB (3.9 ± 0.2 mg S/g biochar). The adsorption capacities in this study for the unmodified biochars (CSB and

MB) were within range of results reported by Sethupathi et al. (2017), with a gas mixture of H₂S (3000 ppm), CO₂ (40%), and CH₄ (59.7%) and biochars prepared from locally available woody and herbaceous substrates (Perilla leaf, Korean oak, Japanese oak, and soybean stover) at temperatures ranging from 400 to 700°C [117]. In their study, the H₂S adsorption capacities ranged from 0.6 - 7.1 mg S/g biochar with the perilla leaf biochar (prepared at 700 °C) having the highest adsorption capacity and the Japanese oak biochar (prepared at 500 °C) having the lowest sulfur capacity. The results, however, were not predictable prior to the start of the experiment since adsorption capacities depend on biochar surface characteristics, and experimental conditions. The limited number of studies on biochar have reported H₂S adsorption capacities up to 273 mg S/g of biochar and the results in the current study were at the lower range of adsorption capacities reported for biochar in the literature [33,100,112]. However, it should be noted that the study is limited in scope since the experiments were conducted on single batches of the unimpregnated and the Fe-impregnated biochars and as such, the variability that could arise from the preparation process (pyrolysis and Fe-impregnation), and sample size of biomass, is not highlighted. Even if the biochars were prepared under the same conditions within the reactor, the inherent differences in mineral content in the biomass obtained from a different crop cycle may lead to larger variations in the results.

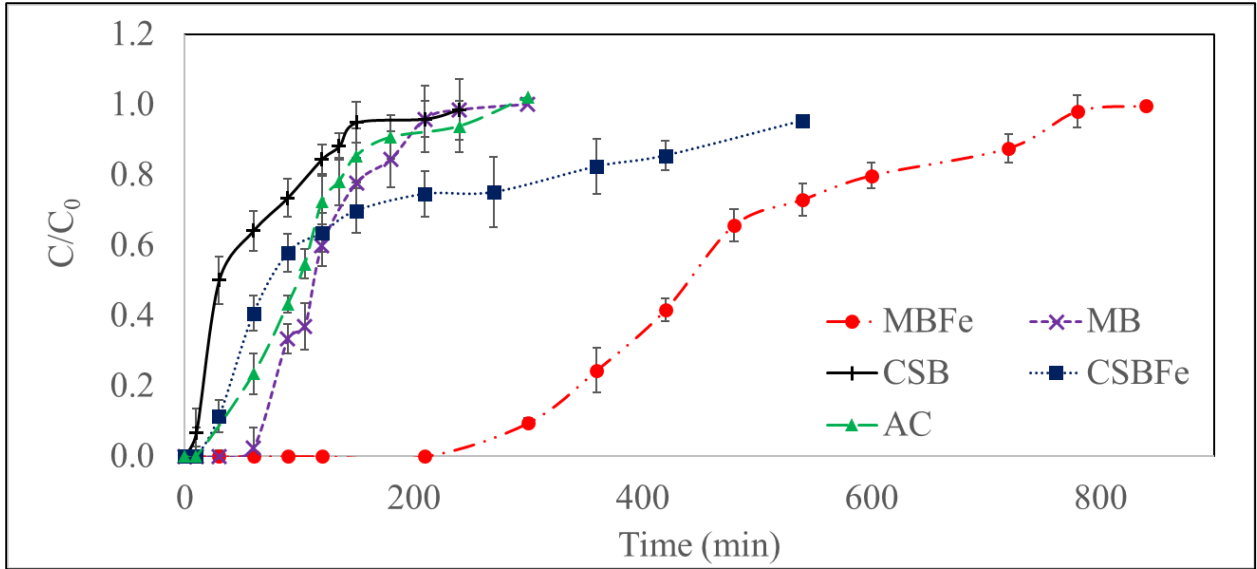


Figure 4.4 Breakthrough curves for H₂S adsorption on raw and Fe-impregnated corn stover biochar (CSB and CSB-Fe), maple biochar (MB and MB-Fe) and activated carbon (AC), where C/C₀ is the ratio of the outlet to the inlet H₂S concentration.

Table 4.2 Saturation time and adsorption capacity of the different adsorbents tested

Adsorbent	Saturation time (min)	Adsorption capacity (mg S/g)	Breakthrough time (min)	Breakthrough capacity (mg S/g)
Corn stover biochar (CSB)	38 ± 9.3	1.7 ± 0.4	10 ± 0	0.51 ± 0
Maple biochar (MB)	99 ± 3.9	3.9 ± 0.2	16.7 ± 7	2.0 ± 0.5
Iron-impregnated corn stover biochar (CSB-Fe)	78 ± 10	3.2 ± 0.4	30 ± 0	1.5 ± 0
Iron-impregnated maple biochar (MB-Fe)	438 ± 13	16.8 ± 0.6	300 ± 0	15.2 ± 0
Activated carbon (AC)	96 ± 6.7	3.9 ± 0.3	60 ± 0	3.0 ± 0

The H₂S adsorption capacity of AC (3.9 ± 0.3 mg S/g biochar) in our study was comparable to the H₂S adsorption capacities of MB, but higher than the CSB by a factor

of 2.35. The adsorption capacity for Darco AC reported by Balsamo et al. (2016) with a gas mixture of 3000 ppm H₂S in N₂ was 6.8 mg S/g biochar [118]. It is likely that the adsorption capacity of AC in the present study would be comparable to the results seen in the aforementioned study if the AC was allowed to be completely saturated with H₂S. Iron impregnated MB had a higher H₂S adsorption capacity compared to AC by a factor of 4.3. Additionally, unmodified MB had a comparable H₂S adsorption capacity compared to AC. Even though AC had a much larger surface area (> 1000 m²/g) compared to both unmodified (161 m²/g for MB) and Fe-impregnated biochar (59.8 m²/g for MB-Fe), it did not have a higher adsorption capacity. This result suggests that even though surface area is an important parameter, it is not the most important factor for H₂S adsorption in carbon-based adsorbents. It has been reported that the amount of surface area on a microporous carbon surface has no effect on the oxidation of H₂S, and can only aid in physical adsorption [110]. Sun et al. (2016) reported that the removal of H₂S by biochar is not controlled by the pore filling physisorption process that is commonly used to determine surface area by N₂ adsorption on the adsorbent [119].

In our study, the confirmation of the presence of Fe₃O₄ in CSB-Fe and MB-Fe highlighted the importance of reactive oxides on the biochar surface, as a multifold increase in H₂S adsorption capacity was observed, likely due the chemical oxidation via redox reactions of the reactive oxides with H₂S [105]. The Fe oxides from the impregnation process were primarily deposited on the biochar surface and pores and significantly affected the H₂S adsorption capacity. The quantity of Fe oxide composites on the surface of CSB-Fe (12,200 ppm) was 57% lower than the amount deposited on MB-Fe (28,600 ppm) and led to a 66% decrease in the adsorption capacity of CSB-Fe

compared to MB-Fe. Huang et al. (2006) conducted similar studies on Cu impregnated activated carbon and found that increasing the Cu content from 16,000 ppm to 40,000 ppm resulted in an increase in H₂S adsorption capacity from 20.3 mg S/g AC to 46.4 mg S/g AC [120]. Lee et al. (2017) showed that Fe hydroxide composites impregnated in activated carbon promoted increased reactivity and adsorption capacity for H₂S. In their study, an H₂S adsorption capacity of 171 mg S/g AC was observed, on 70% (by mass) FeO(OH) dispersed in 30% (by mass) AC, while the unmodified AC had an adsorption capacity of 12 mg S/g AC [116].

The pH of the biochar in our study ranged from 2.8 (CSB-Fe) to 10.2 (CSB), with the Fe-impregnated biochars exhibiting an acidic or neutral pH (MB-Fe pH: 6.97). Xu et al. (2014) proposed that the mechanism for H₂S adsorption on biochar was similar to the one proposed by Adib et al. (1999, 2000) and Boppart (1996) for activated carbon, which stated that the efficiency of the adsorption process was dependent on the attachment of H₂S molecules on the biochar surface [30,31,35,110]. They also suggested that features of activated carbon surfaces, such as local environment of acidic/basic groups along with the presence of alkali metals, are important to the oxidation process of H₂S. The proposed mechanism of H₂S removal using activated carbon involve: 1) H₂S adsorption on the activated carbon surface, 2) gaseous H₂S dissolution in the water film on the carbon surface, 3) dissociation of adsorbed H₂S in the water film into H⁺ and HS⁻, 4) reaction of adsorbed O₂ and H₂S with the formation of elemental sulfur or sulfur dioxide, and 5) further oxidation of SO₂ to H₂SO₄ in the presence of water and metal impurities that promote catalytic oxidation. Shang et al. (2013) compared H₂S removal from biochar and activated carbon and observed a significant increase in the adsorption capacity of biochar

compared to activated carbon [32]. In their study, they highlighted the importance of pH as the dominant factor in H₂S adsorption and found that an increase in biochar pH seemed to correlate with the increase in the adsorption capacity. In our study, biochar pH was not the dominant factor, as MB and AC had lower pH values (9.1 and 8.3, respectively), yet, outperformed CSB (pH = 10.2) in H₂S adsorption capacity. It is more likely that a pH higher than the pK_{a1} (7.2) of H₂S is sufficient to allow the dissociation of H₂S in the water film on the unmodified biochar or AC surface for further reaction, but the presence of reactive oxygen and metal oxides was likely the primary driver for further catalytic oxidation and increased effectiveness. The acidic pH of CSB-Fe (2.8), which was lower than the first ionization dissociation constant (pK_{a1}) of H₂S (7.2), did not lead to a lower H₂S adsorption capacity, either. The higher H₂S removal could be due to the reactive nature of Fe₃O₄ and its direct reaction with dissolved gaseous H₂S in the water film, as opposed to reaction with HS⁻, as reactive oxides on carbon-based adsorbents with a high affinity for sulfur (such as CuO) are known to exhibit that property [121].

Bamdad et al. (2017) stated that since biochar has a heterogeneous surface with many different functional groups, it is complicated to predict a suitable mechanism for the adsorption of acidic gases on the biochar surface [39]. They stated that the original mechanism proposed by Adib et al. (1999) for activated carbon is likely the same for adsorption of acidic gases on biochar, with differences created by the presence of alkali metals and basic functional groups in biochar [30]. Sun et al. (2016) compared the H₂S adsorption performance of biochar to AC and found that adsorption capacity of biochar (70 mg S/g biochar) was 3.7 times higher than AC (19 mg S/g AC) [119]. Ciahotný et al. (2019) also reported that H₂S adsorption on AC is primarily a physical process that takes

place mostly because of van der Waals force interactions [121]. Both biochars used in our study had higher metal concentrations compared to AC (Table 4.1) that should have aided in the process of chemical oxidation in addition to the physical adsorption process. In addition, CSB had higher alkaline metal (Ca and K) concentrations compared to both MB and AC. However, the H₂S adsorption capacity of CSB in the current study was 56.4% lower than both AC and MB. This is most likely due to the chemical form of K and Ca on the biochar surface. The XRD results showed that K was primarily present as KCl and Ca as CaCO₃. KCl, being a neutral salt, would not participate in an acid-base reaction with H₂S. On the other hand, CaCO₃ can participate in an acid-base reaction with H₂S, but it cannot catalytically oxidize H₂S to elemental sulfur/sulfate like its oxide form (CaO), and once it is exhausted further reaction with H₂S is not possible [105]. In addition, the micropore volume of MB (0.095 cm³/g) was 8.6 times higher than the pore volume of CSB (0.011 cm³/g), and micropore volume has been reported to increase H₂S oxidation reaction rates [110]. The results from our study provide evidence to the fact that the speciation of the mineral content in the biochar is important to consider, possibly more than the total mineral content for H₂S adsorption, and the need for detecting and taking into account the effect of micropore volume on H₂S oxidation.

4.3.3 XRD and SEM Results:

The XRD spectra of the fresh and the H₂S saturated biochar show the qualitative changes in the mineral composition and speciation before and after the experiment. Since biochar is primarily amorphous in nature, the XRD spectra produced two broad peaks, while the crystalline components are illustrated by the sharp peaks. The oxides in MB

and CSB were mostly in the form of quartz SiO_2 (as shown by the XRD results in Figures 4.5 – 4.8), a very stable, non-porous and unreactive oxide and most likely did not take part in the oxidation process of H_2S to elemental sulfur or sulfates. It is also important to note that the inherent Fe content of the biochar was not a factor in H_2S adsorption in CSB and MB, as CSB had five times more Fe content (5,500 ppm) and yet, had a lower H_2S adsorption capacity.

The lower fraction of inorganic components in MB led to fewer and smaller peaks, mostly in the form of CaCO_3 and some SiO_2 . The alkaline nature of the unmodified biochars can be attributed to CaCO_3 . The Fe-impregnated biochar samples, CSB-Fe and MB-Fe, however, did not have any CaCO_3 peaks, and likely led to the lowering of biochar pH after the impregnation process. The Fe composites existed as Fe_3O_4 in both Fe-impregnated biochars, but MB-Fe had detectable concentrations of $\text{FeO}(\text{OH})$ as well. The identity of other Fe-composites on the biochar surface could not be confirmed by XRD analysis due concentrations below the detection limit.

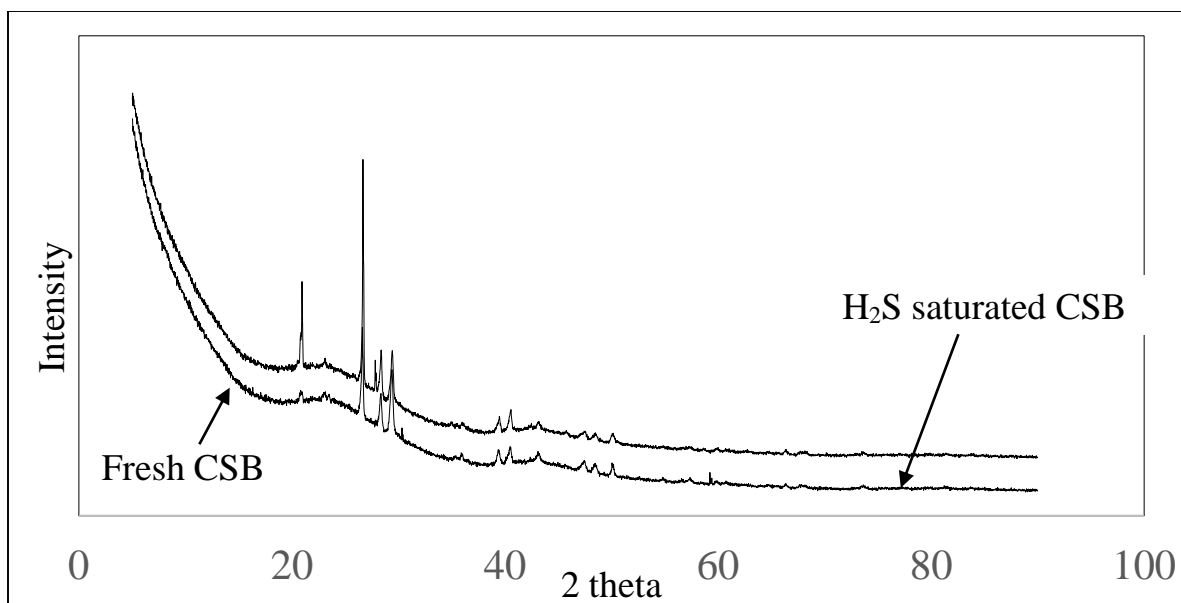


Figure 4.5 XRD spectra for fresh and H₂S saturated corn stover biochar (CSB), where the peaks mainly show the presence of silica (SiO₂), calcium carbonate (CaCO₃), and potassium chloride (KCl).

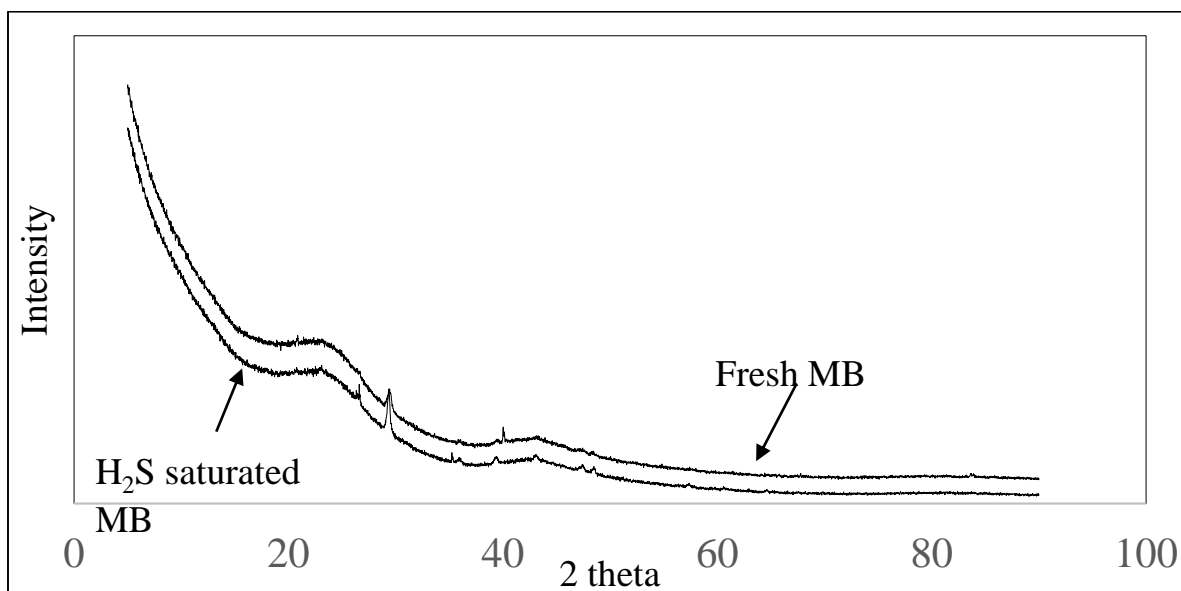


Figure 4.6 XRD spectra for fresh and H₂S saturated maple biochar (MB), where the peaks mainly show the presence of calcium carbonate (CaCO₃). Sulfur peaks were not detected.

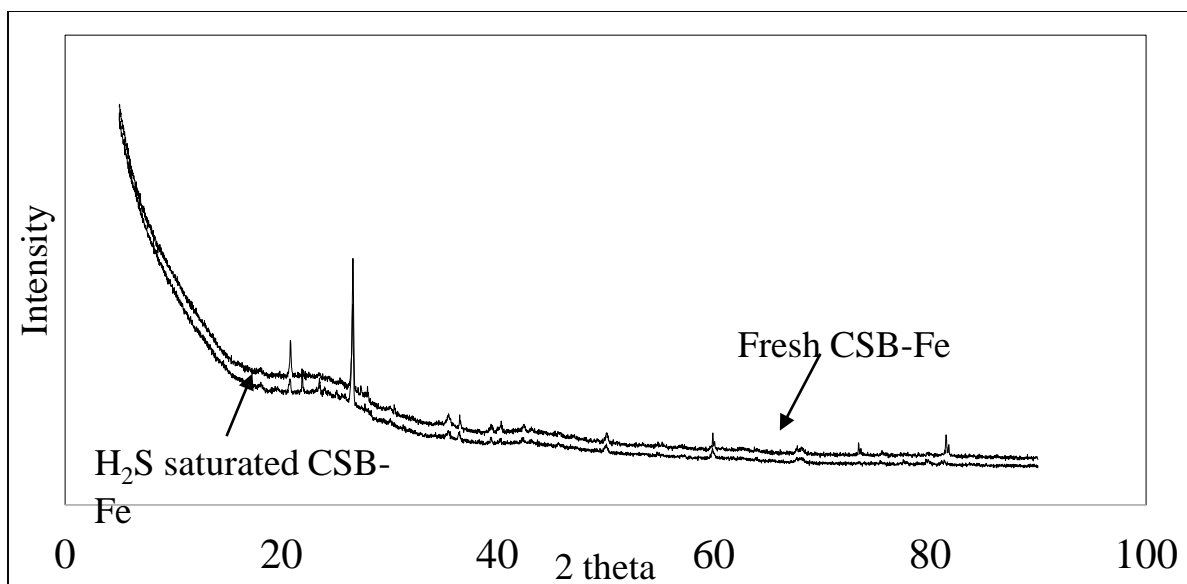


Figure 4.7 XRD spectra for fresh and H₂S saturated Fe impregnated corn stover biochar (CSB-Fe), where the peaks mainly show the presence of silica (SiO₂), and magnetite (Fe₃O₄) in the fresh CSB-Fe. The presence of ferrous sulfate heptahydrate (FeSO₄.7H₂O) is seen at 2 theta = 18.3° and 23.8° in H₂S saturated CSB-Fe.

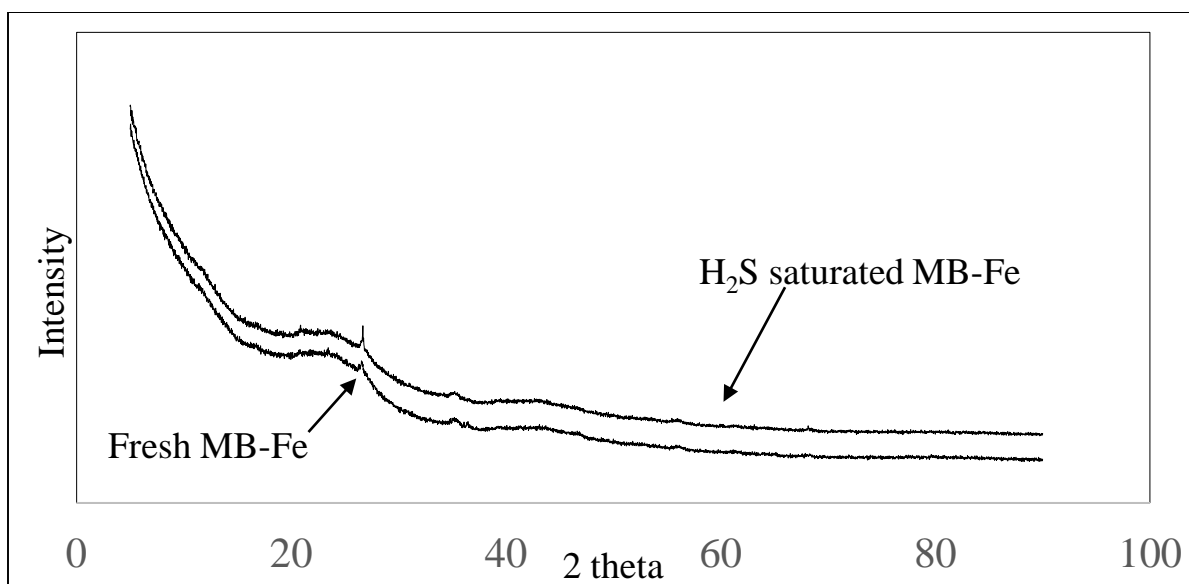


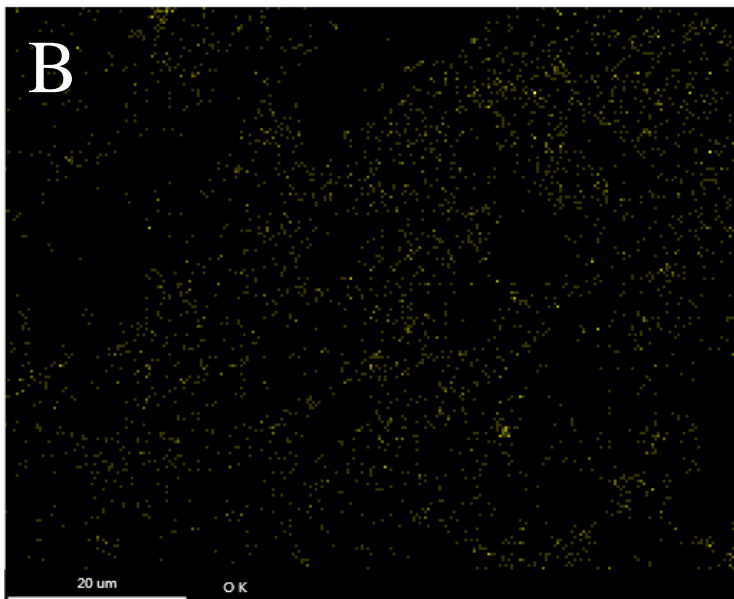
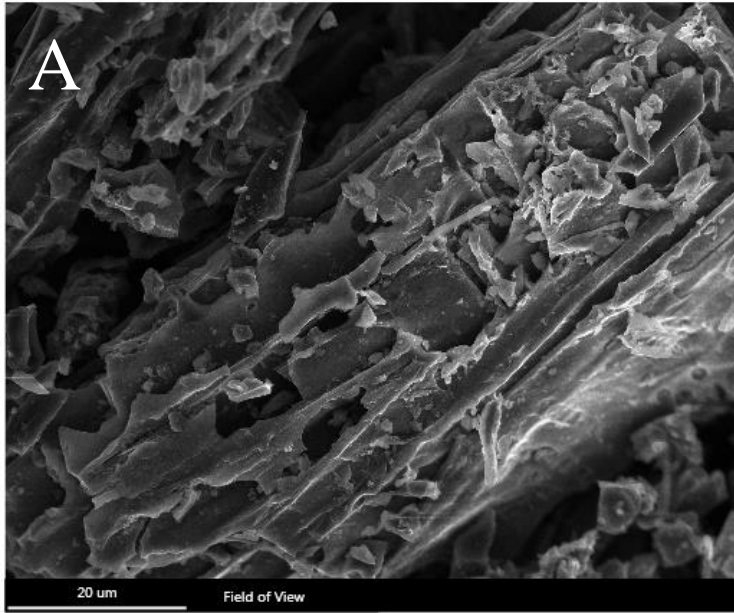
Figure 4.8 XRD spectra for fresh and H₂S saturated iron impregnated maple biochar (MB-Fe), where the peaks show the presence of magnetite (Fe₃O₄), and iron oxide-

hydroxide ($\text{FeO}(\text{OH})$) in the fresh MB-Fe. The presence of ferrous sulfate heptahydrate ($\text{FeSO}_4 \cdot 7\text{H}_2\text{O}$) is seen at $2\theta = 18.3^\circ$ and 23.8° in H_2S saturated MB-Fe.

Crystalline elemental sulfur was detected at 2θ (diffraction angle) = 27.7° in the H_2S -saturated CSB sample, but not in the MB sample. Kanjanarong et al. (2017) conducted XRD analysis on biochar present at the bottom of the column, as it was exposed to the incoming H_2S for the longest period of time and detected two strong peaks at $2\theta = 25^\circ$ and 28° , indicating the formation of elemental S [33]. The authors also conducted a separate analysis on the biochar from the top of the column and found it to be similar to the fresh biochar. The H_2S saturated biochar tested in our study was completely mixed before the XRD analysis. The spent biochar did not show high concentrations of crystalline sulfur compounds, which can be detected by XRD, which indicates that the sulfur was primarily present in its amorphous form, which cannot be detected by XRD. Xu et al. (2014) attempted an additional study using a static H_2S adsorption test that allowed for a longer contact time and a higher retention of sulfur in the biochar [35]. They observed a disappearance of the KCl peak due to its reaction with the sulfates produced from H_2S oxidation. In our study, the intensity of the KCl peak decreased but did not disappear completely, indicating lower amounts of potassium sulfate (K_2SO_4) formation due to the lower amounts of H_2S adsorbed in our dynamic study compared to the results obtained by Kanjanarong et al. (2017) and Xu et al. (2014) [33,35]. In CSB-Fe and MB-Fe, hydrated ferrous sulfate ($\text{FeSO}_4 \cdot 7\text{H}_2\text{O}$) peaks were observed in the XRD spectra, but no other form of sulfur was detected, which makes it likely that hydrated ferrous sulfate was the major crystalline product along with

amorphous elemental sulfur. A similar result was observed by Arcibar-Orozco et al. (2015) for H₂S adsorption on composites of graphite oxide and magnetite (Fe₃O₄), where hydrated ferrous sulfate was detected to be the major crystalline product along with amorphous elemental sulfur [122].

The XRD results were in agreement with the results obtained from SEM analysis. An H₂S saturated biochar (MB) particle is shown in Figure 4.9A. SEM elemental mapping (Figure 4.9C) showed uniform distribution of sulfur (pink dots) on the biochar surface as well as the pores, but oxygen (yellow dots, Figure 4.9B) was primarily concentrated on the surface providing evidence to the possibility of elemental sulfur formation in the pores due to limited oxygen diffusion and sulfate formation on the surface. Kanjanarong et al. (2017) and Xu et al. (2014) both observed similar results from their SEM-EDS results and attributed it to formation of SO₄²⁻ on the surface of the biochar and elemental sulfur formation in the pores of the biochar [33,35]. A similar distribution of sulfur was seen in the Fe-impregnated biochars as well, with the sulfur being attached to Fe and oxygen particles (as FeSO₄), the biochar surface (as SO₄²⁻), as well as the pores (elemental S). Combined with the XRD data, it is likely that along with FeSO₄·7H₂O, there were a multitude of other sulfate products formed on the biochar surface, with elemental sulfur being the major product inside the pores.



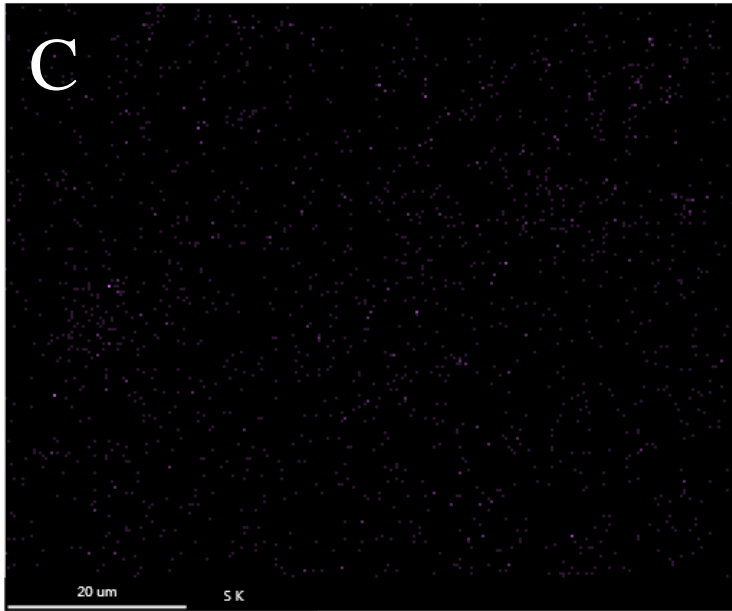


Figure 4.9 SEM elemental mapping of H₂S saturated biochar (A) showing oxygen (B) and sulfur (C) distribution.

4.4 Conclusion:

The results of the study showed that Fe-impregnation can be used to significantly increase the H₂S adsorption capacity of biochar by a factor of 4.3 compared to activated carbon. Iron impregnation also increased the H₂S adsorption capacity of the biochars by a factor of 1.9 – 4.3, when compared to unmodified biochars. Biochar with a 25% moisture content containing reactive oxygen or metal oxides favored the conversion of sulfide into elemental sulfur and sulfates, thereby, positively affecting the H₂S removal capacity.

Biochar pH was not found to be as important as previously speculated, with the more alkaline biochar performing less efficiently. The biochar pH was found to be even less important in the case of Fe-impregnated biochars, as they can effectively bypass the H₂S dissociation step before further reaction, thus shifting the adsorption mechanism.

However, it should be noted that the study does not take the variability associated with

the preparation of the Fe-impregnated and unimpregnated biochars into account. Overall, the results of our study show that Fe-impregnation was effective in increasing the H₂S adsorption capacity of biochar. The importance of metal species for the catalytic oxidation of H₂S was also highlighted in both unmodified and Fe-impregnated biochar, as the total metal content may not provide enough information on the H₂S adsorption capability of the biochar. The results also showed that ferrous sulfate was the major crystalline product in Fe-impregnated biochar and provided evidence to observations from previous research about the formation of sulfates on the biochar surface and elemental sulfur inside the pores. Further studies should be conducted on the effect of increasing iron loading on the biochar surface and the impregnation of other transition metals to improve the efficiency of H₂S adsorption and better understand the reaction mechanism associated with this process.

5 Impact of biochar addition on H₂S production from anaerobic digestion

Abstract:

The effect of two types of biochar addition (corn stover biochar (CSB) and maple biochar (MB)) to remove H₂S in the biogas produced from an anaerobic digester was evaluated in lab-scale systems. The study evaluated the effect of 1) different biochar concentrations, 2) different biochar particle sizes, and 3) iron-impregnated biochar for two different biochar types on H₂S production. At the highest biochar dose (1.82 g biochar/g manure total solids (TS)), only 35.4 ± 5.8 mL and 30.9 ± 2.4 mL H₂S/kg volatile solids (VS) was produced for MB and CSB, respectively, resulting in an average H₂S removal efficiency of 90.5%, compared to the control treatment (351 ± 9.4 mL H₂S/kg VS). No significant effect of particle size was observed in biochar treated reactors (0.5 g biochar/g manure TS), with a H₂S removal efficiency ranging from 26% - 43%. The Fe-impregnated biochar (0.5 g biochar/g manure TS) treated reactors had no H₂S detected in the CSB-Fe system, and 51.3 ± 3.7 mL H₂S/kg VS for MB-Fe, resulting in an H₂S removal efficiency of 98.5%, compared to the control, with 2025 ± 33 mL H₂S/kg VS. Methane in the biochar and control treatments did not vary significantly from each other in all three experiments. The results show that biochar addition in anaerobic digesters was able to significantly reduce H₂S production, without affecting CH₄ production. However, an economic analysis showed that biochar addition was not cost competitive compared to other H₂S removal technologies.

5.1 Introduction:

Biogas produced from anaerobic digestion (AD) consists of 55 - 70% methane (CH_4), which can be used as a source of renewable energy but also contains carbon dioxide (CO_2) (30 - 45%) and traces of hydrogen sulfide (H_2S) (0.01 – 1%) [99]. H_2S gas can corrode piping, mixing motors, and electric generator sets that convert CH_4 into electricity. Market available H_2S scrubbers to reduce high H_2S concentrations in biogas can have high capital costs, operating costs and/or unpredictable efficiencies [82]. Iron oxide scrubbing systems can have capital costs and operating costs ranging from \$0.01 – 0.05 per m^3 of biogas treated, and the costs for biotrickling filters can range from \$0.01 – 0.03 per m^3 of biogas treated [15,82,123]. A possible alternative could be the addition of a carbon-based material (biochar or activated carbon) to the anaerobic digester for in-situ capture of H_2S and simultaneous enhancement of CH_4 production.

Addition of carbon-based conductive materials, such as activated carbon (AC), into anaerobic digesters has led to shorter lag phases and increased CH_4 production from anaerobic digestion, in addition to other benefits such as higher resistance to AD inhibition [124]. These benefits have been attributed to a phenomenon called direct interspecies electron transfer (DIET) [124–127]. Conventionally, IET or interspecies electron transfer is a primary route for CH_4 production, where hydrogen (H_2) acts as the electron carrier between fermentative bacteria and methanogenic archaea [124]. Fermentative bacteria produce H_2 by breaking down volatile fatty acids, and hydrogenotrophic methanogens use that H_2 to reduce CO_2 and produce CH_4 . Several authors have studied the addition of granular activated carbon (GAC) in anaerobic cultures and provided evidence that using conductive materials can bypass the use of H_2

as the indirect carrier of electrons by promoting DIET [124,128]. Liu et al. (2012) suggested that the high conductivities of GAC (3000 $\mu\text{S}/\text{cm}$) resulted in enhanced methanogenesis by providing an electrical connection between fermentation bacteria and CH_4 -producing archaea [129].

Biochar is another carbon-based material that is produced via thermal degradation of organic material under limited oxygen (pyrolysis) at temperatures between 100 °C and 700 °C [27]. due to the lower preparation temperatures of biochar in comparison to activated carbon and the lack of activation step requirement, studies have shown that biochar (\$0.35 - \$1.2/kg) is comparatively cheaper than powdered activated carbon (\$1.1 - \$1.7/kg) [101]. Recent studies have investigated the direct addition of biochar into anaerobic digesters [28,40–42,130]. These studies focused on increasing the CH_4 content or digestion stability upon addition of the biochar but did not monitor or did not focus on the effect of biochar addition on H_2S production.

In a study by Shen et al. (2015), adding biochar made from corn stover directly to an anaerobic digester treating municipal wastewater resulted in an 86% reduction in CO_2 in the biogas, producing biogas with more than 90% CH_4 and less than 5 parts per billion H_2S [42]. The experiments were conducted using thermophilic conditions, with a concentration of initial H_2S (90 ppm) that was lower than the concentrations associated with biogas from dairy manure digesters (1000 – 8000 ppm) [82]. In dairy manure digesters, the TS concentration can vary from 1% to 10%, which would result in large quantities of biochar being to the digesters that could reduce the effective volume for substrate treatment. A lower biochar concentration that adequately desulfurizes biogas, while also providing a measure of CO_2 sequestration may be better for on-farm dairy

manure digesters. Shen et al. (2016) conducted another study using pine and white oak biochar addition to digesters to increase the percent CH₄ in the biogas stream by sequestering CO₂ in mesophilic and thermophilic conditions [28]. The study showed an average CH₄ content of 92.3% (pine biochar) and 89.8% (white oak biochar) in the biochar-amended digesters under mesophilic conditions, but there was no information on the H₂S content in the biogas. Both studies analyzed the particle size distribution of the biochar but did not investigate the effect of different biochar particle sizes on CH₄ production. The study also showed that biochar addition did not impact the total nitrogen (N) and phosphorus (P) under both mesophilic and thermophilic conditions. Studies have also shown that biochar can be used to uptake metal, organic, and inorganic contaminants from soil and water, and surface modified biochar can lead to enhanced uptake of these contaminants [115,131]. Iron (Fe) salts are commonly used for in-situ precipitation of H₂S in anaerobic digestion [64]. It is likely that surface modification of the biochar through Fe impregnation could significantly enhance its H₂S adsorption capacity. To the best of our knowledge, a study focusing on the use of biochar and Fe-impregnated biochar as additives, specifically, for CH₄ enhancement and H₂S reduction from biogas produced by dairy manure digestion at mesophilic temperatures, does not exist.

The overall aim of the study was to test the applicability of corn stover biochar (CSB) and maple wood biochar (MB) as additives in dairy manure digestion for in-situ desulfurization of biogas under mesophilic conditions. The study investigated the effect of 1) four biochar concentrations, 2) three particle sizes, and 3) surface modification through Fe impregnation on CH₄ and H₂S production, ammonium N (NH₄-N), and dissolved phosphorus (P) removal and possible enhancement of CH₄ formation through

DIET. A control experiment using sodium sulfide (Na_2S) solution and biochar was also conducted in order to understand the process of soluble sulfide removal using biochar in an aqueous solution. Finally, a cost analysis was conducted to determine if biochar addition into a digester for H_2S control was cost competitive compared to market available H_2S removal technologies.

5.2 Materials and Methods:

5.2.1 Biochar characterization and properties:

The two types of biochar (CSB and MB) were prepared through pyrolysis under an inert O_2 -free atmosphere (using N_2 gas) at a final temperature of $500\text{ }^\circ\text{C}$. After the final reactor temperature was attained, the material was held at that temperature for 10 mins (ArtiCHAR, Prairie City, Iowa, USA). Each biochar was tested for mineral composition and pH, and then characterized using five methods (described in Section 2.6): 1) N_2 adsorption isotherms for BET surface area, 2) Fourier Transform Infrared Spectroscopy (FTIR) for qualitative detection of functional groups, 3) Scanning Electron Microscopy (SEM) for imaging of the biochar surface, 4) zeta potential for biochar surface charge, and 5) electrical conductivity. The corn stover biochar was chosen to allow a comparison to the study conducted by Shen et al. (2015). The maple biochar was tested for comparison to CSB, since it was expected that the differences in the biochar characteristics (surface area, pore volume, mineral content) would lead to differences in the biogas desulfurization inside the digester.

5.2.2 Sulfide Removal Tests:

The soluble sulfide removal experiment using biochar was a modified version of the tests conducted by Lupitsky et al. (2018) for sulfide removal using zinc nanowires [64]. In the experiment, a solution of 500 mg/L S^{2-} was prepared by dissolving 1.875 g of Na_2S in 500 mL deionized water. These tests were conducted with a biochar concentration of 1 g/L. Both CSB and MB along with their respective Fe-impregnated counterparts (CSB-Fe and MB-Fe) were used for this experiment (see Section 5.2.5 for impregnation process description). The slurry was mixed for 15 hours (overnight) at room temperature using magnetic stirrers. The samples were then filtered using vacuum filtration to separate the biochar and the solution. The biochar was then characterized using SEM and XRD. The filtrate was tested for sulfide concentrations using HACH Method 10254 for high range sulfide concentrations.

5.2.3 Effect of biochar concentration (Experiment 1):

The effect of biochar concentration on H_2S production was conducted using unseparated liquid manure as the manure substrate and anaerobic digester effluent as the inoculum source collected from a covered lagoon digester at Kilby dairy farm in Rising Sun, MD. The farm co-digested 98% (by vol) flushed dairy manure and 2% (by vol) organic substrates containing cranberry waste, chicken fat, meatball fat and ice-cream waste, which was characterized by Lisboa et al. (2013) [7]. The flushed liquid manure and inoculum had total solids (TS) values of 7.03 g/L and 8.63 g/L, respectively, and volatile solids (VS) values of 4.47 g/L and 5.80 g/L, respectively.

The CSB and MB biochar were each tested at four concentrations: 1) 0.1 g biochar/g manure TS (CSB-0.1 and MB-0.1), 2) 0.5 g biochar/g manure TS (CSB-0.5 and

MB-0.5), 3) 1 g biochar/g manure TS (CSB-1 and MB-1), and 4) 1.82 g biochar/g manure TS (CSB-1.82 and MB-1.82). For comparison, the highest concentration (1.82 g biochar/g manure TS) in this study was the lowest concentration in the study conducted by Shen et al. (2015) [42].

5.2.4 Effect of biochar particle size (Experiment 2):

The study on the effect of biochar particle size on H₂S production was conducted using inoculum and unseparated DM obtained from a manure digestion system at the USDA Beltsville Agricultural Research Center (BARC) in Beltsville, MD. The unseparated DM and inoculum had TS values of 30.5 g/L and 21.4 g/L, respectively, and VS values of 22.1 g/L and 13.2 g/L, respectively. Prior to digestion, both biochar types (CSB and MB) were segregated into three different particle sizes using a sieve shaker: larger biochar particles between 841 μm – 707 μm (CSB-L and MB-L), medium biochar particles between 177 μm – 149 μm (CSB-M and MB-M), and small biochar particles less than 74 μm (CSB-S and MB-S). Activated carbon (AC) (Darco G-60, Fisher Scientific, Ontario, Canada) with a particle size of < 74 μm was also used as a treatment to compare its effects on CH₄ and H₂S production to biochar addition (AC-S). All segregated particle sizes of biochar and the activated carbon were added to the digestion reactors at a concentration of 0.5 g biochar/g manure TS.

5.2.5 Effect of biochar surface modification (Experiment 3):

The effect of biochar surface modification on H₂S production was conducted using inoculum and unseparated DM obtained from a mono-digestion system at Mason Dixon farm, Gettysburg, PA. The unseparated DM and inoculum had TS values of 57.8 g/L and 40.8 g/L, respectively, and VS values of 46.8 g/L and 29.9 g/L, respectively. The

two biochar surfaces were modified using a pretreatment step for metal impregnation. There were two treatments: 1) unmodified biochar (CSB and MB) and Fe-impregnated biochar (CSB-Fe and MB-Fe). All biochar substrates were added to the reactors at a concentration of 0.5 g biochar/g manure TS.

For impregnation, 10 g of biochar was mixed with a solution containing 0.97 grams of hydrated iron chloride ($\text{FeCl}_3 \cdot 6\text{H}_2\text{O}$) in 200 mL deionized water. The slurry was stirred using a magnetic stirrer for 48 hours and then dried in an oven for 24 hours at 105 °C. The dried composites were rinsed three times with deionized water to remove contaminants that can easily leach out, and then dried overnight at 105 °C [47].

5.2.6 Experimental Design:

All three experiments were conducted using 300 ml digestion reactors in batch mode. In the experiments, the substrate (dairy manure), digester inoculum, and biochar were added into triplicate reactors, purged with N_2 gas, capped, and incubated at 35 °C. An inoculum to substrate (ISR) ratio of 2:1 was utilized based on the VS concentration. Biogas, CH_4 , and H_2S concentrations were monitored at regular intervals until biogas production had largely ceased to a daily production at less than 1% of the total biogas produced. The quantity of biogas produced was measured using a graduated, gas-tight, wet-tipped 50 mL glass syringe inserted through the septa of the BMP bottles and equilibrated to atmospheric pressure. Biogas samples were collected in 0.5 mL syringes and tested for CH_4 , CO_2 and H_2S concentrations on an Agilent 7890 gas chromatograph (Agilent, Shanghai, China) using a thermal conductivity detector (TCD) at a detector temperature of 250 °C and the oven temperature at 60 °C with helium as the carrier gas. The average CH_4 production in the triplicates from the inoculum control was subtracted

from the other treatments to present the total CH₄ production from the waste substrates only and subtract the CH₄ production attributed to the inoculum source. All cumulative CH₄ and H₂S data presented were normalized by VS addition.

5.2.7 Analytical Methods:

5.2.7.1 Biochar testing:

Nitrogen adsorption isotherms were measured at 77 K (-196.15 °C) using a BET Analyzer (ASAP2020 Micromeritics, Norcross, GA) for the biochar samples. The samples were heated to 150 °C and degassed under a vacuum of <5 μm Hg for six hours. The adsorption isotherms were used to calculate the specific surface area, S_{BET} (BET method) in the range of $0.1 < p/p_0 < 0.55$, and micropore volume S_{micro} (t-plot Method).

The topographic analysis and the elemental composition of the biochar surface, before and after modification, and after completed digestion was conducted using a scanning electron microscopy (SEM-EDS) with a magnification range between 2000x and 10000x using a XEIA3 FIB-SEM (Tescan, Czech Republic). Biochar samples were mounted on a stub and gold coated prior to viewing. The powder XRD patterns of the raw, Fe-impregnated and H₂S saturated biochar were recorded using Bruker D8 Advance Powder X-ray Diffractometer (Billerica, MA, USA), over a scanning interval (2θ) from 5° to 90° with CuK α radiation ($\lambda = 1.54 \text{ \AA}$).

The electrical conductivity and zeta potential were measured on the suspensions using a Zetasizer Nano ZS90 (Malvern Instruments, Westborough, MA). The zeta potential can be used to determine the pH at the point of zero charge (pH_{pzc}), which is an important indicator of the biochar surface charge in a solution. For this test, 10 mg of biochar samples were added to 100 mL of deionized water. The solution was agitated on

a shaker for 24 h at 25 °C. The point of zero charge (pH_{pzc}) was obtained by measuring zeta potential values at different equilibrium pH values. The pH was adjusted using 0.05 M NaOH and 0.05 M HCl. All measurements were conducted in triplicates.

The carbon (C), hydrogen (H), N content, and metal analysis (including heavy metals) of the raw and Fe-impregnated biochar were conducted at Soil Control Labs Inc, California, using dry combustion for C, H, N, and EPA methods (EPA3050B/EPA 6010, 6020) for metals.

5.2.7.2 Manure sampling:

All manure and inoculum samples were brought to the laboratory on ice and tested for TS and VS within 24 hours in triplicate according to Standard Methods [132]. For TS analysis, triplicate 10.0 ml samples were pipetted into pre-weighed porcelain crucibles. The samples were then dried at 105 °C until a constant weight was obtained for the TS concentration. The crucibles were then placed in a furnace at 550 °C until a constant weight was obtained to determine VS concentration.

For ammonia-N, samples before and after digestion were acidified to $\text{pH} < 2$, and centrifuged at 15,000 rpm for 30 min. The supernatant was filtered through a cellulose acetate membrane with pore size of 0.45 μm to obtain a filtrate that was analyzed for ammonium-N using a Lachat Quikchem 8500 (Method 10-107-06-2-O; Lachat Instruments, Loveland, CO).

Dissolved phosphorus was analyzed by modifying the tests for total phosphorus. In the tests, post digested samples were filtered first using 0.45 μm membrane filters to prevent possible dissolution of adsorbed and precipitated P species and then acidified to $\text{pH} < 2$. The samples were then digested with concentrated sulfuric acid and tested using

Method 13-115-01-1-B rev 2006 with the Lachat Quikchem 8500 to obtain the dissolved P fraction.

5.2.8 Cost Analysis:

A cost analysis was conducted using data available from literature for iron oxide scrubbing systems, biotrickling filters for biological desulfurization, and sodium carbonate impregnated activated carbon for H₂S adsorption and compared to Fe-impregnated biochar addition into a digester and in a separate H₂S scrubbing system. The costs (\$) of desulfurization was normalized by the amount of biogas treated for each H₂S scrubbing technology for a biogas flow rate of 1,350 m³/day with an H₂S concentration of 1000 ppm.

5.2.9 Statistical Analysis:

Statistical analysis was conducted to determine significant differences in CH₄, H₂S, TS, VS, NH₄-N, and dissolved P, using t-tests, analysis of variance (ANOVA) and Tukey–Kramer multiple comparisons. All p-values <0.05 were considered significant. All triplicate values are reported as averages with standard errors (SE).

5.3 Results and Discussion:

5.3.1 Biochar Characterization:

The physical and chemical characteristic results (Table 5.1) show that MB had lower Fe, magnesium (Mg), potassium (K), N, and P concentrations than CSB, but a higher C and H concentrations. CSB and MB had a BET surface area of 23.5 and 161 m²/g respectively, which were within the ranges seen for biochar prepared at 500 °C (2 – 400 m²/g), but lower than the surface area of activated carbon (>1000 m²/g) [108,109]. The micropore volume followed a similar trend, with MB (0.095 cm³/g; 3.5 nm) having a

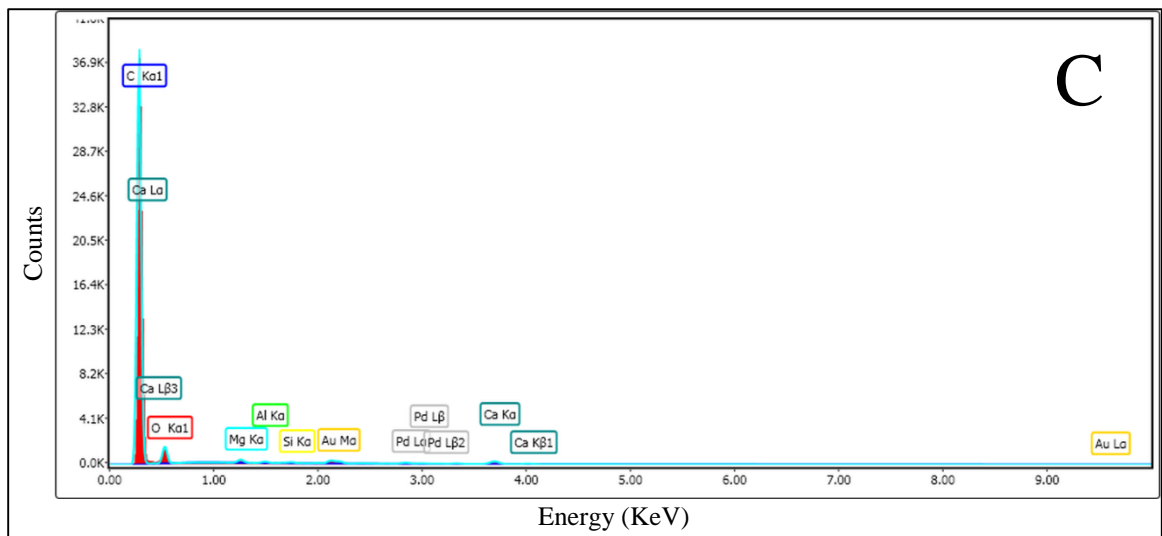
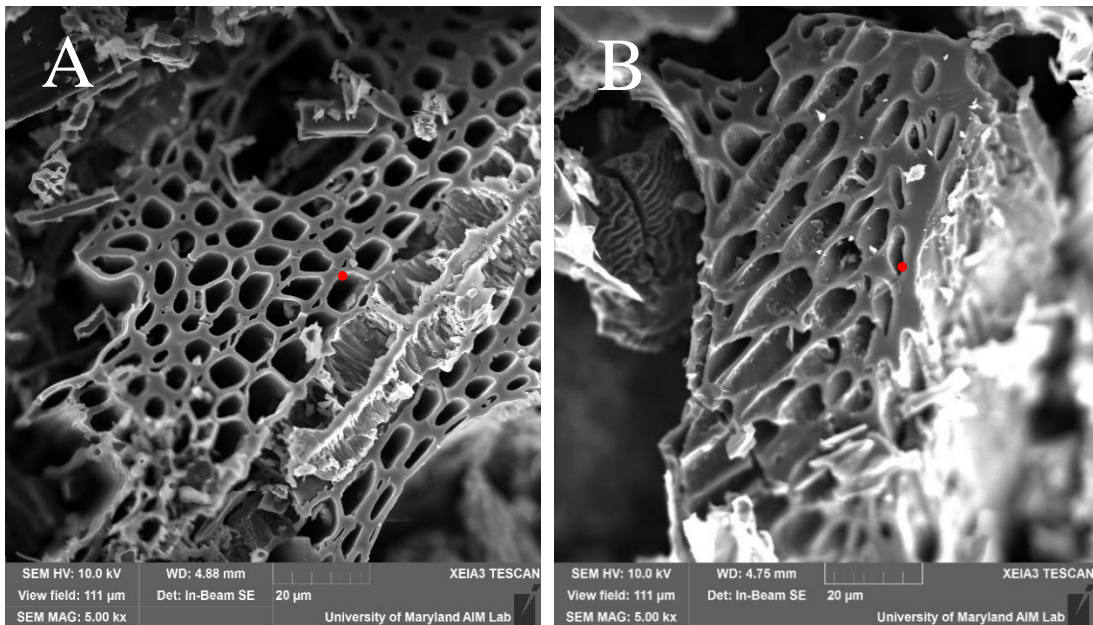
higher pore volume and lower pore width than CSB (0.011 cm³/g; 6.0 nm). Both the biochars were alkaline in nature due to the high preparation temperature (500 °C), with the pH of CSB higher than MB (10.2 and 9.1, respectively) due to the higher metal concentrations and ash content [111].

Table 5.1 Physical and chemical properties of the two biochar types and AC obtained from Soil Control Lab analysis.

Parameter	Corn Stover Biochar (CSB)	Maple Biochar (MB)	Activated Carbon (AC)
Carbon (%)	62.9	81.5	N/A
Hydrogen (%)	3.1	3.4	N/A
Nitrogen (%)	0.95	0.55	0.91
Phosphorus (%)	0.21	0.05	0.14
Potassium (%)	2.34	0.49	0.15
Sulfur (%)	0.04	0.02	0.12
Calcium (%)	1.45	0.96	0.49
Magnesium (%)	0.31	0.09	0.11
Zinc (ppm)	56	43	14
Iron (ppm)	5500	1100	423
Copper (ppm)	12	9.2	8
pH	10.2	9.10	8.3
Ash (%)	29.6	5.8	3.5
Moisture (%)	1.3	0.8	6.4

The carbon content of both biochars were >50%, with MB (81.5%) having a higher C content than CSB (62.9%). The higher ash content in CSB (29.6%) was composed mostly of silica, as previously reported by Shen et al. (2015) and validated by the intense peaks associated with silica in the SEM-EDS data (Figure 5.1D) [42]. Zhao et al. (2018) prepared biochar from corn straw at 500 °C with similar physicochemical parameters (61.8% C, 20.7% ash, and a surface area of 7.7 m²/g) [113]. Similarly, maple biochar prepared by Wang et al. (2015) at 500 °C with a residence time of 30 mins had a

carbon content of 78.9%, 1.4% ash content, and a surface area of 257 m²/g [114]. The EDS data verified that both biochars was primarily composed of C, with smaller amounts of calcium (Ca), Mg, and oxygen (O) in MB, compared to CSB.



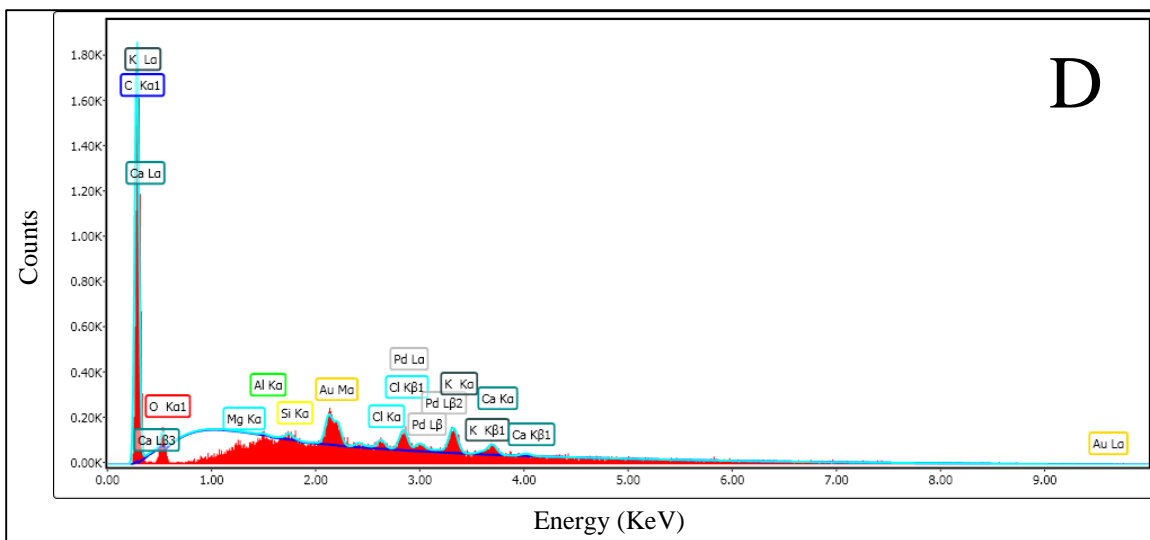
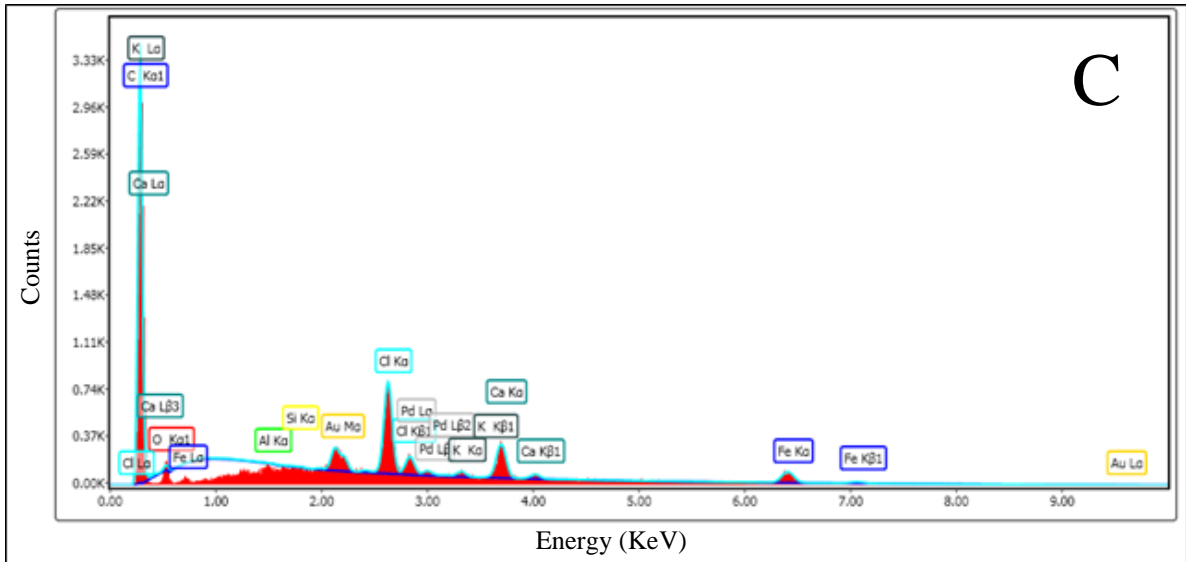
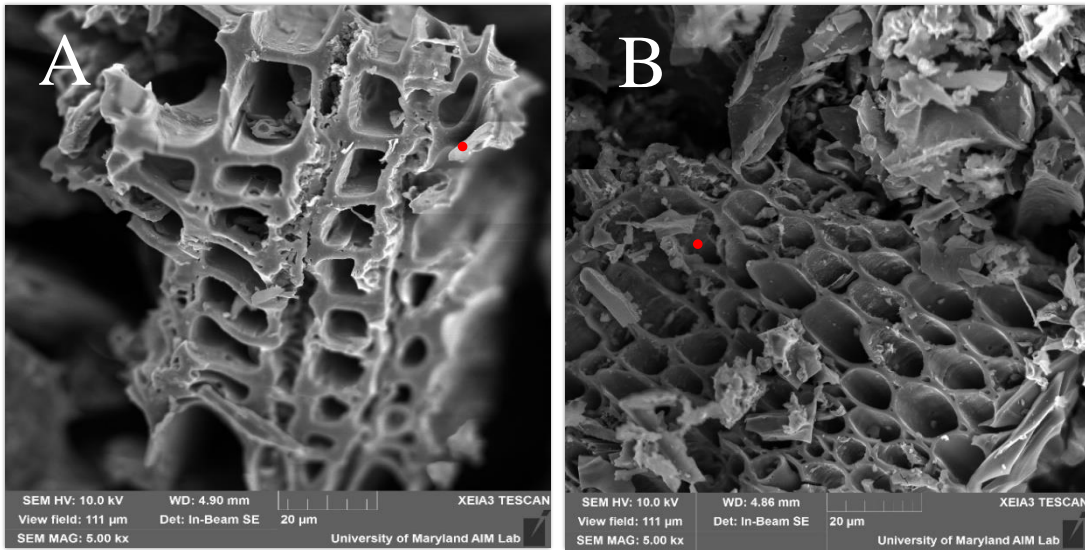


Figure 5.1 SEM image (A) and EDS data (C) of maple wood biochar (MB) and SEM image (B) and EDS data (D) of corn stover biochar (CSB). The EDS data is shown for the red marked points on the SEM images.

The SEM images and EDS data for impregnated CSB-Fe and MB-Fe (Figure 5.2 C & D) highlight the higher Fe concentrations compared to the unmodified CSB and MB. Due to the acidic nature of FeCl_3 , the pH decreased with the increasing Fe concentrations to 2.8 for CSB-Fe and 6.97 for MB-Fe. The iron concentrations increased from 5,500 (CSB) to 17,700 ppm in CSB-Fe, and from 11,000 (MB) to 29,700 ppm in MB-Fe. The impregnation process also changed the micropore volumes of the biochars. MB-Fe had a 58% lower micropore volume ($0.04 \text{ cm}^3/\text{g}$) compared to MB, while CSB-Fe had a 64% lower micropore volume ($0.004 \text{ cm}^3/\text{g}$) compared to CSB. Micropore volume decreases in biochar due to impregnation can be attributed to the blockage of micropores by the impregnating agent and a change in the pore size distribution [115]. The surface area of MB-Fe was reduced by 63%, but the surface area of CSB-Fe increased by 48%. The contrasting effect could be due to the difference in distribution of the resulting Fe-

composites on the biochar surface and pores of CSB-Fe and MB-Fe. The XRD spectra showed the formation of Fe_3O_4 crystals on both CSB-Fe and MB-Fe, but MB-Fe had additional crystals of $\text{FeO}(\text{OH})$ that may have lowered the surface area since they are known to agglomerate [116].



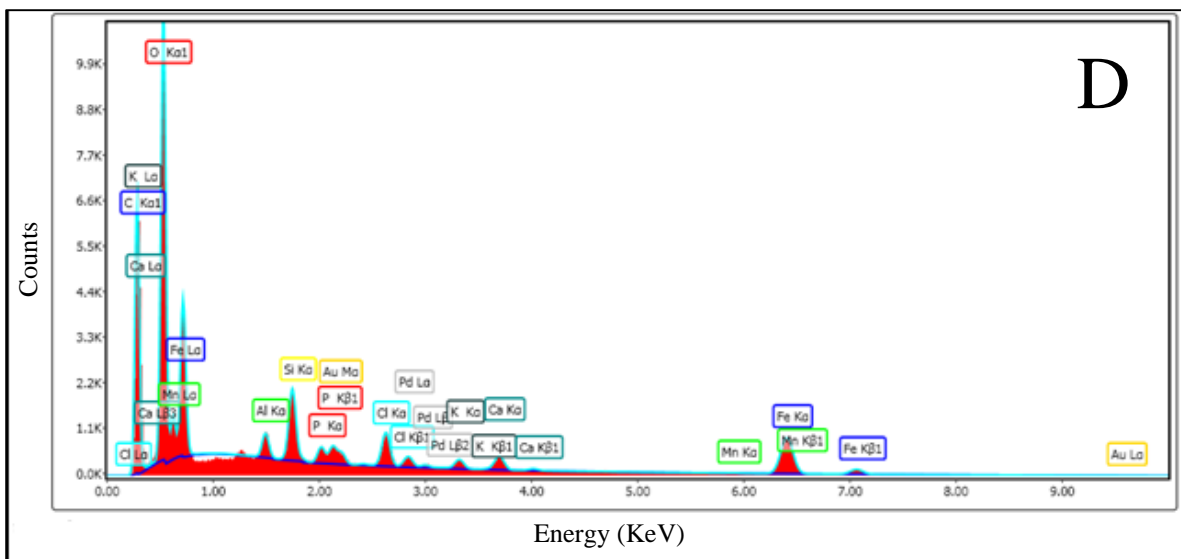


Figure 5.2 SEM image (A) and EDS data (C) of iron impregnated maple biochar (MB-Fe) and SEM image (B) and EDS data (D) of iron impregnated corn stover biochar (CSB-Fe). The EDS data is shown for the red marked points on the SEM images.

5.3.2 Sulfide Removal Test Results:

The results from the sulfide removal test (Table 5.2) showed that biochar can effectively remove soluble sulfides in an aqueous medium. MB-Fe (538 mg S²⁻/g biochar) had the highest H₂S adsorption capacity, followed by CSB-Fe (476 mg S²⁻/g biochar), and MB (439 mg S²⁻/g biochar). CSB had the lowest adsorption capacity (21.6 mg S²⁻/g biochar), and iron impregnation increased the adsorption capacity of CSB by a factor of 22, likely due to the low initial absorption of CSB. It is important to note that the long residence time (15 hours) and vigorous mixing allowed for maximum contact of the sulfide species with the biochar surface, resulting in adsorption capacities higher than the results observed in Chapter 4. Lupitsky et al. (2018) observed similar results where

they reported only 10% removal of dissolved sulfides with a residence time of 1 hour, which, increased to 67% after a residence time of 15 hours [64].

Table 5.2 Sulfide adsorption capacity of biochar in a model aqueous solution of sodium sulfide

Treatment	H₂S adsorption capacity (mg/g biochar)	Iron content (%)
Corn stover biochar (CSB)	21.6	0.55
Iron impregnated corn stover biochar (CSB-Fe)	476	1.77
Maple biochar (MB)	439	0.11
Iron impregnated maple biochar (MB-Fe)	538	2.97

Furthermore, the experiment was conducted in a closed aerobic system and the proposed mechanism for H₂S adsorption on a microporous carbon surface in the literature states H₂S and O₂ can diffuse into the carbon pores after dissolution in the water film on the biochar surface [31,110,112]. Oxygen reacts with the dissolved hydrosulfide ions, forming elemental sulfur and water, with further catalytic oxidation into sulfate promoted by the presence of metals, such as potassium, sodium, magnesium, and iron. Due to the longer residence time and presence of oxygen, the H₂S removal capacity of the biochar was enhanced compared to H₂S adsorption in a biogas scrubbing column, where oxygen was limited. It is likely that the residence time, absence of oxygen, and frequency of mixing will be limiting factors in a real AD system. The SEM and XRD results (Figures 5.3 and 5.4) of MB-Fe highlight the presence of iron and sulfur particles primarily in the form of FeSO₄·7H₂O, indicating catalytic oxidation of sulfide into sulfate as one of the reaction pathways. The presence of sulfur was also seen in the SEM results for MB and

CSB, but the XRD results did not detect the presence of crystalline sulfur, indicating that elemental sulfur formed was in its amorphous state [33].

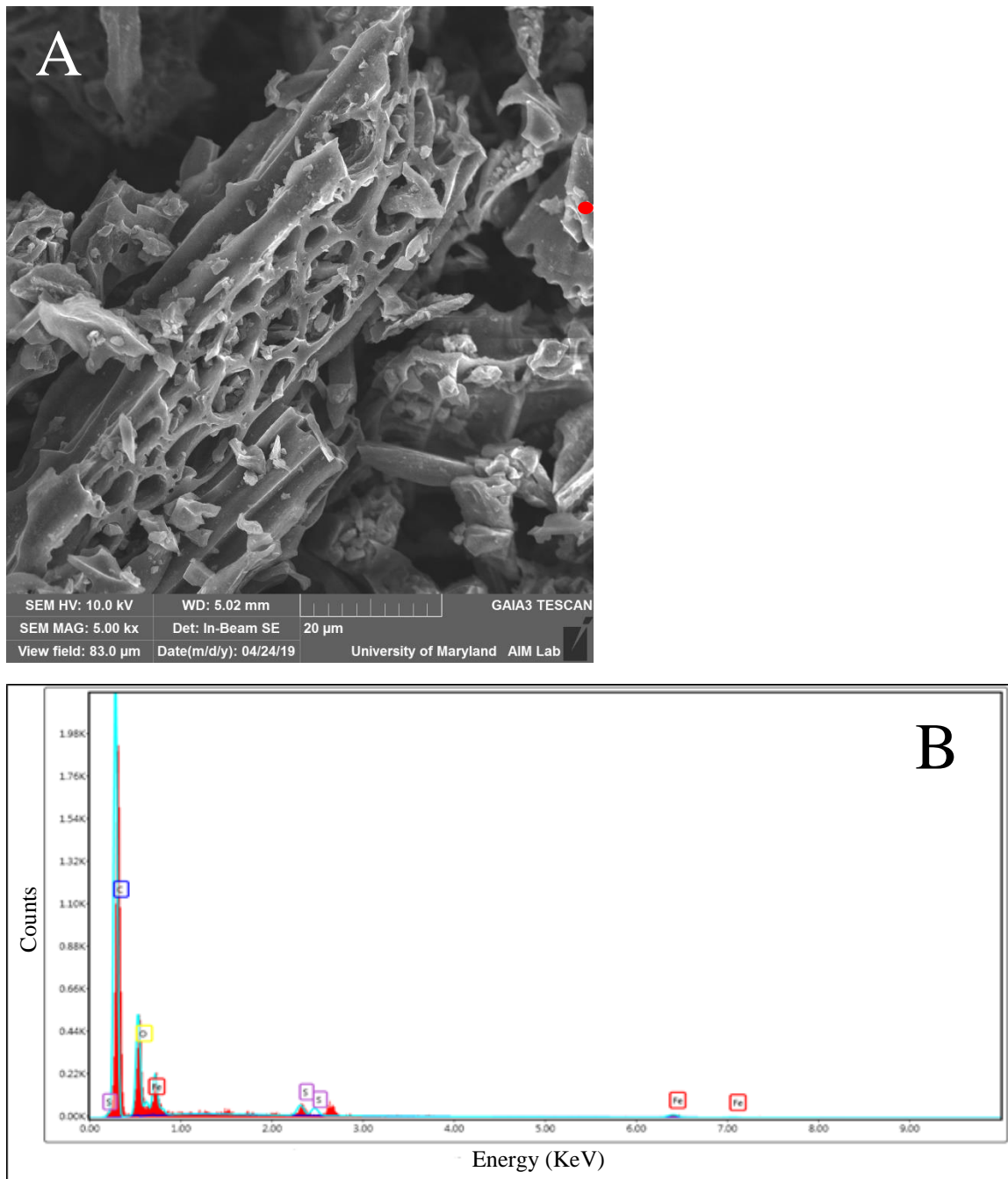


Figure 5.3 SEM image (A) and EDS data (B) of iron impregnated maple biochar (MB-Fe) after sulfide adsorption from model Na_2S aqueous solution. The EDS data is shown for the red marked points on the SEM images.

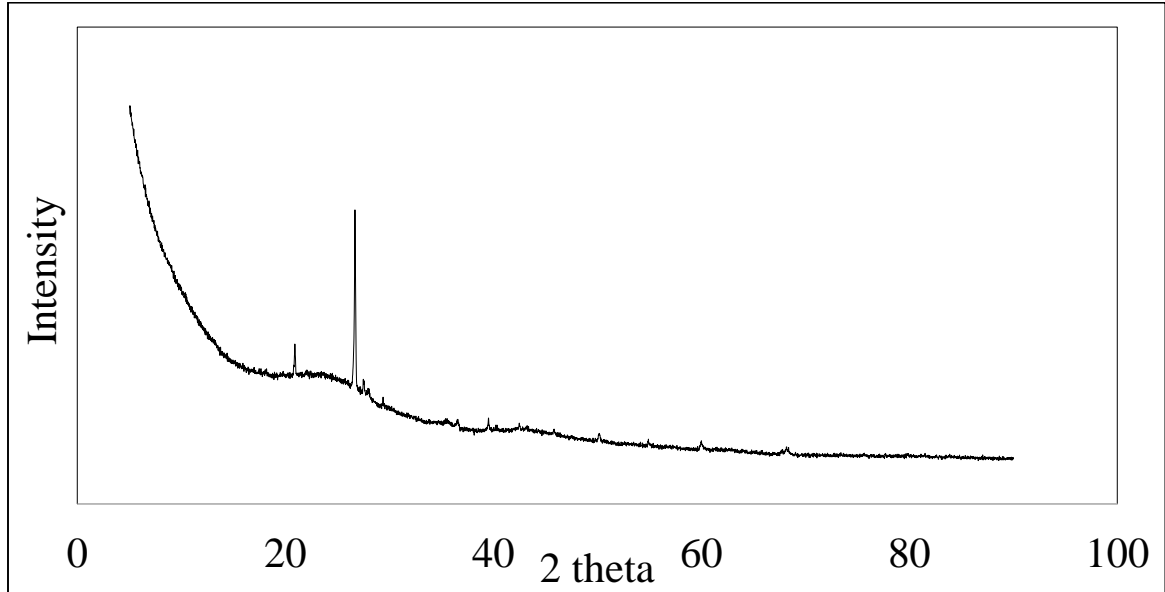


Figure 5.4 XRD spectra for H₂S saturated iron impregnated maple biochar (MB-Fe). The presence of ferrous sulfate heptahydrate (FeSO₄·7H₂O) is seen at 2 theta = 18.3° and 23.8°.

5.3.3 Effect of biochar concentration (Experiment 1):

Addition of biochar to the reactors significantly decreased the H₂S production compared to the DM control (p-value < 0.0001). The normalized H₂S concentration in the biogas decreased as the concentration of biochar increased in the treatments. When no biochar was added into a digester, 351 ± 9.4 mL H₂S/kg VS was produced. At the highest concentration of biochar added (1.82 g biochar/g manure TS), only 35.4 ± 5.8 mL H₂S/kg VS was produced for MB and 30.9 ± 2.4 mL H₂S/kg VS was produced for CSB, a reduction of 90 and 91%, respectively (Figure 5.5). The total volume of H₂S reduction increased with increasing concentration of biochar added, but the increase was

logarithmic, not linear ($R^2 = 0.996$ for CSB and 0.999 for MB). In order to obtain 99% percent removal of H_2S , the required increase in the biochar concentration would be 42%.

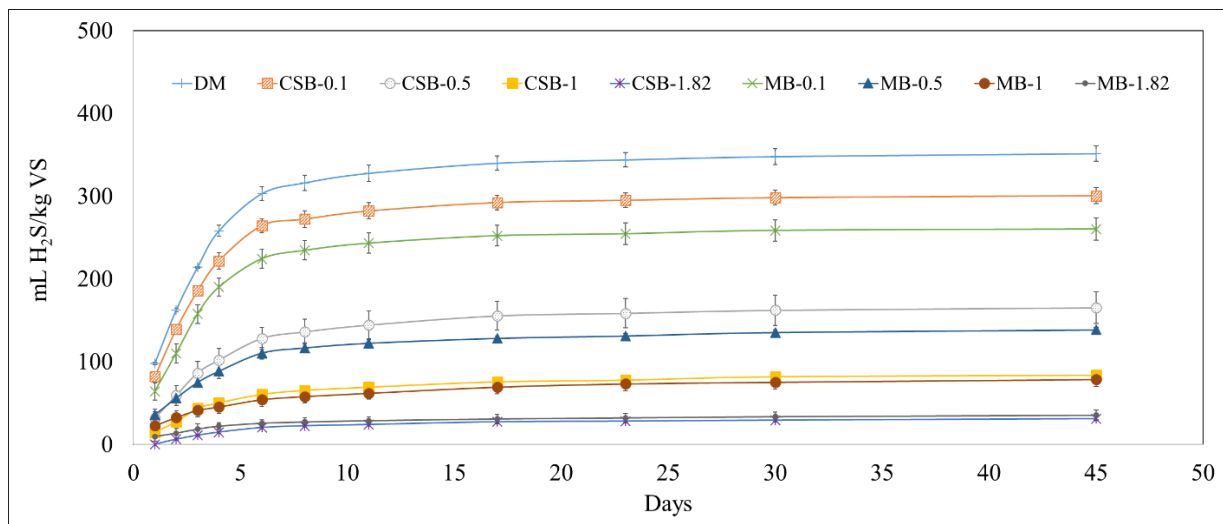


Figure 5.5 Cumulative hydrogen sulfide (H_2S) production normalized by kilograms of volatile solids (VS) with different biochar concentrations, with dairy manure (DM). Corn stover biochar (CSB) and maple biochar (MB) coupled with the different tested concentrations (0.1, 0.5, 1, 1.82 g/g manure TS) are used to differentiate each treatment.

Lower concentrations of added biochar (0.1, 0.5, and 1 g/g manure TS) were not able to completely reduce H_2S concentrations. The presence of organic molecules in the manure can lead to steric hindrance on the binding sites, thereby, reducing the amount of cations and anions adsorbed on the biochar surface [133]. Previous studies have also shown that the presence of multiple cations, anions, and organic matter in an aqueous system would lead to competition among the species with the highest affinity to the binding sites [134]. A decreasing trend was also observed when the volume of H_2S was normalized by the weight of biochar added (Table 5.3). An increase in biochar

concentration increases the probability of interaction with species with a higher affinity to the binding sites and may have blocked access to dissolved H₂S and HS⁻ ions. Over the duration of the incubation period, the biochar pores were also coated with microbial biomass, possibly reducing its effectiveness (Figure 5.6). The percent H₂S removal for each treatment showing a decreasing trend over the incubation period provides some evidence to the hypothesis (Figure 5.7). As previously stated, H₂S oxidation occurs in the micropores within the biochar and the layer of microbial biomass would restrict access to these sites [110]. Incorporating the biochar into a continuous digester will provide a better understanding on the effect of gradual buildup of the microbial biomass layer on the biochar surface, as most of the H₂S was produced within the first week of batch incubation.

Table 5.3 Hydrogen sulfide (H₂S) volume reduction and normalized mass removed per gram of biochar added into the reactor, and percent reductions in comparison to dairy manure (DM).

Treatment	H₂S volume reduction (μL)	Normalized H₂S reduction (mg H₂S/g biochar)	Reduction compared to DM (%)
0.1 g corn stover biochar/g manure total solids (CSB-0.1)	17.9 ± 3.3	0.45 ± 0.08	14
0.5 g corn stover biochar/g manure total solids (CSB-0.5)	65.4 ± 6.8	0.33 ± 0.03	53
1 g corn stover biochar/g manure total solids (CSB-1)	94.1 ± 1.4	0.24 ± 0.00	76
1.82 g corn stover biochar/g manure total solids (CSB-1.82)	113 ± 0.9	0.16 ± 0.00	91
0.1 g maple biochar/g manure total solids (MB-0.1)	32 ± 4.7	0.81 ± 0.12	26
0.5 g maple biochar/g manure total solids (MB-0.5)	74.9 ± 1.1	0.38 ± 0.01	61

1 g maple biochar/g manure total solids (MB-1)	95.9 ± 3.1	0.24 ± 0.01	78
1.82 g maple biochar/g manure total solids (MB-1.82)	111 ± 2.0	0.16 ± 0.00	90

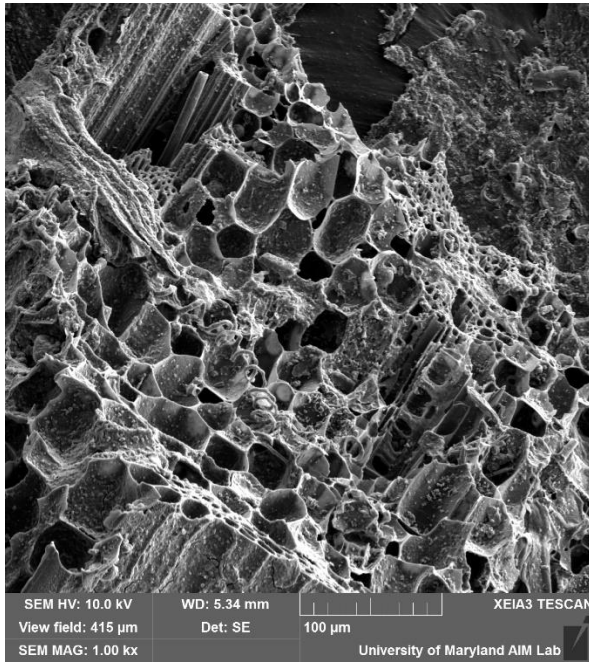


Figure 5.6 SEM image of biochar after digestion showing microbial biomass layers on the biochar surface and pores

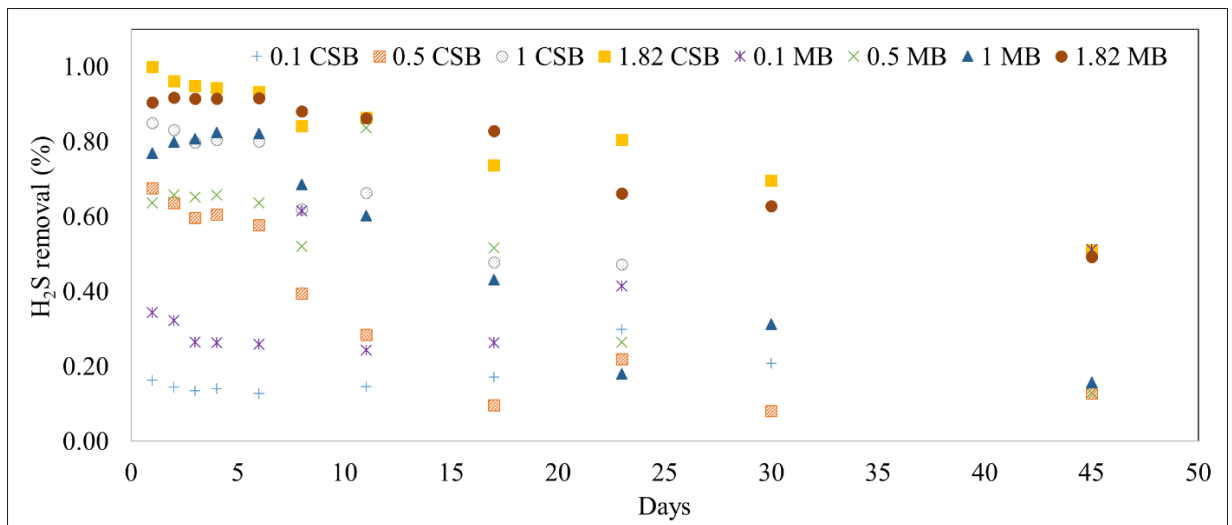


Figure 5.7 Percent hydrogen sulfide (H₂S) removal over the study period with different biochar concentrations, and dairy manure (DM). Corn stover biochar (CSB) and maple biochar (MB) coupled with the different tested concentrations (0.1, 0.5, 1, 1.82 g/g manure TS) are used to differentiate each treatment.

Solution pH is an important factor determining the adsorption of different ions on the biochar surface. The pH of the biochar amended treatment solutions stayed constant with little variation after (7.18 – 7.28) after the incubation period. The zeta potential results showed that $\text{pH}_{\text{pzc}} < 2$ for CSB and $2.35 > \text{pH}_{\text{pzc}} > 2.03$ for MB. Solution pH below the pH_{pzc} allow for protonation of the functional groups present on the biochar surface and provides an overall positive charge to the biochar particle [44]. pH values higher than pH_{pzc} favor the adsorption of positively charged contaminants due to electrostatic attraction by the negative charge on the biochar surface. The presence of metal component traces in the biochar provided microsites with a positive charge that may have aided the adsorption, oxidation, and precipitation of sulfur on the biochar surface [43].

Addition of different biochar concentrations into the reactors did not lead to any significant differences between the treatments in terms of CH₄ production ($0.0801 < p\text{-value} < 1.000$). The cumulative methane production varied between 231 ± 6 mL/g VS (CSB-0.1) and 201 ± 2 mL/g VS (MB-1.82) when normalized by the grams of VS added (Figure 5.8).

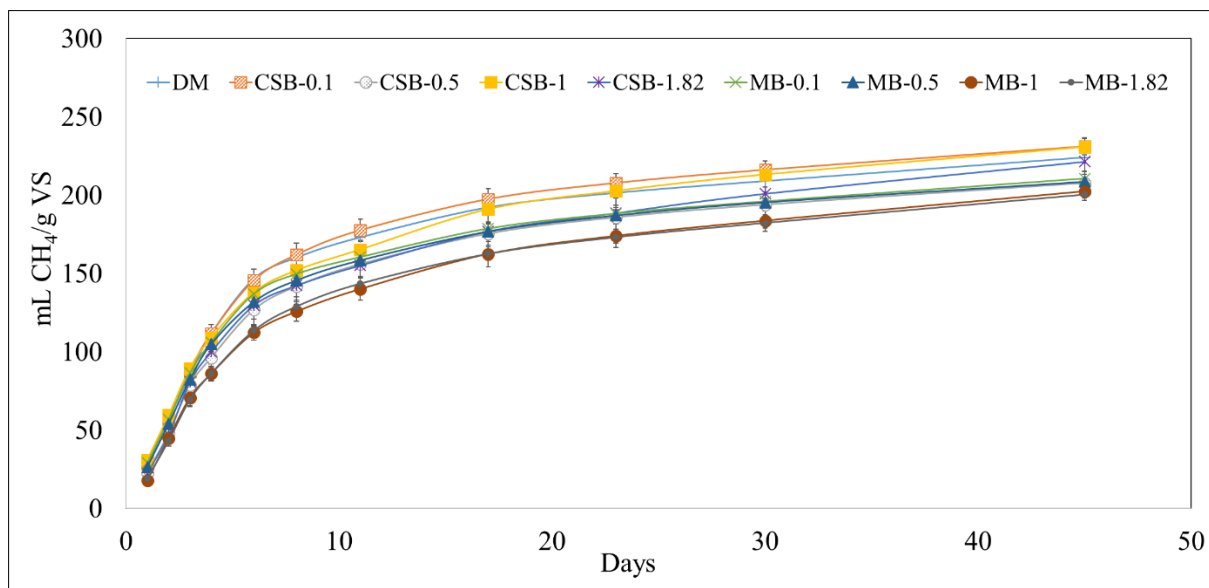


Figure 5.8 Cumulative methane (CH₄) production normalized by grams of volatile solids (VS) with different biochar concentrations, with dairy manure (DM). Corn stover biochar (CSB) and maple biochar (MB) coupled with the different tested concentrations (0.1, 0.5, 1, 1.82 g/g manure TS) are used to differentiate each treatment.

The addition of different biochar concentrations did not significantly affect the NH₄-N (p-value = 0.3640) and dissolved P (p-value=0.1204) concentrations. The NH₄-N concentrations in the biochar amended reactors varied from 143 ± 22 mg/L (CSB-0.1) to 215 ± 46 mg/L (CSB-1.82), with 143 ± 18 mg/L for the DM control. The dissolved P concentrations in the biochar amended reactors varied from 5.62 ± 0.22 mg/L (MB-0.5) to 6.99 ± 0.12 mg/L (CSB-0.1), with 6.21 ± 0.43 mg/L for the DM control. Several authors have conducted studies on the use of biochar for NH₄-N and PO₄³⁻ removal from aqueous solutions. Hou et al. (2016) showed that NH₄⁺ ions were adsorbed onto the biochar surface due to ion exchange and the best results were seen at pH values ranging from 7-9 [135]. However, these studies were conducted on single component systems

with no competing ions interacting with each other and the biochar surface. Pipíška et al. (2017) showed that in a binary system containing cobalt and cadmium ions, the interaction of the metal ions with the biochar surface was affected by the affinity of the two species to the binding sites on the biochar [136]. Dairy manure contains multiple cations, anions and organic matter in the system, and it is likely that the species with the highest affinity to the binding sites would be preferentially captured. The presence of organic matter in the manure can also contribute to steric hindrance for the NH_4^+ and PO_4^{3-} ions, in addition to competition with HS^- ions for the available binding sites [133]. SEM images (Figure 5.6) of the biochar samples after incubation showed layers of microbial biomass on the surface of the biochar that could also have prevented access to the binding sites for NH_4^+ and PO_4^{3-} ions. Liu et al. (2010) showed that the presence of zinc, aluminum, bicarbonate and phosphate ions directly reduced the NH_4^+ adsorption capacity of the adsorbent [137]. Kizito et al. (2015) conducted experiments on using biochar to remove NH_4^+ from swine manure digestate and found that the presence of most metal cations (K, Ca, Mg, Fe, Zn, etc.) negatively affected the sorption capacity of the biochar due to competition for active binding sites [134]. Similarly, phosphate ion adsorption has been shown to be affected by the presence of chloride ions and high concentrations of bicarbonate ions, leading to precipitation inside the biochar pores and adsorption sites [138,139]. The results obtained from the current study suggest that biochar addition into an anaerobic digester may not be effective at reducing $\text{NH}_4\text{-N}$ concentrations due to the presence of interfering cations and anions.

5.3.4 Effect of biochar particle size (Experiment 2):

The three tested biochar particle sizes significantly lowered the normalized H₂S volume compared to DM control and AC-S (p-value <0.0001). The normalized H₂S production for the biochar treated reactors varied from 519 ± 24 (MB-S) to 675 ± 23 (CSB-M) mL H₂S/kg VS (Figure 5.9). Even though the differences in H₂S production between the biochar treated reactors were not significant, MB had a slightly higher percent H₂S reduction than the corresponding CSB particle sizes, similar to the results seen in the first batch test. The mid-range particle sized biochar (CSB-M and MB-M) had the lowest treatment efficiencies (26% for CSB-M and 29% for MB-M, compared to DM control). Overall, the added biochar led to a 26 to 43% reduction in total H₂S volume when compared to DM digestion (Table 5.4). A trend of lowered H₂S percent reductions over time was also observed in this batch study, with 57 to 96% reductions from Day 1 to 2 and decreasing to 13 to 32% reduction by Day 21.

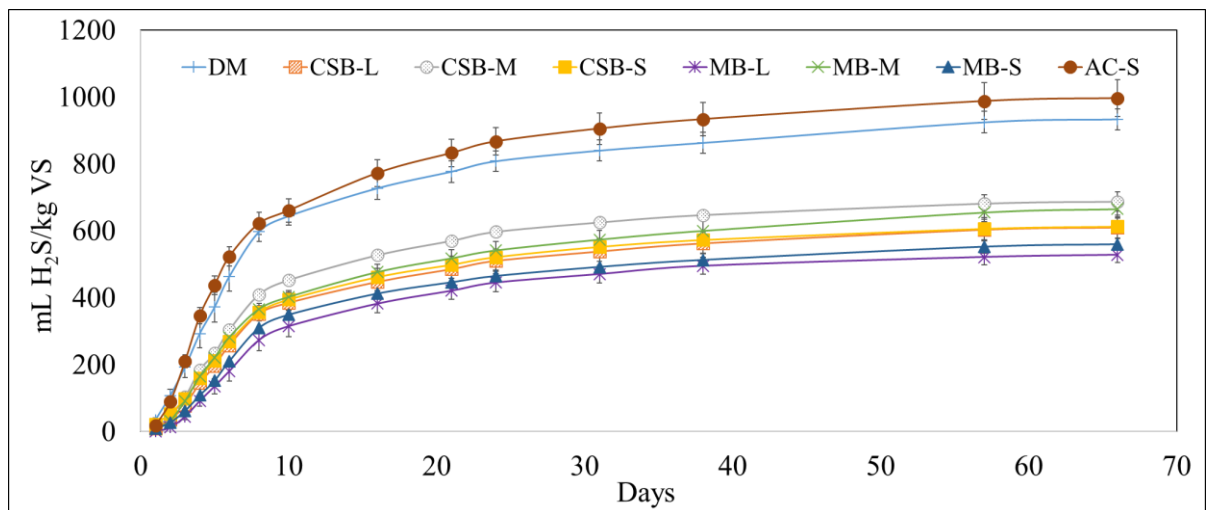


Figure 5.9 Cumulative hydrogen sulfide (H₂S) production normalized by kilograms of volatile solids (VS) with different biochar particle sizes, with dairy manure (DM). Corn

stover biochar (CSB) and maple biochar (MB) coupled with the different tested particle sizes (L,M,S) are used to differentiate each treatment.

Table 5.4 Hydrogen sulfide (H₂S) volume reduction and normalized mass removed per gram of biochar added into the reactor, and percent reductions in comparison to dairy manure (DM).

Treatment	H ₂ S volume reduction (μL)	Normalized H ₂ S reduction (mg H ₂ S/g biochar)	Reduction compared to DM (%)
Corn stover biochar with particles between 841 μm – 707 μm (CSB-L)	329 ± 32.2	0.66 ± 0.06	35
Corn stover biochar with particles between 177 μm – 149 μm (CSB-M)	250 ± 29.1	0.50 ± 0.06	26
Corn stover biochar with particles less than 74 μm (CSB-S)	326 ± 34.0	0.48 ± 0.07	34
Maple biochar with particles between 841 μm – 707 μm (MB-L)	412 ± 23.6	0.65 ± 0.05	43
Maple biochar with particles between 177 μm – 149 μm (MB-M)	273 ± 26.7	0.44 ± 0.05	29
Maple with particles less than 74 μm (MB-S)	380 ± 18.1	0.59 ± 0.08	40

AC addition (996 ± 55 mL H₂S/kg VS) into the reactor did not significantly impact the H₂S concentration in the biogas when compared to the DM control (934 ± 32 mL H₂S/kg VS) (p-value = 0.7938). This result was unexpected, as previous research has shown that AC can be used as an adsorbent for H₂S. However, to the best of our knowledge, the effect of AC on H₂S production when used as a digester additive has not been previously researched. The rate of H₂S production in the AC treated reactors (107 ± 8.2 μL/day) was also significantly higher than the DM control treatments by 24.4% (86 ± 5.5 μL/day) during Day 2 - 5 of incubation (p-value = 0.0225). It has been shown that

certain kinds of sulfate reducing bacteria present in anaerobic digester environments, such as *Geobacter sulfurreducens*, are capable of DIET with GAC as a promoting conductive agent [140]. The results suggest that the interaction of H₂S with AC was following a different reaction pathway than adsorption, but it is not known if the increase in H₂S production rate in the AC amended reactors was due to DIET.

There was no significant impact of particle size differences on the CH₄ production ($0.8668 < p\text{-value} < 1.000$) (Figure 5.10). However, addition of activated carbon led to a significant increase (10.7%) in the normalized CH₄ production (445 ± 3.15 mL CH₄/g VS) compared to DM (402 ± 3.42 mL CH₄/g VS) ($p\text{-value} = 0.0082$). Previous studies have attributed this enhancement in CH₄ production to DIET [113,124]. Additionally, the AC treatment also led to a significantly higher CH₄ production rate (48.2 ± 5.01 mL CH₄/day) compared to DM (30.9 ± 4.06 mL CH₄/day) from Days 2 – 5 ($p\text{-value} = 0.0069$).

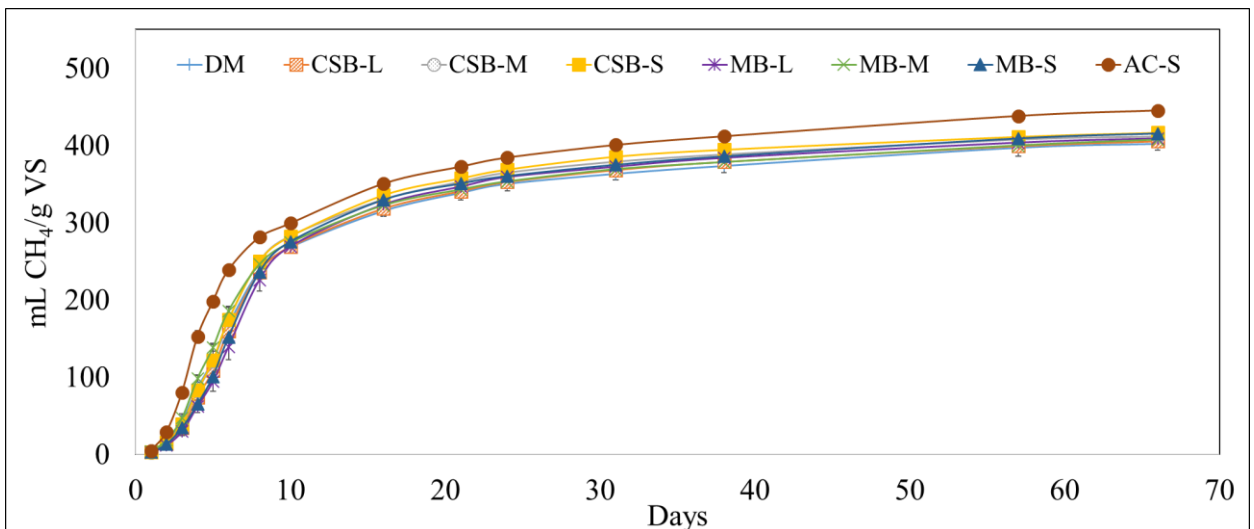


Figure 5.10 Cumulative methane (CH₄) production normalized by grams of volatile solids (VS) for different biochar particle sizes, and dairy manure (DM). Corn stover

biochar (CSB) and maple biochar (MB) coupled with the different tested particle sizes (L, M, S).

A primary concern of adding GAC to anaerobic digesters is the need for separation of the carbon from the digestate prior to use of the effluent as a fertilizer due to the higher cost of the GAC material and advantages of recovery and possible environmental risks with field application [130,141]. To overcome this issue, some authors have investigated the use of biochar, which, has been shown to improve soil properties, and promote DIET. Researchers have found increased CH₄ production rates (22.4 – 40.3 %), shorter lag periods (27.5 – 64.4%) and increase in CH₄ concentrations (~10%) at biochar concentrations varying from 4 g/L to 15 g/L [125,127]. Our results did not show any improvement in lag times, which could be due to the preacclimatization of the substrate used for each batch test in comparison to the previous studies. The dairy manure substrate and the inoculum for this experiment were obtained from the same digester, with negligible lag phase and peak CH₄ concentrations obtained within 2 days. While the amount of biochar added in the present study varied from 0.28 g/L – 9.2 g/L, within the range seen in published literature focusing on DIET, there was not an improvement in CH₄ production, as seen in other studies, only H₂S reduction.

An important controlling factor for DIET is the conductivity of the added biochar/GAC. Biochar used in the current study was prepared at 500 °C with a conductivity of 7.7 μS/cm for MB and 15.4 μS/cm for CSB, whereas, biochar produced at temperatures > 700 °C can have conductivities ranging from 0.5 – 2.3 S/cm due to the increase in conductive graphitic structures [142,143]. This is also supported by results from authors showing that biochar prepared at 900 °C – 1000 °C led to a 28.9 – 30.8%

increase in CH₄ yield, while biochars prepared at 500 °C – 650 °C led to a slight increase or no change in CH₄ production (0.1 – 5.1%) [40].

5.3.5 Effect of biochar surface modification (Experiment 3):

Iron (Fe)-impregnated biochar (CSB-Fe and MB-Fe) led to a significant reduction in the normalized volume of H₂S produced compared to unmodified biochar (p-value < 0.0001). The normalized H₂S production for the Fe-impregnated biochar treated reactors varied from 0 to 51.3 ± 3.7 mL H₂S/kg VS for CSB-Fe and MB-Fe, respectively, compared to DM-only (2025 ± 33 mL H₂S/kg VS), with H₂S removal efficiencies of 100% and 97%, respectively (Figure 5.11; Table 5.5). The Fe-impregnated biochar substrates maintained a consistent average of 98.5% H₂S reduction over time, while the effectiveness of the unmodified biochars decreased over time (Figure 5.12). The incorporation of Fe-impregnated biochar led to an additional Fe loading of 85 and 200 mg/L Fe for CSB-Fe and MB-Fe amended reactors, respectively. Previous research on FeCl₃ as an additive for biogas desulfurization reported the use of 1.25% (12,500 mg/L FeCl₃ or 4300 mg/L Fe) addition for 65% removal of H₂S [144]. Speece (2011) reported that a dosage of 30 – 50 mg FeCl₂/mg S (13.2 – 22 mg Fe/mg S) in the feedstock was practiced in the wastewater industry to precipitate sulfides for odor control, which translates to an iron dosage of 1300 mg/L – 8800 mg/L of Fe required for odor control in a dairy manure digester with sulfur content ranging from 100 – 400 mg/L [13,63]. In the present study, the concentration of Fe added was 85 – 99% lower, but it resulted in an average 98.5% H₂S removal throughout the incubation period.

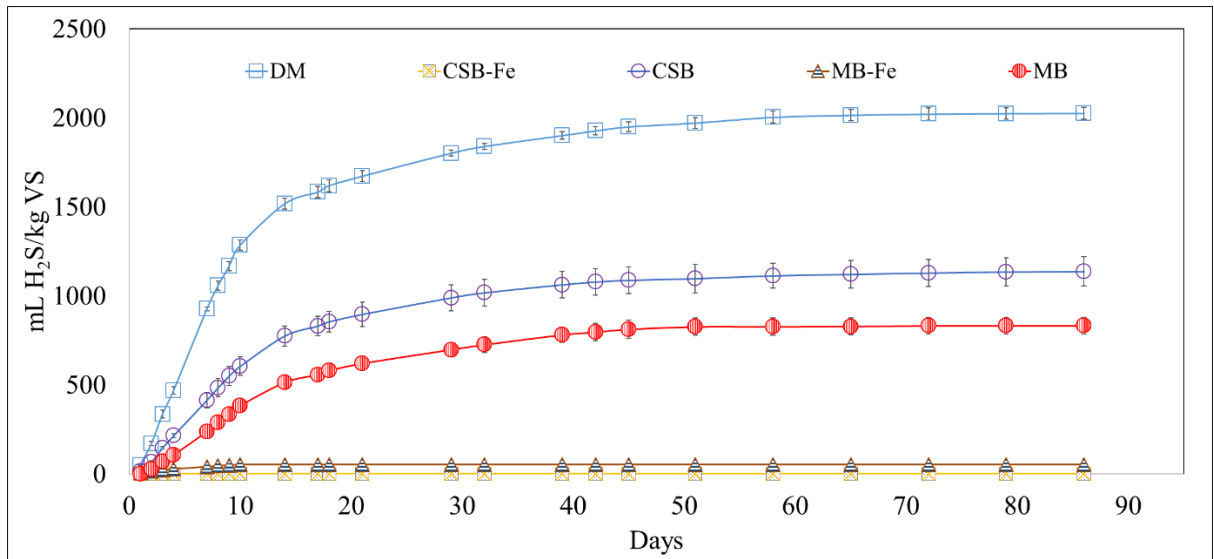


Figure 5.11 Cumulative hydrogen sulfide (H₂S) production normalized by volatile solids (VS) for dairy manure (DM), unmodified and Fe-impregnated corn stover biochar (CSB, CSB-Fe) and maple biochar (MB, MB-Fe).

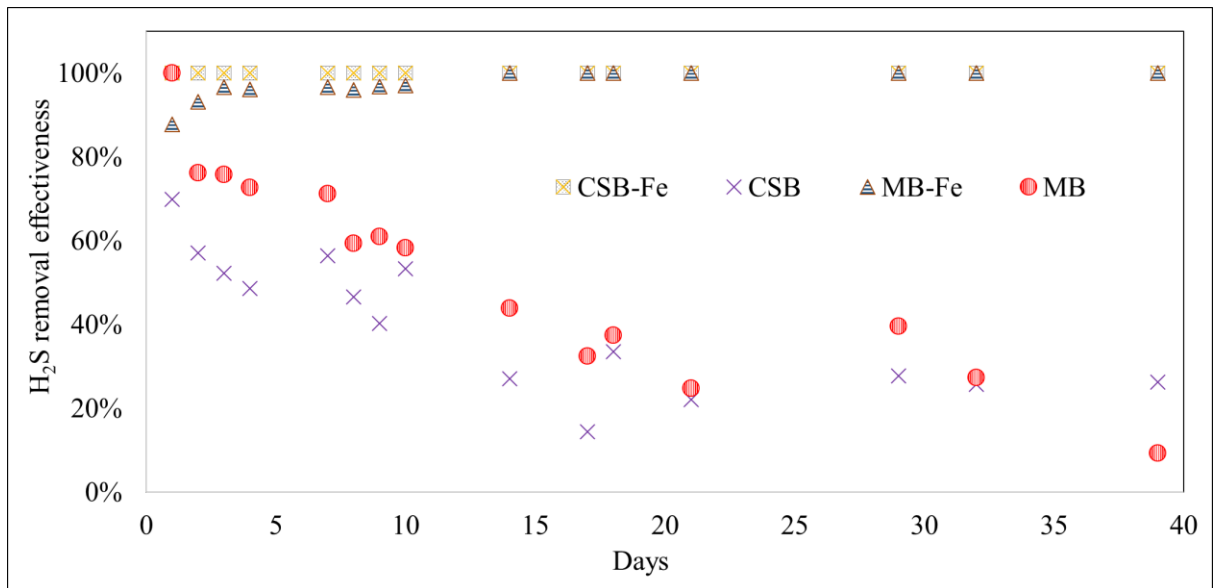


Figure 5.12 Hydrogen sulfide (H₂S) removal effectiveness over time for unmodified and Fe-impregnated corn stover biochar (CSB, CSB-Fe) and maple biochar (MB, MB-Fe).

Table 5.5 Hydrogen sulfide (H₂S) volume reduction and normalized mass removed per gram of biochar added into the reactor, and percent reductions in comparison to dairy manure (DM) digestion.

Treatment	H₂S volume reduction (μL)	Normalized H₂S reduction (mg H₂S/g biochar)	Reduction compared to DM (%)
Iron impregnated corn stover biochar (CSB-Fe)	3440 ± 0	4.6 ± 0.0	100
Unmodified corn stover biochar (CSB)	1509 ± 82	2.0 ± 0.1	44
Iron impregnated maple biochar (MB-Fe)	3350 ± 3.7	4.5 ± 0.0	97
Unmodified maple biochar (MB)	2026 ± 48	2.7 ± 0.1	59

Surface modification using iron-impregnation affected the conductivities of the biochar, however, it was four orders of magnitude lower than biochars prepared at >700 °C seen in other studies (18.3 μS/cm for modified CSB and 44.7 μS/cm for MB). The change in the conductivities did not significantly impact the CH₄ production for the Fe-impregnated biochar treatments (273 ± 6 and 296 ± 11 mL CH₄/g VS for CSB-Fe and MB-Fe, respectively) compared to the DM-only treatment (285 ± 17 mL CH₄/g VS; p-value = 0.7860, 0.8594) (Figure 5.13). All three experiments showed no significant differences on the rate and total CH₄ production due to biochar addition.

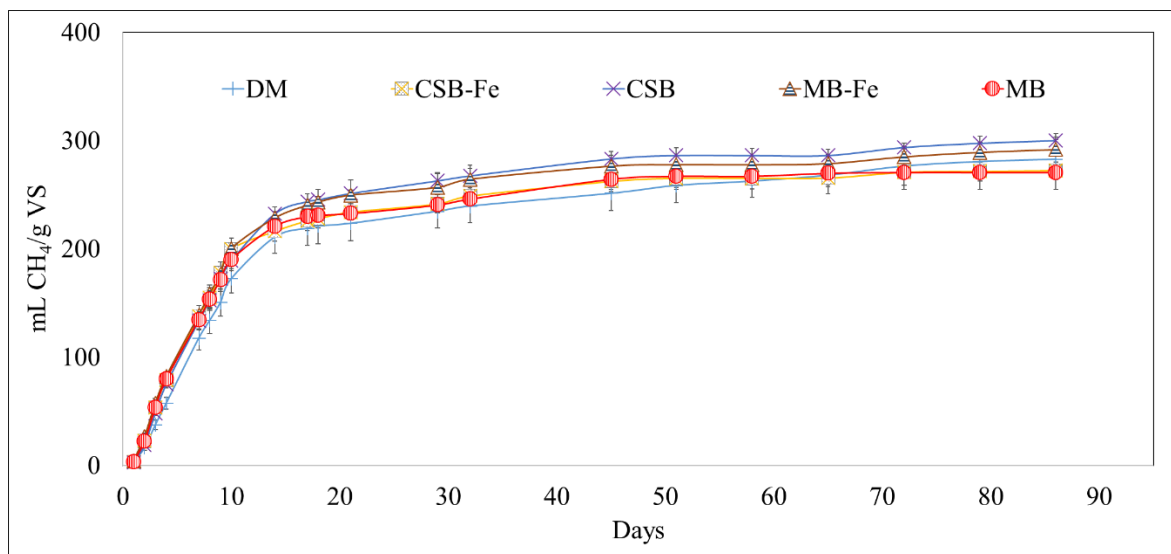


Figure 5.13 Cumulative methane (CH₄) production normalized by volatile solids (VS) for dairy manure (DM), unmodified and Fe-impregnated corn stover biochar (CSB, CSB-Fe) and maple biochar (MB, MB-Fe).

The sorption of anions on the surface of modified biochar has been attributed to chemical adsorption or electrostatic attraction to the positively charged metal oxide particles embedded on the surface [43]. Surface area and selectivity for cations and anions can be changed by the activation (chemical or physical) or surface modification of biochar, which can effect sorption of different pollutants. The high surface area of biochar was suitable for embedding Fe-particles that provided a positive charge and chemical properties to increase H₂S capture. Metal impregnated biochar-based composites have been shown to remove negatively charged anions from aqueous solutions [43,45].

The surface areas of CSB and MB changed upon pretreatment for Fe-impregnation. Iron-impregnation led to a 48% increase in the surface area of CSB (34.9 m²/g) and a 63% decrease in the MB surface area (59.8 m²/g). It has been reported that

pretreatment of biochar using metal chlorides and nitrates results in a modification in the surface area of the biochar [43]. Micháleková-Richveisová et al. (2017) prepared modified biochars from garden wood waste, wood chips, and corncob through pretreatment with $\text{Fe}(\text{NO}_3)_2$, which resulted in a decrease in the surface area of the biochar due to the filling of micro and mesopores with iron [49]. However, van Vinh et al. (2015) prepared Zn-modified biochar prepared from pine cones using a similar pretreatment step and the modification process led to an increase in the biochar surface area [145]. The authors attributed the increase in surface area to the formation of new porous structures from the chemical treatment. Even though surface modification changed the surface areas of the biochars, the effectiveness of Fe-impregnated biochars for arsenic and phosphate removal increased in both studies. In our study as well, the change in the biochar surface area for CSB and MB from Fe-impregnation increased its effectiveness for H_2S removal.

5.3.6 Cost Analysis:

Abatzoglou and Boivin (2009) compared the cost of iron-based adsorbents and sodium carbonate (Na_2CO_3) impregnated AC for a farm producing 1,350 m^3/day of biogas, with 1000 ppm H_2S [19]. The authors reported that the cost per unit of biogas treated would be similar for the two H_2S scrubbing technologies ($\$0.031/\text{m}^3$ biogas treated for Fe adsorbents, and $\$0.034/\text{m}^3$ biogas treated for Na_2CO_3 impregnated AC) based on treating 1.35 m^3 $\text{H}_2\text{S}/\text{day}$ or 1.89 kg $\text{H}_2\text{S}/\text{day}$. Using these same data parameters, it can be calculated that the amount of daily addition of MB-Fe and CSB-Fe into the digester required to desulfurize the biogas (98.5% removal on average) would be 420 kg of MB-Fe, with 84 grams of impregnated Fe, and 411 kg of CSB-Fe, with 33 grams of

impregnated Fe. Thompson et al. (2016) reported that biochar costs range from \$0.35 - \$1.2/kg, with an average value of \$0.78/kg of biochar [101]. The calculated daily cost of biochar for biogas desulfurization would be \$328 and \$321 for MB-Fe and CSB-Fe, respectively. The cost of iron was assumed to be negligible compared to biochar production process since industrial grade (98%) iron chloride costs \$200 - \$500 per ton of material and would only add \$0.05 to the total cost of biochar. When normalized by the amount of biogas treated, the cost was determined to be \$0.24/m³ biogas treated. However, if the biogas is desulfurized in an external scrubber, the costs would be lower since the adsorption capacity would be higher. MB-Fe was estimated to have an adsorption capacity of 16.8 mg S/g biochar (Chapter 4) and in such a case, the normalized cost is estimated to be \$0.06/m³ of biogas treated.

Table 5.6 Cost of hydrogen sulfide (H₂S) treatment currently available desulfurization technology compared to results from this study (values obtained from literature data for biogas flow rate of 1,350 m³/day with 1000 ppm H₂S).

Technology	Cost of H₂S treatment (\$/m³ treated biogas)	Reference
Iron-based adsorbents	0.031	[19]
Impregnated Activated Carbon	0.034	[19]
Biological Desulfurization	0.030	[82]
Impregnated Biochar as an additive	0.24	values obtained from the current study.
Impregnated Biochar adsorbent	0.06	values obtained from Chapter 4.

5.4 Conclusions:

The study showed that biochar can be used in-situ to reduce H₂S concentrations in an anaerobic digestion system. The study showed an increasing trend in the percent reduction of H₂S as the biochar concentrations increased, with the highest tested concentration showing > 90% H₂S removal. Differences in biochar particle size had no significant impact in the H₂S removal efficiency, indicating that the surface area of the biochar is not an important factor for H₂S removal. Iron-impregnation resulted in an average 98.5% H₂S removal efficiency compared to 52% H₂S removal efficiency for unmodified biochars. Furthermore, iron-impregnated biochar addition into a digester was more effective than direct addition of iron chloride compounds at 85 – 99% lower Fe concentrations inputs needed. As expected, the aqueous sulfide adsorption tests resulted in enhanced biochar H₂S adsorption capacities, due to the reaction taking place in an aerobic environment with a long residence time, but the adsorption capacities decreased when the biochar was added into an anaerobic environment with dairy manure, due to a lower residence time, other competing species, and absence of oxygen. Even though previous studies have shown that biochar can be effective in NH₄⁺ and PO₄³⁻ removal in mono-component systems, it was not effective in a dairy manure system due to possible competition with other species. Direct addition biochar into a digester for desulfurization was not cost competitive in comparison to market available H₂S removal technologies. Future studies should further investigate the DIET capabilities of biochar to increase CH₄ production, understand the mechanism controlling H₂S adsorption in impregnated and unimpregnated biochars within the AD system, and increasing the selectivity of biochar for H₂S to make it more cost competitive.

6 Fluidized bed combustion of poultry litter at farm-scale: a case study on the environmental impacts using a life cycle approach

Abstract:

Combustion can concentrate the phosphorus in poultry litter into an ash product that is easier to transport out of the Eastern shore, where land application of poultry litter is limited. The aim of this study was to investigate the efficacy and sustainability of poultry litter combustion through a life cycle assessment (LCA). The combustion process converted 568 tons of poultry litter into 59.3 tons of ash over a sixteen-month period. The thermal energy production was 858.6 MWh, with 12.5 MWh in the form of electricity, and a process efficiency of 55.3%. The two scenarios analyzed for the LCA assessment included 1) the impacts associated with the actual results of the combustion process, and 2) the impacts associated with the process operating under improved operational conditions (increased biomass feed rate (0.246 tons/hr), yearly run-time (6,720 hours), and net positive electricity output). In the first scenario, the climate change potential (CCP) was 32% less than the CCP associated with LPG production and use for heating the poultry houses, but, a lower than expected electrical energy production resulted in net environmental losses in twelve out of eighteen impact categories. The environmental impacts of the second scenario were 48 – 98% lower, when compared to the first scenario. In the sensitivity analysis, the effects of changing the electricity input for operating the FBC system by 10% resulted in the highest overall average (4.8%) change in all impact categories, indicating the necessity of a net positive electrical energy output for an increased sustainability of the process.

6.1 Introduction:

The broiler industry in the US was estimated to produce about 44.4 million tons of poultry manure, containing 2.2 million tons of N, 0.7 million tons of P and 1.4 million tons of K in 2008 [146]. Maryland is the ninth largest poultry producer in the U.S., with the industry providing 41% of all farm income in the state. The Eastern Shore of Maryland in the United States is known for intensive poultry production. The Delmarva Poultry industry estimated a total of 605 million broiler chickens in 2018, generating an estimated 1.1 million tons of litter, bedding, and feathers. It is estimated that 750,000 tons of poultry litter have been remediated or managed alternatively based on the new proposed nutrient management strategies for Maryland from 2000 - 2010 [56].

Poultry litter includes a mixture of manure and the bedding material, including wood chips, waste feed, and feathers removed from poultry houses. The litter and manure component of this waste has a high nitrogen (N) (2.9 - 4.4%), phosphorus (P) (3.2 – 5.5%), and potassium (K) (2.2 – 3.8%) content and is used as an organic fertilizer, thus recycling the nutrients [147–149]. Direct spreading of poultry litter on agricultural farms in Maryland, especially on the Eastern shore, has resulted in phosphorus-enriched soils [57]. Poultry litter contains plant-available nitrogen and phosphorus at a ratio less than 2:1 but the crops grown on the Eastern Shore of Maryland require five times more N than P (on a mass basis) [150]. As a result, land application of poultry litter as an N source simultaneously results in three to four times higher application of P than the crops need. Leaching of nutrients from these soils over the years has contributed to the eutrophication of the Chesapeake Bay [150].

Combustion significantly reduces the mass of a substrate, which makes the final product easier to transport to the fields for fertilization. The concentrated ash form has been shown to be an advantageous soil amendment, with positive effects on plant growth compared to standard fertilizer, as it can be applied separately from an N source to meet the P needs of the crops [151,152]. This can be beneficial for areas such as the Eastern Shore, where application of poultry litter to meet the N needs of the crops leads to overapplication of P. The heating value of poultry litter ranges from 9,000 to 13,500 kJ/kg, depending on the material and moisture content, which is approximately half the value of coal [147,153]. Even though there are challenges to combustion of poultry litter, it has a high energy content and produces an ash product that can be used as a P and K source, making it a valuable resource for valorization.

Commercial combustion of poultry litter to produce heat and electrical energy has been implemented in both Europe and the United States [148]. There has been a growing interest in combusting poultry litter to provide on-farm heating requirements due to increasing propane prices, greenhouse gas (GHG) emissions associated with propane combustion, and eutrophication of water bodies due to leaching of nutrients from land spreading of poultry litter, especially in areas with high N and P in the soil. Kelleher et al. (2002) and Lynch et al. (2013) stated that fluidized bed technology can be used to produce heat and electricity from poultry litter, either by itself or mixed with other domestic or industrial wastes due to its ability to handle low-grade fuels [147,154]. A manure to energy system that generates heat using a fluidized bed combustion (FBC) process was investigated in this study. In the process, the thermal energy generated was used to heat the poultry houses, with excess heat used in an organic Rankine cycle device

(ORC) to produce electricity. The ORC turbine is an advanced power generation technology that uses organic chemicals with low critical temperature and pressure, low specific volume, low viscosity and surface tension, and high thermal conductivity as working fluids [155].

Life cycle assessment (LCA) is an evaluation of environmental impacts through a systematic, inclusive, and analytical approach for any product or service [53]. An LCA quantifies the inputs and outputs of a system, product, service or a process, as defined by a system boundary, and evaluates the environmental impacts for each input and output [54]. LCA is most commonly used in comparing the environmental impact of a product or service with a comparable alternative in order to determine which product has a lower environmental impact [53]. LCA can also be used to estimate the environmental impact of a product at each stage of its life (cradle to grave) in order to identify the process stages that have the highest negative environmental impacts. Billen et al. (2015) conducted a LCA of poultry litter combustion and concluded that surplus electricity production from litter utilization prevented GHG emissions equivalent to 655 kg of CO₂ per metric ton of poultry litter due to avoided impacts from coal combustion [156]. Williams et al. (2016) conducted a LCA of turkey litter combustion and found reductions in energy demand (14%), eutrophication potential (55%), and acidification potential (70%) compared to direct use as a fertilizer [157]. However, these studies were conducted in UK conditions, where poultry litter is managed differently. European regulations require poultry barns with cement floors to be cleaned out completely after each flock is removed. Poultry houses in Maryland have the litter on top of dirt or clay floors instead of cement floors. Since only the top layer of the poultry litter is removed

after each flock, the composition of the poultry litter can be different after each flock [158]. This study also quantified the avoided use of liquefied propane gas (LPG) for space heating the poultry houses in addition to benefits of electricity production from the FBC unit.

The aim of this study was to provide a quantification of the environmental impacts of burning poultry litter for energy generation and utilization. The LCA was used to evaluate and track the effectiveness of the technology in reducing the cradle to grave environmental impacts when compared to the use of LPG for heating the poultry houses. The specific objectives were to: 1) use the material use, emissions, and energy production data obtained from sixteen months of sampling to estimate the environmental impacts of the actual process and compare it to liquefied propane gas (LPG) production and use, and 2) use expected data to estimate the environmental impacts of an improved process scenario. It was anticipated that the environmental impacts of the improved process would be lower than the actual data due to higher electricity production and biomass usage during system operation.

6.2 Methods:

6.2.1 System Description:

A fluidized bed combustion (FBC) system for poultry litter combustion was installed in Rhodesdale, MD designed to produce 600 kW of heat for the poultry houses and 65 kW of electrical energy. The FBC system performance in terms of energy generation, biomass consumption, ash production, time of operation, and litter and ash characteristics was monitored for 16 months.

After each poultry flock, the poultry litter was removed and stored for FBC operation, with excess heat was used for electricity production. The flock dates that were used in the FBC unit are shown below:

- Flock 1: December 17th, 2016 to February 12th, 2017
- Flock 2: March 8th, 2017 to May 4th, 2017
- Flock 3: May 19th, 2017 to July 18th, 2017
- Flock 4: August 1st, 2017 to September 29th, 2017
- Flock 5: October 18th, 2017 to December 18th, 2017
- Flock 6: January 5th, 2018 to March 5th, 2018

The litter was stored in a covered storage shed before being fed into the FBC system using a sensor-controlled scraping system connected to a conveyor belt. The combustion system employed a fluidized bed type technology, where multiple streams of hot air are used to suspend the fuel particles that were combusted within the furnace. The fluidization of the particles leads to an increase in surface area due to the constant turbulence and breaking up of larger particles into smaller sizes [156]. The increased surface area leads to improved contact between the particles and oxygen in air. The ash produced from the combustion process was then transferred to sealed bags for potential transport off-farm for use as a fertilizer or soil amendment.

The thermal energy generated by the combustion of the poultry litter was used to heat up the poultry houses by replacing LPG usage. The excess heat was used to power the ORC for electricity production without additional fuel use or emissions. The electrical energy was used on-farm. It is important to note that the FBC system required electricity

from the grid to operate, and the electrical energy required to operate the system (parasitic load) was higher than the electrical energy generated during the study period.

6.2.2 Analytical Methods:

Triplicate poultry litter samples were tested for calorific value, total solids (TS), and volatile solids (VS) at the University of Maryland. For the calorific value, one gram of poultry litter sample was pelletized using a Pellet Press (Parr Instruments, Moline, IL) and tested for gross heat using a PARR 1261 Bomb Calorimeter (Parr Instruments, Moline, IL). The percent efficiency of the FBC system was calculated by dividing the total generated thermal and electrical energy by the calorific value of the poultry litter obtained from lab test results. The biomass to energy conversion efficiency was calculated by dividing the total amount of energy generated by the total amount of biomass combusted in the FBC system. For TS analysis, triplicate 25 g samples were added into pre-weighed porcelain crucibles. The samples were then dried at 105 °C until a constant mass was obtained for the TS concentration (presented on a wet weight basis in the study). For the VS analysis (presented on a wet weight basis in the study), the crucibles with the dried material were placed in a furnace at 550 °C until a constant mass was obtained between two measurements. The poultry litter, bed ash, and fly ash samples were sent to Agrolabs Inc., Delaware, for the following analyses: organic nitrogen, ammonium nitrogen, nitrate nitrogen, total nitrogen, phosphorus, potassium, sulfur, calcium, magnesium, sodium, manganese, copper, iron, aluminum, boron, zinc, pH, % moisture, % dry matter, % ash, bulk density, % organic matter, % organic carbon, soluble salts, and sodium adsorption ratio using A3769 Method for manure analysis [159]. The carbon to nitrogen (C:N) ratio measurements on the poultry litter samples were conducted

at the USDA facility in Beltsville, MD using a LECO CHN 2000 Analyzer (LECO, St. Joseph, MI).

6.2.3 Impact Assessment Methodology:

This LCA study followed the ISO 14040 and 14044 standards [160,161] which recommends: 1) a clearly defined goal and purpose of the study; 2) a clearly defined scope with a functional unit, system boundary, and impact assessment methods; 3) an inventory of the data used for the analysis that can be related back to the functional unit; 4) sensitivity analyses; 5) categories of environmental impacts analyzed; and 6) a discussion of limitations of the analysis.

The LCA of the FBC system for poultry litter combustion was performed using SimaPro software (Version 9.0). The environmental impacts were estimated using the Recipe 1.10/World (May 2014) midpoint (H) impact assessment method. The following 18 impact categories included in this method were estimated: climate change potential (CCP), ozone depletion potential (ODP), terrestrial acidification potential (TAP), freshwater eutrophication potential (FEP), marine eutrophication potential (MEP), human toxicity potential (HTP), photochemical oxidant formation (POF), particulate matter formation (PMF), terrestrial ecotoxicity potential (TEP), freshwater ecotoxicity potential (FETP), marine ecotoxicity potential (METP), ionizing radiation (IR), agricultural land occupation (ALO), urban land occupation (ULO), natural land occupation (NLO), metal depletion (MD), fossil depletion (FD), and water depletion (WD). The results presented focus on the CCP, TAP, FEP, and MEP due to its relevance to renewable energy production from waste resources and the health of the Chesapeake Bay region.

6.2.3.1 Goal and Scope of the study:

The goal of the study was to quantify the environmental impacts of generating heat and electricity from the combustion of poultry litter. The scope was from cradle to grave, including storage of poultry litter and its combustion, production of heat, conversion of the generated heat into electricity using the ORC system, and co-production of ash as a fertilizer (Figure 6.1). Construction materials and assembly of the plant were also considered in the model (Ecoinvent version 3.0). Transport of the poultry manure to the FBC system was not included in the study, as the FBC was located at the farm site and did not require additional transportation for use. During the study period, the litter and the ash produced from the combustion process was never transported out of the farm, and hence, not included in the LCA assessment.

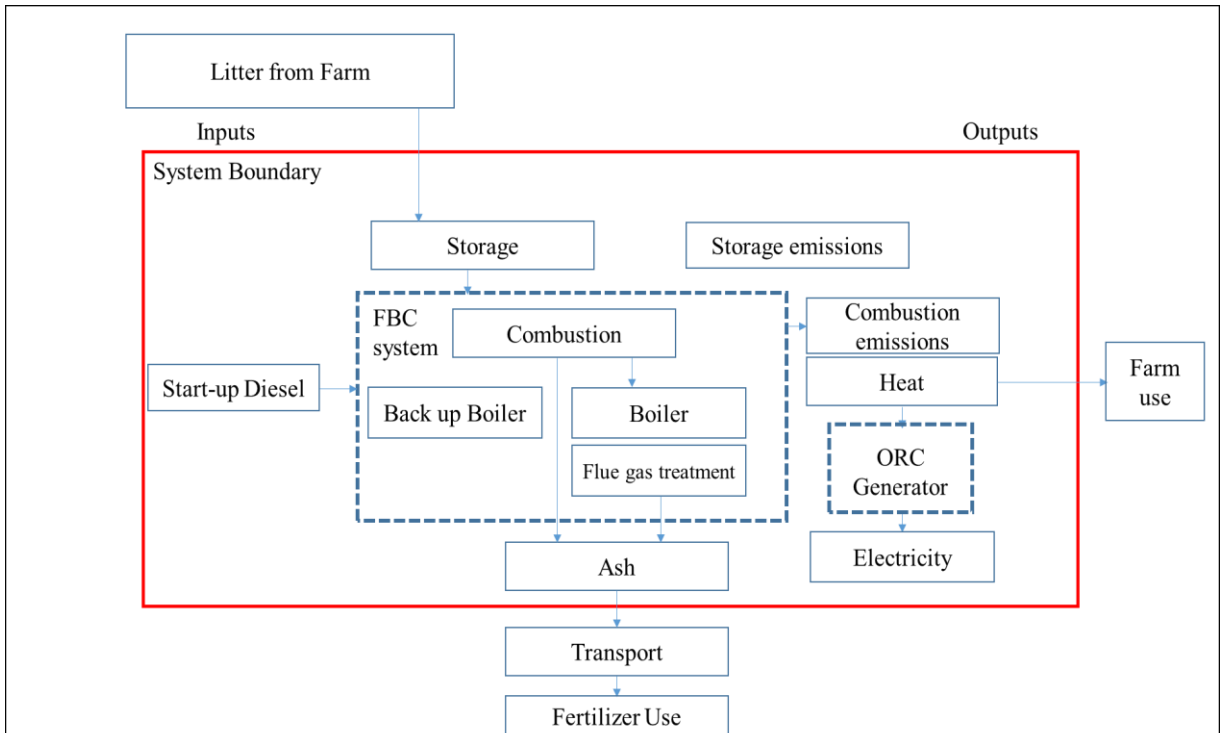


Figure 6.1 System boundary of the combustion of poultry litter for heat and electricity production.

The impacts of manure production were also not included in the study, as poultry is bred for meat and eggs and not for the manure. As such, the impacts associated with poultry production would be the same for all the studied scenarios [156]. Two main scenarios were considered for the impact assessment:

1. Baseline scenario: impacts from the actual operating conditions and outputs of the FBC unit monitored over the study period was used.
2. Improved operational scenario: Assumed that the FBC system operated for 6,720 hours annually (77% annual runtime, instead of 30% in the baseline scenario), combusted 1,655 tons of poultry litter annually at a 0.246 tons/hr feed rate (instead of 0.176 tons/hr in the baseline scenario), and a net positive electricity output.

The Maryland electricity average consumption data from EIA in 2017 was used for the analysis, with the generation source estimated to be a combination of coal, natural gas, and nuclear power (approximately 2:1:1 ratio) [162]. The impacts of these two scenarios were compared to the impacts associated with the production and use of liquefied propane gas (LPG) to generate the same amount of energy, as conventionally propane was historically used to heat the poultry houses.

The functional unit for the impact assessment was defined as the ‘generation of 1 MJ of energy’. The input and output flows of the system were calculated based on the total amount of energy produced from poultry litter combustion after 16 months of monitoring. During this time, the FBC system operated for 3,226 hours and processed a total of 568 metric tons of poultry litter, with a maximum of 198 tons processed during flock 1 and a minimum of 38.5 tons processed during Flock 4.

6.2.3.2 LCA inventory:

The poultry litter storage emissions were not monitored, and therefore, literature data was used to obtain ammonia (NH₃) and nitrous oxide (N₂O) emissions [163]. Methane (CH₄) emissions from storage were assumed to be negligible [164]. Emissions of carbon dioxide (CO₂), carbon monoxide (CO), sulfur dioxide (SO₂), oxides of nitrogen (NO and NO₂ combined as NO_x), particulate matter (PM), and volatile organic compounds (VOCs) from the FBC process were obtained from the emissions testing data from an independent third-party contractor using USEPA Reference test methods 1-2, 3A, 4, 5/202, 6C/7E, 10, and 25A (Table A.2). N₂O emissions were obtained from literature data related to combustion of poultry litter in FBC systems [156]. CO₂ emissions were considered to be biogenic as the organic carbon in poultry litter is of biogenic origin and the renewable energy generated can replace energy from fossil fuels [156]. Diesel use for FBC start-up was obtained from data logs. For the comparison, it was assumed that a unit of energy from poultry litter is equivalent to a unit of thermal energy from LPG and electrical energy from the grid. Sand use in the FBC system was obtained from literature data of a similar poultry litter combustion system in Netherlands [165]. The impacts associated with the LPG production and use, sand use, and diesel use were obtained from the Ecoinvent version 3.0 database in SimaPro. The LCA inventory data for all the data are shown in the Appendix B.

6.2.3.3 Sensitivity Analyses:

In the sensitivity analysis, each variable of interest (electricity use for FBC operation, startup diesel for bringing the FBC system up to temperature, combustion emissions, emissions from poultry litter storage, and construction material input) was

modified by $\pm 10\%$, while keeping the other variables constant for the baseline scenario. The percent change in environmental impact in each impact category for every variable of interest was then calculated by comparing it to the environmental impacts in the original baseline scenario.

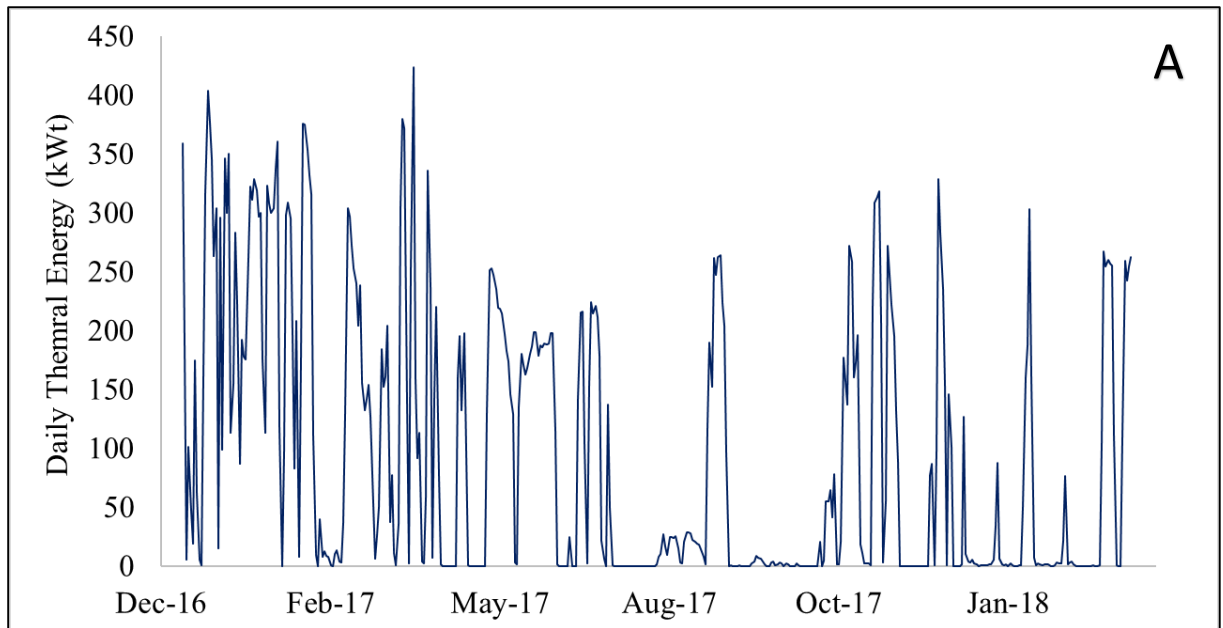
6.3 Results and Discussion:

6.3.1 Energy production from the FBC system:

The total energy supplied to the two poultry houses for heating the six flocks was 1,504,727 kWh, which included energy from the FBC unit (858,569 kWh) and energy from back up diesel use when the FBC unit was not operational (646,158 kWh) (Table 6.1). The thermal energy production from the FBC unit was more continuous during the initial project period (Flocks 1 – 2 from Dec 2016 – May 2017), with the highest runtime (853 hours), biomass use (198 tons), and amount of energy produced (299,584 kWh) during Flock 1 (Figure 6.2A). The FBC operated for a total of 3,226 hours and combusted 568 tons of poultry litter, with an average feed rate of 0.176 tons/hr. During Flock 4, the FBC had the lowest runtime (211 hours), thermal energy production (58,186 kWh), and biomass use (38.5 tons) due to repairs and maintenance work on the system. The electrical energy production ranged from 0.7% to 4.0% of the total energy produced per flock, with a cumulative electric energy production of 12,527 kWh during the study period, with most of the potential energy from the poultry litter used for heating the houses and not delivered to the ORC (Figure 6.2B).

Table 6.1 Energy production from the fluidized bed combustion (FBC) system over the six flocks tested.

Flock	Runtime (hours)	FBC Total Thermal Energy (kWh)	FBC Total Electrical Energy (kWh)	Farm Energy (kWh)	Biomass Use (Metric ton)	Biomass to Energy Conversion Efficiency (kWh/ton biomass)	Efficiency (%)
1	853	299,586	2,144	648,219	198	1523	54.9
2	631	156,031	1,400	256,858	103	1525	55.0
3	819	138,836	3,098	128,033	91.8	1546	55.7
4	211	58,186	2,157	61,722	38.5	1568	56.5
5	482	140,821	1,000	340,278	93.2	1523	54.9
6	229	65,110	2,727	69,618	43.1	1575	56.8
Total	3,226	858,569	12,527	1,504,727	568	1534	55.3



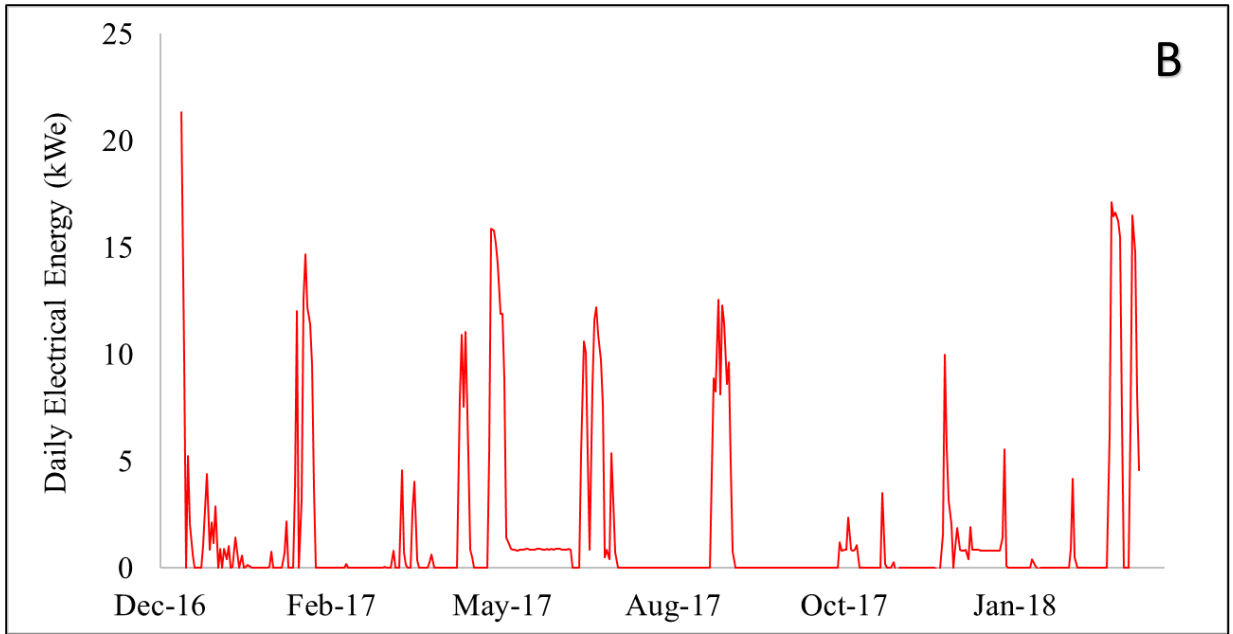


Figure 6.2 Daily thermal (A) and electrical (B) energy production from the fluidized bed combustion (FBC) unit used to heat two poultry houses and provide electricity over sixteen months (six flocks) of monitoring.

The energy efficiency of the FBC system was consistent, with an average of 55.3% of the calorific value of the poultry litter converted into total energy, with an average energy output of 1,534 kWh/ton poultry litter combusted. The parasitic electric load for operating the FBC unit (131,072 kWh) was higher than the electricity generated during the study period, with a net negative electricity output (-112,700 kWh). It was anticipated (improved operational scenario) that the FBC system would operate for 6,720 hours annually (77% annual runtime), and utilize 1,655 tons of poultry litter annually at a 0.246 tons/hr feed rate, resulting in an energy production efficiency of 67.4%, and a biomass to energy conversion efficiency of 1,985 kWh/ton poultry litter combusted. Cotana et al. (2014) reported that in practical applications of small-scale biomass fueled

ORC systems (< 30 kW_e capacity), the thermal energy production efficiency varied from 60% - 70%, along with 15% efficiency in electricity production [155].

6.3.2 Poultry Litter and Ash Product Characteristics:

The heating value of the poultry litter varied from 2,055 to 2,737 cal/g, while the VS content varied from 40.1% to 56.7%. The two parameters followed a similar trend, with higher VS fractions leading to higher heating values (Figure 6.3). The dry matter content of the poultry litter averaged 60.8%. Percent carbon varied from 21.66% to 27.55%, while the percent nitrogen varied from 2.77% to 3.42%. The average values for these parameters are shown in Table 6.2 The FBC process concentrated the phosphorus and minerals in the poultry litter in the final ash product, as expected, with an average concentration increase of 459% in the bed ash and 633% in the fly ash (Table 6.3). The potassium (2.40% ± 0.1) and phosphorus content (1.98% ± 0.1) in the poultry litter formed a substantial part of the fly ash product (15.0% ± 1.1 for phosphorus and 19.4% ± 1.4 for potassium), with negligible concentrations of carbon and nitrogen. Chastain et al. (2012) calculated the average poultry litter heating value from literature data to be 2,461 cal/g with a moisture content of 24% [148]. The total percent N (2.87%), P (3.28%), and K (2.87%) in their study were similar to the present study as well.

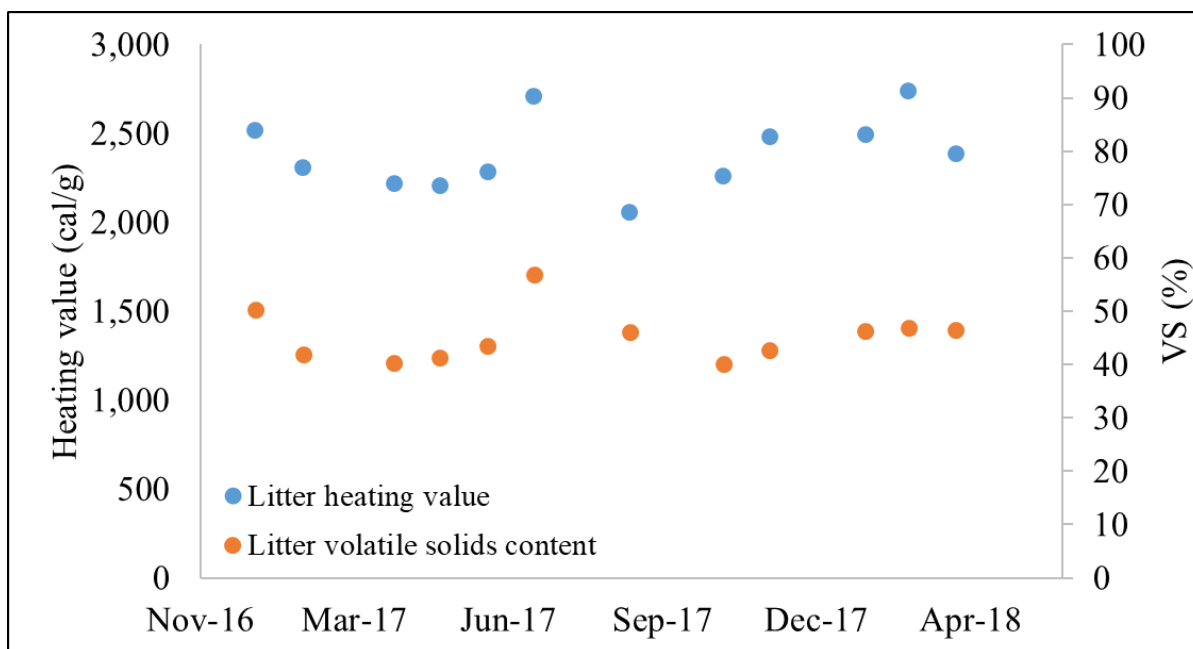


Figure 6.3 Heating value and volatile solids (VS) variation over the 16 months of sampling.

Table 6.2 Average physical characteristics (wet weight basis) of the poultry litter input to the fluidized bed combustion unit during the sixteen-month study.

TS (%)	VS (%)	Carbon (%)	Nitrogen (%)	C:N ratio	Gross Heat (cal/g)
60.8 ± 1.5	45.1 ± 1.4	23.9 ± 0.5	3.1 ± 0.1	7.8 ± 0.2	2386 ± 60

Table 6.3 Elemental composition of the poultry litter, bed ash, and fly ash, and percent change in the bed ash and fly ash compared to the poultry litter substrate.

Elements	Poultry Litter	Bed Ash	Fly Ash	Change in bed ash (%)	Change in fly ash (%)
Phosphorus (%)	2.0 ± 0.1	13.4 ± 1.5	15.0 ± 1.1	577	658
Sulfur (%)	0.7 ± 0.0	3.4 ± 0.3	4.4 ± 0.3	379	520
Potassium (%)	2.4 ± 0.1	11.4 ± 1.2	19.4 ± 1.4	375	708
Sodium (%)	0.6 ± 0.0	3.0 ± 0.3	4.6 ± 0.3	376	630
Calcium (%)	1.7 ± 0.2	9.1 ± 1.0	9.3 ± 0.8	423	434

Magnesium (%)	0.50 ± 0.1	2.3 ± 0.3	2.7 ± 0.2	369	451
Zinc (ppm)	469 ± 22	2274 ± 288	2565 ± 168	385	447
Iron (ppm)	548 ± 92	3506 ± 186	4515 ± 174	540	724
Manganese (ppm)	355 ± 21	1840 ± 232	2256 ± 146	418	535
Copper (ppm)	254 ± 13	938 ± 87	1767 ± 147	269	596
Aluminum (ppm)	206 ± 23	2131 ± 153	2810 ± 116	934	1264

The FBC system combusted 568 tons of poultry litter and converted it to 59.3 tons of ash, which is 10.5% of the original mass of poultry litter. Plant macronutrients with a fertilizer value, namely, K, and P in the poultry litter were also concentrated in the ash product. The bed ash and fly ash had an average P content of 13.4% and 15.0%, respectively, and an average K content of 11.4% and 19.4%, respectively. Most of the P (63%) and K (72%) were concentrated in the fly ash fraction. The ash contained negligible concentrations of carbon (C) and nitrogen (N), as the combustion process resulted in complete conversion of C and N into its gaseous forms (CO, CO₂, NO_x, and N₂ gas). On a per ton basis, the wet poultry litter contained 31 kg of N, 19.8 kg of P and 24 kg of K. The bed ash and fly ash formed 39.6% (23.5 tons) and 60.4% (35.8 tons) respectively, of the total ash produced. The bed ash contained 134 kg of P (as P₂O₅) and 114 kg of K (as K₂O) on a per ton basis, while the fly ash contained 150 kg of P (as P₂O₅) and 194 kg of K (as K₂O) on a per ton basis. The mixed ash product (bed ash + fly ash) contained an estimated 144 kg of P (as P₂O₅), and 163 kg of K (as K₂O), with negligible concentrations of N on a per ton basis (Table A.1).

6.3.2 Life Cycle Environmental Impacts:

6.3.2.1 Climate Change potential:

The climate change potential of poultry litter combustion corresponded to 0.053 kg CO_{2eq}/MJ of energy, which was 32% less than the CCP associated with LPG production and use (0.078 kg CO₂ eq/MJ of energy) (Table 6.4; Figure 6.4). When converted to a mass basis, the total CCP impact due to GHG emissions (N₂O and CO) corresponding to the combustion of one kilogram of poultry litter was 0.0775 kg CO₂ eq/kg poultry litter combusted. N₂O emissions from the combustion process (0.260 g/kg PL) and storage emissions (0.070 g/kg PL) had the highest contribution to CCP, as N₂O is 298 times more potent GHG than CO₂. On the other hand, CO is a weaker GHG compared to CO₂, and the CO emissions (0.750 g/kg PL) had a minimal impact on CCP.

Table 6.4 Impact on climate change potential from poultry litter combustion, electricity production and liquefied propane (LPG) use for heating based on 1 MJ of energy. A negative value indicates a net positive environmental impact.

Scenario	Baseline	Improved operation
Impact category	Climate change	
Functional Unit	1 MJ of energy	
Unit	kg CO ₂ eq	
Combustion emissions only	0.014	0.011
Poultry litter storage only	0.039	0.003
Combustion unit and generator	0.002	0.0004
Startup diesel use	0.005	0.004
Electricity use from grid	0.028	0
Combustion of Poultry Litter (total)	0.053	0.018
Renewable electricity production	0	-0.005
LPG production and use	-0.078	-0.074

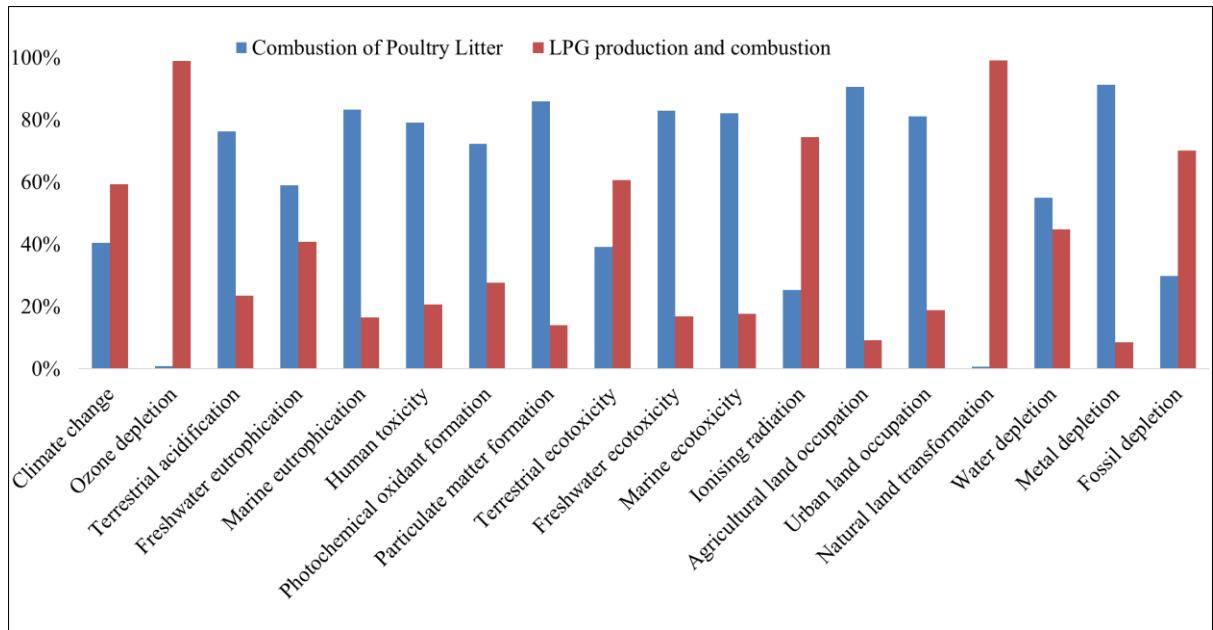


Figure 6.4 Environmental impacts of poultry litter combustion in the baseline scenario compared to LPG production and combustion.

The total impact of combusting poultry manure on climate change was a combination of direct emissions of GHGs and upstream emissions originating from the construction and assembly of the plant, emissions associated with storage of poultry litter, start-up diesel use, and electricity required for daily operation of the FBC system. It was expected that the FBC system would produce excess electricity, especially during the summer when heating requirements for the poultry houses are lower. However, due to the system not performing at its highest efficiency throughout most of the study period, the electricity produced was not sufficient to offset the parasitic load required for daily operation of the system. As a result, the net electricity input had the highest impact on CCP (53.1%) for the combustion of poultry litter. The electricity input accounted for GHG emissions of 0.028 kg CO₂ eq/MJ of energy. Emissions associated with poultry

litter storage and start-up diesel use contributed to 7.3% and 8.9% of the GHG emissions, respectively.

In the improved operational scenario, the combustion process had 66% less impact (0.018 kg CO₂ eq/MJ of energy) on CCP than the baseline scenario due to the increased biomass feed rate, yearly run-time (6,720 hours), and energy output/biomass feed ratio. The expected energy output/biomass feed ratio was 1,985 kWh/ton of poultry litter in the improved operational scenario, while it was 19.4% lower (1,512 kWh/ton of poultry litter) in the actual scenario. As a result, the amount of poultry litter required to produce 1 MJ of energy decreased from 0.184 kg to 0.140 kg in the improved operational scenario. The increased thermal energy output avoided impacts on CCP corresponding to 0.074 kg CO₂ eq/MJ of energy due to the replacement of LPG production and use (Figure 6.5).

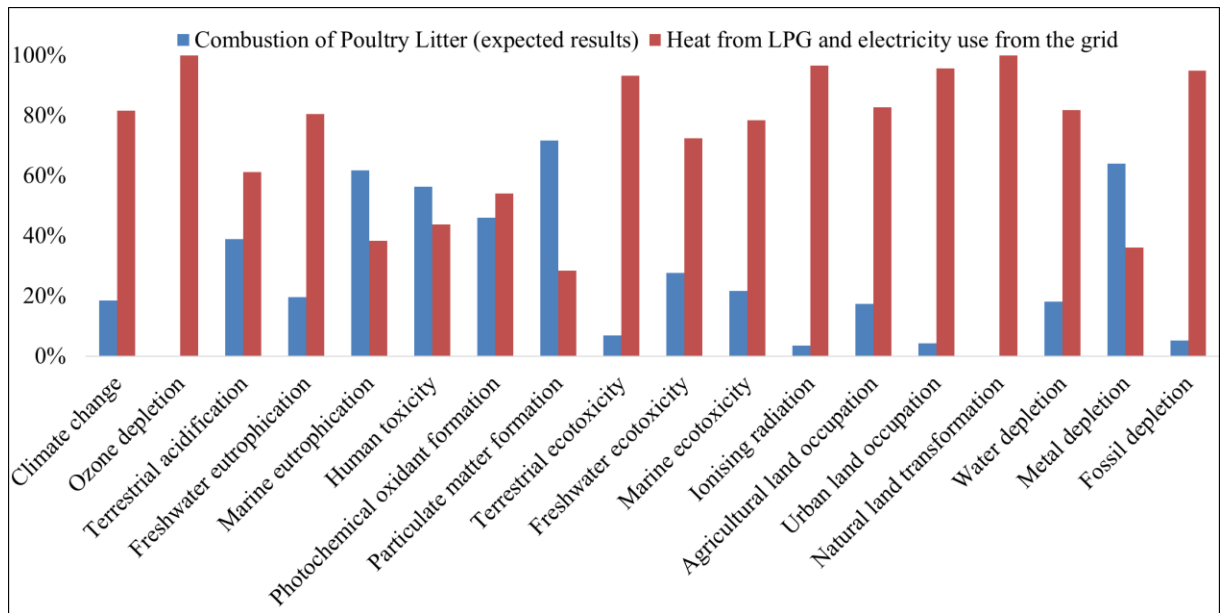


Figure 6.5 Environmental impacts of poultry litter combustion with renewable energy production in the improved operational scenario compared to LPG production and combustion and replacement of electricity production in Maryland.

The other important factor was the increased total electrical energy output in the improved operational scenario (181,104 kWh), which was 5.51% of the total energy produced in this scenario. As a result, the FBC system had a net electrical energy output of 68,404 kWh (after parasitic load subtraction). The excess renewable electricity led to avoided impacts on CCP from the production of electricity from fossil fuel sources (0.005 kg CO₂ eq/MJ of energy). The contribution of combustion emissions to CCP was the highest in the improved operational scenario (60.7%), followed by start-up diesel use (20.4%), and emissions from storage (16.4%).

Williams et al. (2016) found a net 3% decrease in CCP from burning turkey litter due to the use of natural gas for electricity production [157]. However, they included the loss of soil carbon from not applying the litter on land in their analysis and suggested that this led to the net effect being minimal. Billen et al. (2015), however, argued that the loss of soil carbon has no negative impact as it was not clear if carbon fertilization was necessary in most cases [156]. In addition, they also stated that carbon neutral sources for increasing organic matter content, such as compost, are easily available at low prices. In their assessment, the combustion of poultry litter resulted in avoided impacts from electricity from coal, corresponding to 655 g CO₂ eq/kg of poultry litter. In the case of natural gas use for electricity production, the avoided impacts corresponded to 357 g CO₂ eq/kg of poultry litter. In the present study, instead of electrical energy, the avoided impacts were associated with offsetting thermal energy from LPG corresponding to 424 g CO₂ eq/kg of poultry litter.

6.3.2.2 Eutrophication and Terrestrial Acidification potential:

The ReCiPe model makes the assumption that marine eutrophication is most affected by the leaching of different forms of N into the ocean, while freshwater eutrophication is attributed to the leaching of different forms of P. Gaseous species of N such as ammonia and NO_x have lower impacts on MEP but have the highest impact on TAP along with SO_x. The Chesapeake Bay is not considered to be fresh or marine but a brackish water body, so both FEP and MEP need to be highlighted in the study.

In the baseline scenario, electricity usage from the grid had the highest impact on MEP (5.0×10^{-6} kg N eq/MJ of energy), followed by NO_x emissions from the combustion process (3.0×10^{-6} kg N eq/MJ of energy), and NH₃ emissions from poultry litter storage (2.95×10^{-6} kg N eq/MJ of energy) (Table B.1; Figure B.1). FEP was primarily affected by the material use for the FBC system (78.5%) followed by electricity use for its operation (20.6%). The overall TAP corresponded to 4.1×10^{-4} kg SO₂ eq/MJ of energy and it also followed a similar trend with electricity use for FBC operation having the highest contribution (64.3%), followed by NH₃ emissions from storage (19%), and NO_x and SO_x emissions from the combustion process (10.6%).

Poultry litter has low amounts of sulfur (0.71%) and up to 90% of sulfur present in poultry litter can react with the oxides of calcium produced during the combustion process to form Ca-S complexes [153]. As a result, the emission of SO_x from poultry litter combustion (0.005 g/kg PL) is significantly lower than emissions from coal combustion (0.830 g/kg PL) [147,156]. The flue gas from the combustion process also had lower concentrations of NO_x (0.42 g/kg poultry litter), compared to coal combustion (1.1 g/kg poultry litter), but more than the emissions from natural gas combustion (0.34

g/kg poultry litter) [156]. However, due to the electricity requirement to operate the FBC unit, the total TAP and MEP of the combustion process had 69% and 80% higher impacts, respectively, when compared to LPG production and usage, resulting in a net negative environmental impact (Figure 6.5).

In the improved operational scenario, TAP and MEP were reduced by 74.6% and 58.3%, respectively, compared to the baseline scenario. As a result, a net environmental benefit of 6.1×10^{-5} kg SO₂ eq/MJ of energy was seen in TAP, but the increased efficiencies were not able to offset the impacts on MEP due to the volatilization of NH₃ from storage and NO_x emissions from the combustion process (Figure A.4). Freshwater eutrophication potential was 30.7% higher in the baseline scenario compared to the use of LPG, but due to the improved efficiencies and a net positive electricity production in the improved operational scenario, the FEP associated with the combustion process was 75.7% lower than the impacts associated with LPG and electricity use from the grid.

6.3.2.3 Other Environmental Impact categories:

The results for the other environmental categories for the baseline scenario (Figure A.1) show that the electricity use for plant operation and the material use for the FBC unit were the main contributors to all the impacts, except for PMF. Combustion of poultry litter in the FBC unit had the highest contribution towards PMF, due to emissions of particulate matter < 10 µm, SO₂, and NO_x. Human toxicity potential was most affected by the material use and the start-up diesel use for bringing the FBC to its optimum temperature. Ozone depletion potential was also affected by the material use due to the use of a fluorocarbon refrigerant in the heat exchanger system, but emissions are expected to be negligible during the lifetime of the system due to the airtight enclosure

surrounding the heat exchanger system. As expected, steel and aluminum use in the construction of the FBC unit had the highest contribution towards MD (89%). When compared to the avoided production and use of LPG for heat production, a net environmental gain was only observed in six (CCP, ODP, TEP, IRP, NLT, and FD) out of the eighteen impact categories.

In the improved operational scenario, the material usage in the construction of the FBC unit had the highest contribution in nine out of the eighteen impact categories, followed by start-up diesel use in four out of the eighteen categories (Figure B.2). The reduction in all other environmental impacts due to the improved efficiencies in the improved operational scenario ranged from 48 – 98% when compared to the actual conditions in the first scenario. Due to the higher electricity production in the improved operational scenario, a net environmental gain was observed in fourteen out of the eighteen impact categories, indicating the necessity for improved efficiencies for heat and electricity production when operating the FBC unit.

6.3.3 Sensitivity Analysis:

The effects of changing the electricity input for running the FBC system resulted in the highest average (4.8%) change in the impact category values, while the emissions from the litter storage had the lowest average change (0.4%) (Table 6.5; Figure 6.6). The litter was only stored for two weeks before being utilized for energy generation, leading to comparatively lower N₂O and NH₃ emissions. The 10% change in electrical energy input resulted in a 7.9% change in FD due to the use of coal and natural gas for electricity production in Maryland. Both the combustion emissions from the FBC process and electrical energy input resulted in a 5.3% change in CCP, which was the highest impact

out of all the variables tested. The material of construction had the highest impact on metal depletion, as expected. Freshwater eutrophication potential was also primarily affected (7.9% change) by the material of construction, while MEP was equally impacted by the electrical energy input, and the combustion emissions containing nitrogen. As previously discussed, the ReCiPe model attributes marine eutrophication to different forms of N emissions into the ocean, while freshwater eutrophication is attributed to different forms of P. The sensitivity analysis provided support to the notion that improved efficiencies for heat and electricity production would lead to a more sustainable process, as it would eliminate the impacts associated with the electrical energy input for FBC operation.

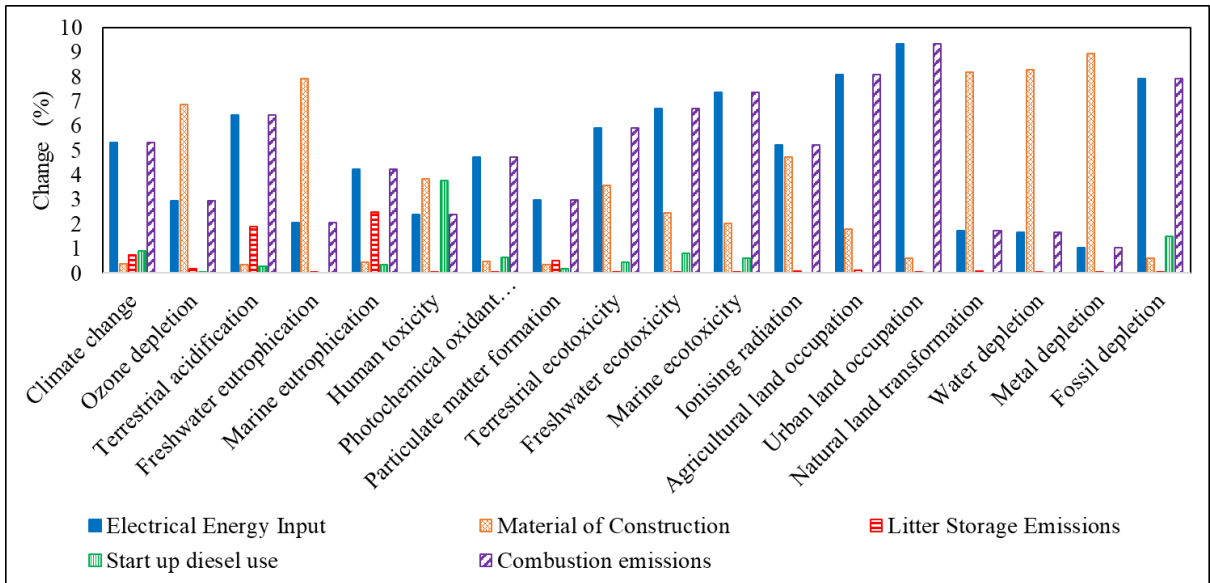


Figure 6.6 Percent change in impact categories upon 10% change in the five variables tested for the sensitivity analysis.

6.4 Land Application Considerations:

Even though several studies have been conducted on alternative disposal technologies for poultry litter, peer-reviewed articles on LCA of these technologies are limited. Billen et al. (2015) and Williams et al. (2016) conducted LCA analyses on poultry litter combustion and turkey litter combustion, respectively, while Jeswani et al. (2019) conducted an LCA assessment on poultry litter gasification [156,157,166]. All authors concluded that combustion and gasification of poultry litter were attractive alternatives to land application, especially in areas with areas with high concentration of poultry farms. However, it is difficult to ascertain if such alternative waste disposal technologies can lead to environmental benefits, if the poultry industry was not as concentrated in certain areas [157]. Poultry litter application on land in areas that are deficient in nutrients such as N and P would be the preferred mode of disposal, as it can offset the use of inorganic fertilizers such as urea and triple superphosphate. In addition, PL increases soil organic matter, leading to improvement of both the physical and chemical attributes [153].

Unmanaged and excessive agronomic utilization of poultry litter can, however, result eutrophication of water bodies, spread of pathogens, and GHG emissions. The primary pathways for these environmental concerns include leaching losses of soluble P, NH_4^+ , and NO_3^- to water bodies, emissions of N_2O and NO_x , and buildup of heavy metals into the soil [146]. In addition, ammonia volatilization also results in N losses, especially within the first two weeks of land application [167]. According to Meisinger and Jokela (2000), ammonia losses from poultry litter can vary, in the range of 20-45% of total ammonia nitrogen (TAN), while Wolf et al. (1988) reported a loss of 37% of total N in

the form on NH_3 when the poultry litter was surface applied [168,169]. However, the percent loss decreased to 1 – 8 % of the total N when the litter was incorporated into the soil. The factors that determine the loss of ammonia from land application of manure are dependent on manure characteristics, application management, soil conditions, and environmental factors [168].

Leaching losses of soluble P, NH_4^+ , and NO_3^- to water bodies also depend on several parameters, as described above for NH_3 emissions to air. As a result, obtaining emission data for land spreading of manure is not straightforward and subject to large uncertainties. The other important thing to consider are all the emissions associated with the use of inorganic fertilizer that should be subtracted from the emissions associated with land application of poultry litter in order to understand its environmental benefits. Ammonia emissions associated with inorganic fertilizer use are also dependent on the amount and type of fertilizer, soil pH, wind speed and application method, while the N_2O and NO emissions are dependent on the water filled pore space, among other factors [170].

Furthermore, the use of poultry litter as a fertilizer also avoids the production of N, P, and K fertilizer that have significant environmental impacts in all impact categories. While the use of poultry litter ash can be a substitute for phosphorus and potassium fertilizers, it cannot offset the environmental burdens associated with inorganic N fertilizer production and usage. Due to all the uncertainties and complications associated with the use of poultry litter and poultry litter ash as a fertilizer, it was excluded from the impact assessment and the focus of the study was directed towards the impacts associated with the combustion process only.

It should be noted that poultry manure ash has several advantages over untreated manure due to its value as a P and K fertilizer that is 75% – 90% less bulky which makes it easier to transport [57,156]. The absence of nitrogen in the ash prevents harmful gaseous emissions of NH_3 and N_2O , while also allowing for its application separately based on only the P needs of the soil, thus reducing potential P run-off that could have resulted from the application of the litter on the basis of N requirements for the crop. Furthermore, the low percentage of water-soluble inorganic P (1.45%) in the ash compared to raw poultry litter (55%) could potentially lead to reduced run-off when used as a fertilizer or soil amendment [57]. Codling et al. (2002) showed that even with the low concentration of water-soluble P, it was an effective P fertilizer for crops [171]. The LCA assessment does not take pathogen destruction into account. Poultry manure may cause diseases due to emissions of pathogens into air and water after land application and [156,167]. Even though land application of poultry litter has rarely been associated with foodborne outbreaks, the combustion process does produce a pathogen-free ash product and flue gases due to temperatures in excess of 850 °C inside the furnace. This should be taken into consideration when alternative poultry litter management technologies are analyzed for sustainability, especially in areas with a high concentration of poultry farms [172].

6.5 Limitations of the study:

As previously mentioned, the study only focused on the FBC combustion process, and as such, it is limited in scope as it does not take the implications and emissions associated with the land application of the poultry litter and the ash byproduct into account. One of the most important results from the analysis was that the use of this

technology by itself can help reduce impacts on climate change potential, but a more complete analysis of the impacts on land application would provide a better understanding on how the process can affect climate change. It is also important to note that the LCA assessment was conducted on a demonstration project that did not function as expected. Even though the study incorporated an improved operational scenario, it is likely that a fully functional FBC system would result in energy production and operational efficiencies that varies from the two scenarios analyzed in this study. Currently, poultry litter combustion systems are commercially functioning in Europe and the UK, with previous studies discussing its benefits, but LCA studies have disagreed on the best way to incorporate the impacts of land application. The study also does not take the decommissioning and disposal of the plant into account and recycling the materials may significantly reduce impacts in material depletion.

6.6 Conclusions:

The use of poultry litter for energy production in an FBC system can be a sustainable alternative means of manure management, but it may only be applicable in regions where it is readily available, with restricted land application. The added benefits included the production of a dry and odorless ash without volatile N emissions. The ash product also had a lower mass than the original litter, which can be transported to a region with P deficiency more easily. However, in this study, the FBC system was not able to function optimally (lower than expected biomass feed rate, operating hours, and energy output/biomass feed ratio), due to differences in poultry litter characteristics, varying moisture content, and the increased presence of foreign matter that interfered with the combustion process. As a result, a lower than expected total energy output and

an overall net negative electricity output was observed. The life cycle assessment of the FBC system showed that it is theoretically possible under ideal conditions to obtain net environmental gains from poultry litter combustion for heating poultry houses and renewable electricity production, especially in the climate change potential category. Due to the complications associated with the operation of the FBC system, the avoided use of LPG for space heating was able to offset the environmental impacts associated with only six out of the eighteen impact categories. In the improved operational scenario, the impacts on the environment were significantly lower compared to the first scenario, indicating the need for a net positive electrical energy output that can be used for FBC operation, and other on-farm operations to increase the sustainability of the process.

7 Conclusions

7.1 Intellectual Merit and Broader Impacts:

Chapter 2 evaluated the anaerobic degradability and quantified the methane potential and H₂S reduction potential of a gummy waste resource when it was co-digested with dairy manure. The results of the study showed how increasing the GVW percentage as a co-digestion substrate increased CH₄ production while significantly decreasing H₂S production compared to mono-digestion of dairy manure. This research demonstrated the effect of co-digestion of a carbon rich substrate, such as GVW, on both CH₄ yield and H₂S concentrations, which has not been shown in previous co-digestion research. In addition, the co-digestion study did not focus on single substrates co-digestion, which is often the focus of previous research, but instead illuminated the effects of co-digestion mixtures that are used in the farm setting on CH₄ and H₂S production, and the degradability of the digested mixture. Even though co-digestion of GVW with dairy manure would have provided an estimate on the methane potential of the mixture, it may not provide sufficient information for AD practitioners trying to understand the fraction of GVW that can be added for maximum benefits. Co-digestion of GVW with dairy manure, grease waste, and food waste lowered the H₂S yield and maximum H₂S concentration compared to mono-digestion of dairy manure due to its low sulfur content. Co-digestion of industrial byproducts and food waste mixtures in farm-scale biogas digesters could provide economic incentives for farmers through tipping fees and increased biogas production while redirecting valuable waste products from landfills. The results also show how co-digestion tests should be tested for both CH₄ and H₂S production in order to provide beneficial information for researchers and AD

practitioners to comply with recommended H₂S limits, while receiving tipping fees for adding these organic-rich substrates to their AD systems. If co-digestion of a particular substrate can reduce the H₂S concentration in the biogas while increasing the CH₄ generation, it can potentially lead to increased energy generation and reduced generator down-times. Future research should be conducted on organic feedstocks with a high C:S ratio to better understand its impact on CH₄ and H₂S yields.

Chapter 3 aimed to integrate field data (biogas, CH₄ and H₂S production, electricity generation, scrubber efficiency) from full-scale functioning AD and H₂S scrubber systems with economics and maintenance time, thus, creating a framework to enable better-informed decisions in the future. The results provided 1) long term unbiased data on H₂S removal efficiency of different scrubbing units, 2) their related capital, operational, and maintenance costs, 3) the effect of scrubber management on its efficiency, and 4) possible solutions to real world problems faced by farmers with anaerobic digesters on their farms. The study especially highlighted the substantial effect of scrubber operation and management on its performance, including comparing the results to well-managed scrubbers in the US. The H₂S scrubber systems that were better managed with more time and labor investment compared to the scrubber systems studied in this study, resulted in more efficient and consistent scrubbing performance. It is also important to note that due to the high levels of H₂S in the biogas, the H₂S sensors were replaced multiple times in the monitoring system, which resulted in gaps in the biogas collection period. The costs and technical expertise associated with multiple replacements of the sensor may not be feasible for farmers even though an H₂S monitoring system is essential for ensuring a high-quality biogas output. The corrosiveness of the H₂S in the

biogas and failure of the equipment over the 2-year study highlights the difficulty of quantifying H₂S concentrations in un-cleaned biogas due to the damaging levels of H₂S. Eventually, the high levels of the H₂S in the pre-scrubbed gas damaged the equipment beyond repair over two years of testing. Future studies should quantify and incorporate long-term costs (5+ years) associated with engine overhauls, down-times, repairs, etc. undertaken due to H₂S related damage to better understand the economic benefits of H₂S scrubbers.

Chapters 4 and 5 were important because it investigated the reaction of gaseous and dissolved H₂S with the biochar surface and the effect of iron as an impregnation agent to enhance the H₂S adsorption capacity of the biochar. Fe-impregnation was observed to significantly increase the H₂S adsorption capacity of biochar in a biogas scrubbing column, when compared to unmodified biochar. Biochar pH was not found to be as important as previously speculated, with the more alkaline biochar performing less efficiently. The biochar pH was found to be even less important in the case of Fe-impregnated biochars, as they can effectively bypass the H₂S dissociation step before further reaction, thus shifting the adsorption mechanism. The importance of metal oxides for the catalytic oxidation of H₂S was also highlighted in both unmodified and Fe-impregnated biochar, as the mineral content by itself may not be sufficient to predict the H₂S adsorption capability of the biochar. The results of the study also showed that biochar can be effective as an in-situ desulfurization agent of biogas under mesophilic conditions. The study showed an increasing trend in the percent reduction of H₂S as the biochar concentrations increased, with no significant biochar particle size effect. Iron-impregnation resulted in nearly complete H₂S removal efficiency compared to

approximately 50% H₂S removal efficiency for unmodified biochars. Furthermore, iron-impregnated biochar addition into a digester was significantly more effective than direct addition of iron chloride compounds. Even though previous studies have shown that biochar can be effective in NH₄-N and dissolved P removal in mono-component systems, it was not effective in a dairy manure system due to possible competition with other species. However, direct addition biochar into a digester for desulfurization was not cost competitive in comparison to market available H₂S removal technologies at this point of time. It is expected that the results of the study would help create a market for biochar to as a possible alternative to activated carbon for H₂S adsorption from biogas, and as an additive for in-situ biogas desulfurization in the future. Future studies should further investigate if biochar can help increase CH₄ production, while increasing the selectivity for H₂S to make it more cost competitive.

Chapter 6 aimed to provide a quantification of the environmental impacts of burning poultry litter for energy generation and utilization. The results showed that poultry litter combustion is a waste-to-energy process that can be considered as a viable and sustainable means of its disposal, but it may only be applicable in regions where it is readily available, with restricted land application. Even though the FBC system was not able to function optimally in the study due to differences in poultry litter characteristics, varying moisture content, and the increased presence of foreign matter that interfered with the combustion process, it is expected that the results would help to frame recommendations that can optimize the process and lead to a higher adoption of this technology in poultry farming areas with N and P saturated soils. The life cycle assessment of the FBC system showed that it is possible to obtain net environmental

gains from poultry litter combustion for heating poultry houses and renewable electricity production and the anticipated performance of the process would have led to net environmental gains in fourteen out of the eighteen impact categories. Future studies should incorporate an additional study on the emissions and leaching of nutrients from the soil after poultry litter and ash application to better understand the benefits of avoided land application of the poultry litter.

Appendix A: Nutrient Load Reduction and Emissions after combustion

Table A.1 Overall nutrient load reductions for all flocks and their respective fractions in the bed ash, fly ash, and total ash product.

Poultry Litter (568 metric tons combusted)		
Nutrient	Concentration (%)	Mass of nutrient (kg/ton poultry litter)
Nitrogen (% N)	2.41	24.1
Phosphorus (% P ₂ O ₅)	1.98	19.8
Potassium (% K ₂ O)	2.40	24.0
Bed Ash (23.5 metric tons generated)		
Nutrient	Concentration (%)	Mass of nutrient (kg/ton bed ash)
Nitrogen (% N)	0	0.0
Phosphorus (% P ₂ O ₅)	13.4	134
Potassium (% K ₂ O)	11.4	114
Fly Ash (35.8 metric tons generated)		
Nutrient	Concentration (%)	Mass of nutrient (kg/ton fly ash)
Nitrogen (% N)	0.2	2
Nitrogen (% N)	15	150
Phosphorus (% P ₂ O ₅)	19.4	194
Total Ash (59.3 metric tons generated)		
Nutrient	Concentration (%)	Mass of nutrient (kg/ton ash)
Nitrogen (% N)	0.1	1
Phosphorus (% P ₂ O ₅)	14.4	144
Potassium (% K ₂ O)	16.3	163

Table A.2 Emission test results for the FBC system with a heat input of 2.7 MMBtu/hr

Contaminants	Emissions (g/hr)	Emission rate (g/MMBtu)	Emission Standard (g/MMBtu)
Filterable Particulate Matter	6.3 ± 2.6	2.33	N/A
Condensable Particulate Matter	163 ± 7.8	60.5	N/A
Total Particulate Matter	170 ± 5.2	62.8	104
Nitrogen Oxide	120 ± 42	44.4	136
Sulfur Oxide	1.4 ± 0.2	0.54	N/A
Carbon Monoxide	215 ± 69	79.5	N/A
Volatile organic carbon	1.6 ± 0.5	0.60	N/A

Appendix B: Life Cycle Assessment Detailed Results

Table B.3 LCA inventory for combustion of poultry litter

Functional Unit – 1 MJ of energy produced from poultry litter combustion						
Item	Description	Value per ton poultry litter	Monitoring data	Expected Data	Units	Notes
Storage Emissions	CH ₄	Negligible	Negligible	Negligible		Not monitored during the study. Moore et al., (2011) for N ₂ O and NH ₃ data, Reijnders and Huijbregts, (2005) for negligible CH ₄ . Storage for an average time period of two weeks
	N ₂ O	70 g/ton PL	0.00001288	0.0000098	kg/MJ	
	NH ₃	174 g/ton PL	0.000032016	0.00002436	kg/MJ	
Litter Storage Facility	Area Required	0.0022 m ² /ton PL	4.048E-07	0.000000308	m ² /MJ	20 m ² (5m x 4m) for 38 tons PL storage capacity from Google Maps. Lifetime storage = 9120 tons in 20 years
Net Efficiency	Electricity Generation Efficiency		1.13%	3.93%		Data obtained from 16 months of monitoring electricity and heat production data
	Heat Generation Efficiency		54.30%	67.40%		
Material Input	Poultry Litter Combusted	1 ton	0.184	0.14	kg/MJ	
Calorific Value		9.98 GJ/ton PL	0.1		kg/MJ	Data obtained from 16 months of tests conducted using a

						bomb calorimeter on poultry litter samples obtained from the farm
Air Emissions	SO _x	5 g/ton PL	0.00000092	0.0000007	kg/MJ	Data obtained from 3 rd party air emissions test conducted in April 2018, CO ₂ assumed to be biogenic and not included in the assessment. N ₂ O emission data from Billen et al., (2015)
	Particulates	593 g/ton PL	0.000109112	0.00008302	kg/MJ	
	CO ₂	569 m ³ /ton PL	0.104696	0.07966	m ³ /MJ	
	NO _x	419 g/ton PL	0.000077096	0.00005866	kg/MJ	
	N ₂ O	260 g/ton PL	0.00004784	0.0000364	kg/MJ	
	CO	750 g/ton PL	0.000138	0.000105	kg/MJ	
	Volatile Organic Carbon (VOC)	5.7 g/ton PL	1.0488E-06	0.000000798	kg/MJ	
Auxiliaries	Diesel Start up	8.19 L/ton PL	0.00150696	0.0011466	L/MJ	Data obtained from 16 months of monitoring diesel use data FBC start up and back up heat production
	Diesel Back up	187.4 L/ton PL	0.0344816	0.026236	L/MJ	
	Sand	14 kg/ton PL	0.002576	0.00196	kg/MJ	Sand for Fluidized bed
Ash	Poultry litter Bed Ash	41.4 kg/ton PL	0.0076176	0.005796	kg/MJ	Data obtained from total amount of bed ash and fly ash production during the study period

	Poultry litter Fly Ash	63.1 kg/ton PL	0.0116104	0.008834	kg/M J	Data obtained from total amount of bed ash and fly ash production during the study period
	Ash Transport		0.000230736 (12 km), 0.00461472 (240 km)	0.00017556 (12 km), 0.0035112 (240 km)	kg/M J	TKM for 12 km transport and max 240 km transport to Chester county, PA
	Poultry litter K content in ash (bed + fly)	4.72 + 12.24 kg/ton PL	0.00312064	0.0023744	kg/M J	Data obtained from 16 months of bed ash and fly ash sample collection for PK content
	Poultry litter P content in ash (bed + fly)	5.55 + 9.47 kg/ton PL	0.00276368	0.0021028	kg/M J	
Poultry Litter Nutrient Content	Poultry litter N content	24.1 kg/ton PL	0.0044344	0.003374	kg/M J	Data obtained from 16 months of poultry litter sample collection for NPK content
	Poultry litter P content	19.8 kg/ton PL	0.0036432	0.002772	kg/M J	
	Poultry litter K content	24 kg/ton PL	0.004416	0.00336	kg/M J	

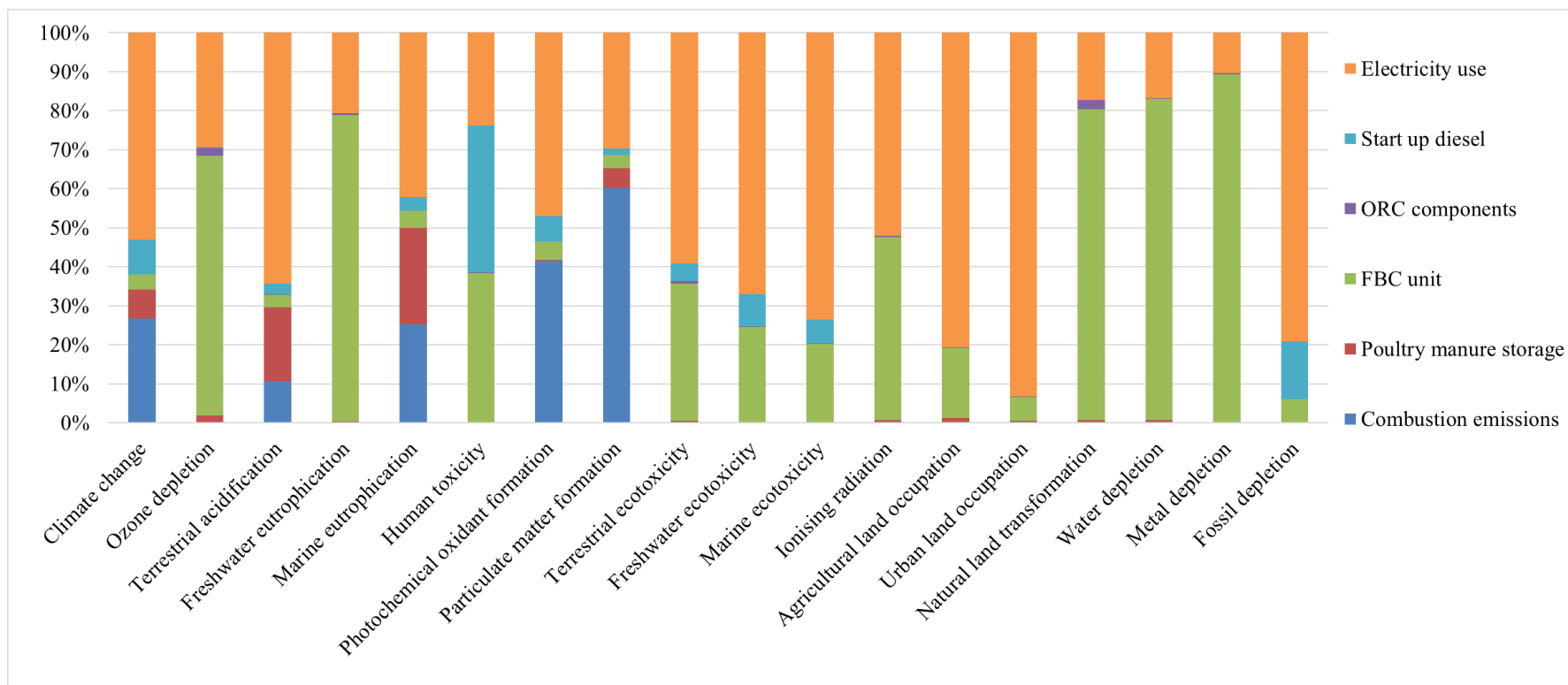


Figure B.1 Distribution of environmental impacts of poultry litter combustion in the baseline scenario.

Table B.4 Environmental impacts in the baseline scenario

Impact category	Unit	Total	Combustion emissions	Poultry manure storage	FBC unit	ORC components	Startup diesel
Functional Unit – 1 MJ of energy							
Climate change	kg CO ₂ eq	5.32E-02	1.43E-02	3.86E-03	2.07E-03	2.64E-05	4.73E-03
Ozone depletion	kg CFC-11 eq	8.84E-11	0.00E+00	1.65E-12	5.89E-11	1.68E-12	1.92E-13
Terrestrial acidification	kg SO ₂ eq	4.14E-04	4.41E-05	7.87E-05	1.35E-05	1.57E-07	1.17E-05
Freshwater eutrophication	kg P eq	1.89E-06	0.00E+00	6.49E-09	1.49E-06	9.32E-09	0.00E+00
Marine eutrophication	kg N eq	1.19E-05	3.01E-06	2.95E-06	5.34E-07	2.19E-09	4.11E-07
Human toxicity	kg 1,4-DB eq	7.11E-03	0.00E+00	9.89E-06	2.71E-03	1.84E-05	2.68E-03
Photochemical oxidant formation	kg NMVOC	2.01E-04	8.35E-05	1.18E-07	9.62E-06	6.28E-08	1.29E-05
Particulate matter formation	kg PM10 eq	2.09E-04	1.26E-04	1.03E-05	7.19E-06	4.12E-08	3.51E-06
Terrestrial ecotoxicity	kg 1,4-DB eq	7.90E-07	0.00E+00	3.86E-09	2.78E-07	4.80E-09	3.62E-08
Freshwater ecotoxicity	kg 1,4-DB eq	2.63E-04	0.00E+00	2.96E-07	6.43E-05	3.12E-07	2.16E-05
Marine ecotoxicity	kg 1,4-DB eq	3.50E-04	0.00E+00	2.83E-07	7.04E-05	5.02E-07	2.13E-05
Ionizing radiation	kBq U235 eq	2.99E-04	0.00E+00	2.19E-06	1.40E-04	9.87E-07	0.00E+00
Agricultural land occupation	m ² a	8.42E-04	0.00E+00	1.07E-05	1.51E-04	7.41E-07	0.00E+00
Urban land occupation	m ² a	7.50E-04	0.00E+00	3.65E-06	4.55E-05	1.07E-06	0.00E+00
Natural land transformation	m ²	2.78E-07	0.00E+00	2.14E-09	2.22E-07	6.36E-09	0.00E+00
Water depletion	m ³	1.52E-02	0.00E+00	9.87E-05	1.26E-02	2.11E-05	0.00E+00
Metal depletion	kg Fe eq	2.84E-03	0.00E+00	3.36E-06	2.53E-03	9.59E-06	0.00E+00
Fossil depletion	kg oil eq	1.06E-02	0.00E+00	6.48E-06	6.27E-04	8.17E-06	1.57E-03

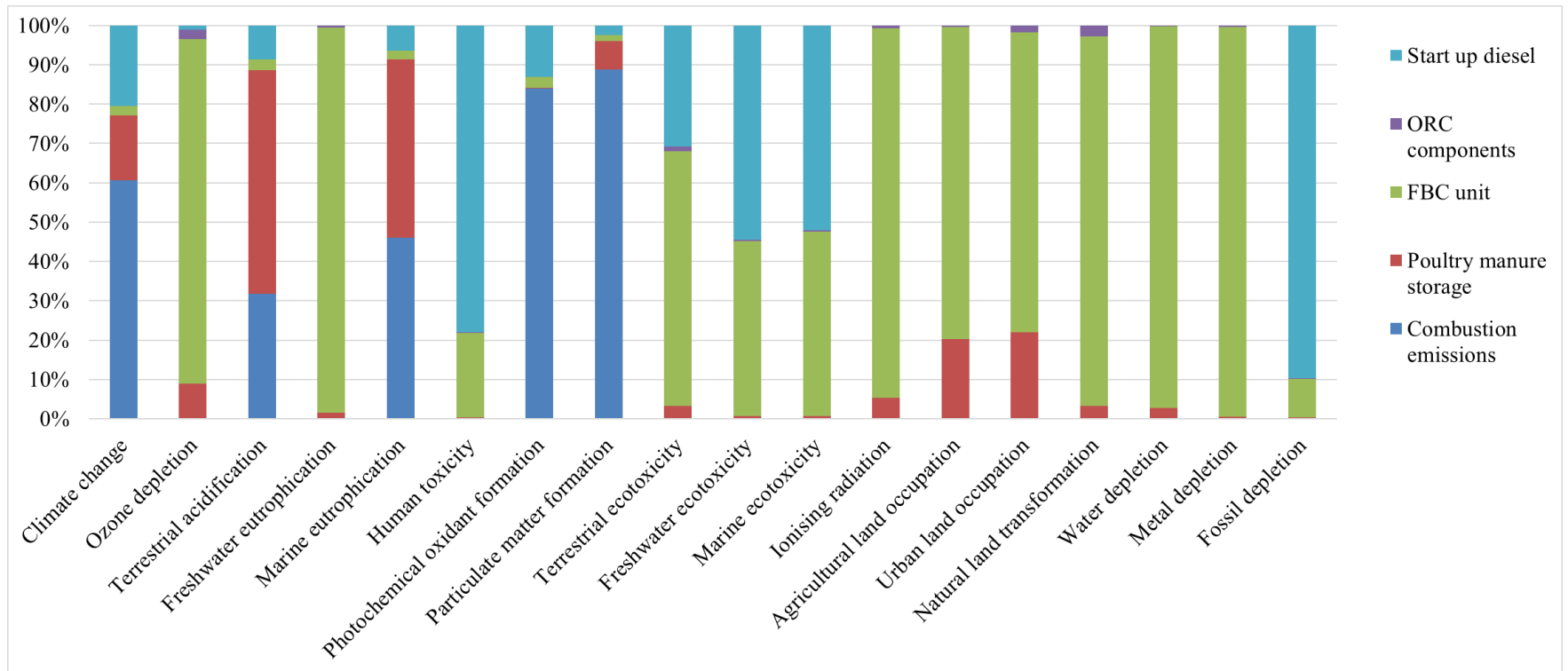


Figure B.2 Distribution of environmental impacts of poultry litter combustion in the improved operational scenario.

Table B.5 Environmental impacts in the improved operational scenario

Impact category	Unit	Total	Combustion emissions	Poultry manure storage	FBC unit	ORC components	Startup diesel
Functional Unit – 1 MJ of energy							
Climate change	kg CO ₂ eq	1.79E-02	1.08E-02	2.94E-03	4.36E-04	5.58E-06	3.65E-03
Ozone depletion	kg CFC-11 eq	1.42E-11	0.00E+00	1.26E-12	1.24E-11	3.55E-13	1.48E-13
Terrestrial acidification	kg SO ₂ eq	1.05E-04	3.35E-05	5.99E-05	2.85E-06	3.32E-08	9.00E-06
Freshwater eutrophication	kg P eq	3.20E-07	0.00E+00	4.94E-09	3.13E-07	1.97E-09	0.00E+00
Marine eutrophication	kg N eq	4.96E-06	2.29E-06	2.25E-06	1.13E-07	4.63E-10	3.17E-07
Human toxicity	kg 1,4-DB eq	2.65E-03	0.00E+00	7.53E-06	5.72E-04	3.89E-06	2.07E-03
Photochemical oxidant formation	kg NMVOC	7.55E-05	6.34E-05	9.01E-08	2.03E-06	1.32E-08	9.93E-06
Particulate matter formation	kg PM10 eq	1.08E-04	9.60E-05	7.86E-06	1.52E-06	8.69E-09	2.71E-06
Terrestrial ecotoxicity	kg 1,4-DB eq	9.06E-08	0.00E+00	2.94E-09	5.87E-08	1.01E-09	2.80E-08
Freshwater ecotoxicity	kg 1,4-DB eq	3.05E-05	0.00E+00	2.25E-07	1.36E-05	6.59E-08	1.67E-05
Marine ecotoxicity	kg 1,4-DB eq	3.16E-05	0.00E+00	2.16E-07	1.49E-05	1.06E-07	1.65E-05
Ionizing radiation	kBq U235 eq	3.14E-05	0.00E+00	1.67E-06	2.95E-05	2.08E-07	0.00E+00
Agricultural land occupation	m ² a	4.01E-05	0.00E+00	8.11E-06	3.18E-05	1.56E-07	0.00E+00
Urban land occupation	m ² a	1.26E-05	0.00E+00	2.78E-06	9.59E-06	2.25E-07	0.00E+00
Natural land transformation	m ²	4.98E-08	0.00E+00	1.63E-09	4.68E-08	1.34E-09	0.00E+00
Water depletion	m ³	2.73E-03	0.00E+00	7.51E-05	2.65E-03	4.45E-06	0.00E+00
Metal depletion	kg Fe eq	5.39E-04	0.00E+00	2.56E-06	5.35E-04	2.02E-06	0.00E+00
Fossil depletion	kg oil eq	1.35E-03	0.00E+00	4.93E-06	1.32E-04	1.72E-06	1.21E-03

Appendix C: Calculation of Adsorption capacity

$$\frac{x}{M} = \frac{QM_w}{\omega V_m} (C_i \cdot t_s - \int_0^{t_s} C(t) dt)$$

In equation (1), x/M is the adsorption capacity (mg/g of sorbent), Q is the inlet flow rate (m^3/s), M_w is the molecular weight of H_2S (g/mol), ω is the weight of biochar in the column (g), V_m is the ideal gas molar volume (L/mol), C_i is the inlet concentration (ppm), t_s is the saturation time (s), and $C(t)$ is the outlet H_2S concentration at time = t .

Calculations for Maple biochar (MB).

Area under the curve for two points $t_i = 0 - 240$ min; $t_j = 10 - 300$ min = $\frac{1}{2}(t_j - t_i)\{C(t_1) + C(t_2)\}$

Table C.1 Concentration of H_2S in the outlet of the biochar column as a function of time

Time (t) (sec)	H_2S (C(t)) (ppm)	Area under the curve for $t_i = 0 - 240$ min; $t_j = 10 - 300$ min
0	0	0
600	0	0
1,800	0	22,051
3,600	24.5	322,319
5,400	334	316,689
6,300	370	436,327
7,200	599	1,238,606
9,000	777	1,459,115
10,800	845	1,623,324
12,600	959	1,750,000
14,400	985	3,575,067
18,000	1,001	

$$\int_0^{t_s} C(t) dt \approx \sum \frac{1}{2}(t_j - t_i)\{C(t_1) + C(t_2)\} = 10,743,499$$

Table C.2 Operational parameters for H_2S adsorption using a biochar adsorption column

Q (m ³ /s)	M _w (g)	ω (g)	V _m (L/mol)	C _i (ppm)	t _s (s)
0.00000167	34	3	22.4	1,000	18,000

$$\frac{x}{M} = 6.13 \text{ mg/g biochar}$$

Bibliography

1. Smil, V. *Energy transitions: global and national perspectives*; ABC-CLIO, 2016; ISBN 1440853258.
2. Energy Information Administration USA Primary Energy Production by Source Available online: <https://www.eia.gov/totalenergy/data/annual/>.
3. Pham, T.P.T.; Kaushik, R.; Parshetti, G.K.; Mahmood, R.; Balasubramanian, R. Food waste-to-energy conversion technologies: Current status and future directions. *Waste Manag.* **2015**, *38*, 399–408.
4. Mata-Alvarez, J.; Dosta, J.; Romero-Güiza, M.S.; Fonoll, X.; Peces, M.; Astals, S. A critical review on anaerobic co-digestion achievements between 2010 and 2013. *Renew. Sustain. Energy Rev.* **2014**, *36*, 412–427.
5. El-Mashad, H.M.; Zhang, R. Biogas production from co-digestion of dairy manure and food waste. *Bioresour. Technol.* **2010**, *101*, 4021–4028.
6. Zhang, C.; Xiao, G.; Peng, L.; Su, H.; Tan, T. The anaerobic co-digestion of food waste and cattle manure. *Bioresour. Technol.* **2013**, *129*, 170–176.
7. Lisboa, M.S.; Lansing, S. Characterizing food waste substrates for co-digestion through biochemical methane potential (BMP) experiments. *Waste Manag.* **2013**, *33*, 2664–2669.
8. Moody, L.B.; Burns, R.T.; Bishop, G.; Sell, S.T.; Spajic, R. Using biochemical methane potential assays to aid in co-substrate selection for co-digestion. *Appl. Eng. Agric.* **2011**, *27*, 433–439.
9. Zhang, C.; Su, H.; Baeyens, J.; Tan, T. Reviewing the anaerobic digestion of food waste for biogas production. *Renew. Sustain. Energy Rev.* **2014**, *38*, 383–392.

10. Braguglia, C.M.; Gallipoli, A.; Gianico, A.; Pagliaccia, P. Anaerobic bioconversion of food waste into energy: A critical review. *Bioresour. Technol.* **2018**, *248*, 37–56.
11. Xu, F.; Li, Y.; Ge, X.; Yang, L.; Li, Y. Anaerobic digestion of food waste – Challenges and opportunities. *Bioresour. Technol.* **2018**, *247*, 1047–1058.
12. Chen, J.L.; Ortiz, R.; Steele, T.W.J.; Stuckey, D.C. Toxicants inhibiting anaerobic digestion: A review. *Biotechnol. Adv.* **2014**, *32*, 1523–1534.
13. Speece, R.E. *Anaerobic biotechnology and odor/corrosion control for municipalities and industries*; Nashville (Ten.): Archae press, 2008; ISBN 9781578430529.
14. Syed, M.; Soreanu, G.; Falletta, P.; Béland, M. Removal of hydrogen sulfide from gas streams using biological processes - a review. *Can. Biosyst. Eng.* **2006**, *48*, 2.1-2.14.
15. Steven McKinsey Zicari Removal of hydrogen sulfide from biogas using cow manure compost, Cornell University, Ithaca, NY, 2003.
16. Schieder, D.; Quicker, P.; Schneider, R.; Winter, H.; Prechtel, S.; Faulstich, M. Microbiological removal of hydrogen sulfide from biogas by means of a separate biofilter system: Experience with technical operation. *Water Sci. Technol.* **2003**, *48*, 209–212.
17. Gabriel, D.; Deshusses, M.A.; Gamisans, X. *Desulfurization of biogas in biotrickling filters*; Wiley Online Library, 2013;
18. Persson, M.; Jonsson, O.; Wellinger, A. Biogas Upgrading To Vehicle Fuel Standards and Grid. *IEA Bioenergy* **2007**, 1–32.

19. Abatzoglou, N.; Boivin, S. A review of biogas purification processes. *Biofuels, Bioprod. Biorefining* 2009.
20. Petersson, A.; Wellinger, A. Biogas upgrading technologies—developments and innovations. *IEA Bioenergy* **2009**, 20.
21. Ramos, I.; Pérez, R.; Fdz-Polanco, M. Microaerobic desulphurisation unit: A new biological system for the removal of H₂S from biogas. *Bioresour. Technol.* **2013**, 142, 633–640.
22. Krayzelova, L.; Bartacek, J.; Díaz, I.; Jeison, D.; Volcke, E.I.P.; Jenicek, P. Microaeration for hydrogen sulfide removal during anaerobic treatment: a review. *Rev. Environ. Sci. Biotechnol.* **2015**, 14, 703–725.
23. Gabelman, A. *Adsorption basics: Part 1*; 2017; Vol. 113;.
24. Bauer, F.; Hulteberg, C.; Persson, T.; Tamm, D. Biogas upgrading – Review of commercial technologies. *Swedish Gas Technol. Centre, SGC* **2013**, 82.
25. Ryckebosch, E.; Drouillon, M.; Vervaeren, H. Techniques for transformation of biogas to biomethane. *Biomass and Bioenergy* **2011**, 35, 1633–1645.
26. Muñoz, R.; Meier, L.; Diaz, I.; Jeison, D. A review on the state-of-the-art of physical/chemical and biological technologies for biogas upgrading. *Rev. Environ. Sci. Biotechnol.* **2015**, 14, 727–759.
27. Hale, S.; Hanley, K.; Lehmann, J.; Zimmerman, A.; Cornelissen, G. Effects of Chemical, Biological, and Physical Aging As Well As Soil Addition on the Sorption of Pyrene to Activated Carbon and Biochar. *Environ. Sci. Technol.* **2011**, 45, 10445–10453.
28. Shen, Y.; Linville, J.L.; Ignacio-de Leon, P.A.A.; Schoene, R.P.; Urgun-Demirtas,

- M. Towards a sustainable paradigm of waste-to-energy process: Enhanced anaerobic digestion of sludge with woody biochar. *J. Clean. Prod.* **2016**, *135*, 1054–1064.
29. Lehmann, J.; Joseph, S. *Biochar for environmental management: science, technology and implementation*; Routledge, 2015; ISBN 1134489536.
30. Adib, F.; Bagreev, A.; Bandosz, T.J. Effect of surface characteristics of wood-based activated carbons on adsorption of hydrogen sulfide. *J. Colloid Interface Sci.* **1999**, *214*, 407–415.
31. Adib, F.; Bagreev, A.; Bandosz, T.J. Adsorption/oxidation of hydrogen sulfide on nitrogen-containing activated carbons. *Langmuir* **2000**, *16*, 1980–1986.
32. Shang, G.; Shen, G.; Liu, L.; Chen, Q.; Xu, Z. Kinetics and mechanisms of hydrogen sulfide adsorption by biochars. *Bioresour. Technol.* **2013**, *133*, 495–499.
33. Kanjanarong, J.; Giri, B.S.; Jaisi, D.P.; Oliveira, F.R.; Boonsawang, P.; Chaiprapat, S.; Singh, R.S.; Balakrishna, A.; Khanal, S.K. Removal of hydrogen sulfide generated during anaerobic treatment of sulfate-laden wastewater using biochar: Evaluation of efficiency and mechanisms. *Bioresour. Technol.* **2017**, *234*, 115–121.
34. Bagreev, A.; Bandosz, T.J. H₂S adsorption/oxidation on unmodified activated carbons: Importance of prehumidification. *Carbon N. Y.* **2001**, *39*, 2303–2311.
35. Xu, X.; Cao, X.; Zhao, L.; Sun, T. Comparison of sewage sludge- and pig manure-derived biochars for hydrogen sulfide removal. *Chemosphere* **2014**, *111*, 296–303.
36. Suliman, W.; Harsh, J.B.; Abu-Lail, N.I.; Fortuna, A.M.; Dallmeyer, I.; Garcia-Perez, M. Influence of feedstock source and pyrolysis temperature on biochar bulk

- and surface properties. *Biomass and Bioenergy* **2016**, *84*, 37–48.
37. Feng, W.; Kwon, S.; Borguet, E.; Vidic, R. Adsorption of hydrogen sulfide onto activated carbon fibers: effect of pore structure and surface chemistry. *Environ. Sci. Technol.* **2005**, *39*, 9744–9749.
 38. Mochizuki, T.; Kubota, M.; Matsuda, H.; D’Elia Camacho, L.F. Adsorption behaviors of ammonia and hydrogen sulfide on activated carbon prepared from petroleum coke by KOH chemical activation. *Fuel Process. Technol.* **2016**, *144*, 164–169.
 39. Bamdad, H.; Hawboldt, K.; MacQuarrie, S. A review on common adsorbents for acid gases removal: Focus on biochar. *Renew. Sustain. Energy Rev.* **2018**, *81*, 1705–1720.
 40. Meyer-Kohlstock, D.; Haupt, T.; Heldt, E.; Heldt, N.; Kraft, E. Biochar as additive in biogas-production from bio-waste. *Energies* **2016**, *9*, 247.
 41. Mumme, J.; Srocke, F.; Heeg, K.; Werner, M. Use of biochars in anaerobic digestion. *Bioresour. Technol.* **2014**, *164*, 189–197.
 42. Shen, Y.; Linville, J.L.; Urgun-Demirtas, M.; Schoene, R.P.; Snyder, S.W. Producing pipeline-quality biomethane via anaerobic digestion of sludge amended with corn stover biochar with in-situ CO₂ removal. *Appl. Energy* **2015**, *158*, 300–309.
 43. Sizmur, T.; Fresno, T.; Akgül, G.; Frost, H.; Moreno-Jiménez, E. Biochar modification to enhance sorption of inorganics from water. *Bioresour. Technol.* **2017**, *246*, 34–47.
 44. Tan, X.; Liu, Y.; Zeng, G.; Wang, X.; Hu, X.; Gu, Y.; Yang, Z. Application of

- biochar for the removal of pollutants from aqueous solutions. *Chemosphere* **2015**, *125*, 70–85.
45. Yao, Y.; Gao, B.; Chen, J.; Yang, L. Engineered biochar reclaiming phosphate from aqueous solutions: mechanisms and potential application as a slow-release fertilizer. *Environ. Sci. Technol.* **2013**, *47*, 8700–8708.
 46. Agrafioti, E.; Kalderis, D.; Diamadopoulos, E. Ca and Fe modified biochars as adsorbents of arsenic and chromium in aqueous solutions. *J. Environ. Manage.* **2014**, *146*, 444–450.
 47. Frišták, V.; Micháleková-Richveisová, B.; Víglašová, E.; Ďuriška, L.; Galamboš, M.; Moreno-Jiménez, E.; Pipiška, M.; Soja, G. Sorption separation of Eu and As from single-component systems by Fe-modified biochar: kinetic and equilibrium study. *J. Iran. Chem. Soc.* **2017**, *14*, 521–530.
 48. Rajapaksha, A.U.; Chen, S.S.; Tsang, D.C.W.; Zhang, M.; Vithanage, M.; Mandal, S.; Gao, B.; Bolan, N.S.; Ok, Y.S. Engineered/designer biochar for contaminant removal/immobilization from soil and water: Potential and implication of biochar modification. *Chemosphere* **2016**, *148*, 276–291.
 49. Micháleková-Richveisová, B.; Frišták, V.; Pipiška, M.; Ďuriška, L.; Moreno-Jimenez, E.; Soja, G. Iron-impregnated biochars as effective phosphate sorption materials. *Environ. Sci. Pollut. Res.* **2017**, *24*, 463–475.
 50. Gwenzi, W.; Chaukura, N.; Noubactep, C.; Mukome, F.N.D. Biochar-based water treatment systems as a potential low-cost and sustainable technology for clean water provision. *J. Environ. Manage.* **2017**, *197*, 732–749.
 51. Rosales, E.; Meijide, J.; Pazos, M.; Sanromán, M.A. Challenges and recent

- advances in biochar as low-cost biosorbent: From batch assays to continuous-flow systems. *Bioresour. Technol.* **2017**, *246*, 176–192.
52. Mohan, D.; Kumar, S.; Srivastava, A. Fluoride removal from ground water using magnetic and nonmagnetic corn stover biochars. *Ecol. Eng.* **2014**, *73*, 798–808.
 53. Horne, R.; Grant, T.; Verghese, K. *Life cycle assessment: principles, practice and prospects*; Csiro Publishing, 2009; ISBN 0643094520.
 54. Vigon, B.W.; Vigon, B.W.; Harrison, C.L. *Life-cycle assessment: Inventory guidelines and principles*; Citeseer, 1993;
 55. Delmarva Poultry Industry DPI Facts & Figures Available online:
<http://www.dpichicken.org/facts/facts-figures.cfm>.
 56. Ridlington, E.; Landers, T. *An Unsustainable Path*; 2011;
 57. Codling, E.E. Laboratory characterization of extractable phosphorus in poultry litter and poultry litter ash. *Soil Sci.* **2006**, *171*, 858–864.
 58. Belgiorno, V.; De Feo, G.; Della Rocca, C.; Napoli, R.M.A. Energy from gasification of solid wastes. *Waste Manag.* **2003**, *23*, 1–15.
 59. Marculescu, C.; Stan, C. Poultry processing industry waste to energy conversion. *Energy Procedia* **2011**, *6*, 550–557.
 60. Joseph, P.; Tretsiakova-McNally, S.; McKenna, S. Characterization of cellulosic wastes and gasification products from chicken farms. *Waste Manag.* **2012**, *32*, 701–709.
 61. Weiland, P. Biogas production: Current state and perspectives. *Appl. Microbiol. Biotechnol.* **2010**, *85*, 849–860.
 62. Moody, L.B.; Burns, R.T.; Bishop, G.; Sell, S.T.; Spajic, R. Using Biochemical

Methane Potential Assays to Aid in Co-substrate Selection for Co- digestion.
Trans. ASABE **2011**.

63. Belle, A.J.; Lansing, S.; Mulbry, W.; Weil, R.R. Anaerobic co-digestion of forage radish and dairy manure in complete mix digesters. *Bioresour. Technol.* **2015**, *178*, 230–237.
64. Lupitsky, R.; Alvarez-Fonseca, D.; Herde, Z.D.; Satyavolu, J. In-situ prevention of hydrogen sulfide formation during anaerobic digestion using zinc oxide nanowires. *J. Environ. Chem. Eng.* **2018**, *6*, 110–118.
65. Pipatmanomai, S.; Kaewluan, S.; Vitidsant, T. Economic assessment of biogas-to-electricity generation system with H₂S removal by activated carbon in small pig farm. *Appl. Energy* **2009**, *86*, 669–674.
66. Corro, G.; Pal, U.; Bañuelos, F.; Rosas, M. Generation of biogas from coffee-pulp and cow-dung co-digestion: Infrared studies of postcombustion emissions. *Energy Convers. Manag.* **2013**, *74*, 471–481.
67. RedCorn, R.; Fatemi, S.; Engelberth, A.S. Comparing End-Use Potential for Industrial Food-Waste Sources. *Engineering* **2018**, *4*, 371–380.
68. Delgado, P.; Bañón, S. Determining the minimum drying time of gummy confections based on their mechanical properties. *CYTA - J. Food* **2015**, *13*, 329–335.
69. Lansing, S.; Martin, J.F.; Botero, R.B.; da Silva, T.N.; da Silva, E.D. Methane production in low-cost, unheated, plug-flow digesters treating swine manure and used cooking grease. *Bioresour. Technol.* **2010**, *101*, 4362–4370.
70. Ugoji, E.O. Anaerobic digestion of palm oil mill effluent and its utilization as

- fertilizer for environmental protection. *Renew. Energy* **1997**, *10*, 291–294.
71. Angelidaki, I.; Ahring, B.K. Codigestion of olive oil mill wastewaters with manure, household waste or sewage sludge. *Biodegradation* **1997**, *8*, 221–226.
 72. Bujoczek, G.; Oleszkiewicz, J.; Sparling, R.; Cenkowski, S. High Solid Anaerobic Digestion of Chicken Manure. *J. Agric. Eng. Res.* **2000**, *76*, 51–60.
 73. Witarsa, F.; Lansing, S. Quantifying methane production from psychrophilic anaerobic digestion of separated and unseparated dairy manure. *Ecol. Eng.* **2015**, *78*, 95–100.
 74. Kaparaju, P.; Luostarinen, S.; Kalmari, E.; Kalmari, J.; Rintala, J. Co-digestion of energy crops and industrial confectionery by-products with cow manure: batch scale and farm scale evaluation. *Water Sci. Technol.* **2002**, *45*, 275–280.
 75. Li, Y.; Zhang, R.; Liu, X.; Chen, C.; Xiao, X.; Feng, L.; He, Y.; Liu, G. Evaluating methane production from anaerobic mono- and co-digestion of kitchen waste, corn stover, and chicken manure. *Energy and Fuels* **2013**, *27*, 2085–2091.
 76. Belle, A.J.; Lansing, S.; Mulbry, W.; Weil, R.R. Methane and hydrogen sulfide production during co-digestion of forage radish and dairy manure. *Biomass and Bioenergy* **2015**, *80*, 44–51.
 77. Xie, S.; Higgins, M.J.; Bustamante, H.; Galway, B.; Nghiem, L.D. Current status and perspectives on anaerobic co-digestion and associated downstream processes. *Environ. Sci. Water Res. Technol.* **2018**.
 78. Chastain, J.P.; Camberato, J.J. Dairy manure production and nutrient content. *Confin. Anim. Manure Manag. Certif. Progr. Man. Dairy Version* **2004**, 1–16.
 79. Tampio, E.; Ervasti, S.; Paavola, T.; Heaven, S.; Banks, C.; Rintala, J. Anaerobic

- digestion of autoclaved and untreated food waste. *Waste Manag.* **2014**, *34*, 370–377.
80. Administration, O.S. and H. OSHA safety and health standards. 29 CFR 1910.1000. *Occup. Saf. Heal. Adm. Revis.* **1997**, *1*, 444.
81. Krich, K.; Augenstein, D.; Batmale, J.P.; Benemann, J.; Rutledge, B.; Salour, D. *Biomethane from dairy waste*; 2005;
82. Shelford, T.J.; Gooch, C.A.; Lansing, S.A. Performance and Economic Results for Two Full-Scale Biotrickling filters to remove H₂S from Dairy Manure-derived Biogas. *Appl. Eng. Agric.* **2019**, *0*.
83. Gooch, C.A.; Hogan, J.S.; Glazier, N.; Noble, R. Use of post-digested separated manure solids as freestall bedding: A case study. *2006 Natl. Mastit. Counc. Annu. Meet.* **2006**.
84. Key, N.; Sneeringer, S. Climate Change Policy and the Adoption of Methane Digesters on Livestock Operations. *Ssrn* **2012**.
85. Allegue, L.B.; Hinge, J. Biogas upgrading Evaluation of methods for H₂S removal. *Danish Technol. Inst.* **2014**, *31*.
86. Oliver, J.P.; Gooch, C.A. Microbial underpinnings of H₂S biological filtration. **2016**.
87. Shelford, T.; Gooch, C. Hydrogen Sulfide Removal From Biogas: Iron Sponge Basics. **2017**.
88. Weather underground Available online:
<https://www.wunderground.com/history/daily/us/md/rising-sun/KILG> (accessed on Oct 17, 2019).

89. Cord-Ruwisch, R.; Kleinitz, W.; Widdel, F. Sulfate-reducing Bacteria and Their Activities in Oil Production. *J. Pet. Technol.* **1987**, *39*, 97–106.
90. Kohl, A.L.; Nielsen, R.B. *Gas Purification*; 1997; Vol. 10; ISBN 978-0-88-415220-0.
91. Mehta, A. The economics and feasibility of electricity generation using manure digesters on small and mid-size dairy farms. *Available SSRN 2638078* **2002**.
92. Mulbry, W.; Selmer, K.; Lansing, S. Effect of liquid surface area on hydrogen sulfide oxidation during micro-aeration in dairy manure digesters. *PLoS One* **2017**, *12*, 1–12.
93. Ramos, I.; Fdz-Polanco, M. Microaerobic control of biogas sulphide content during sewage sludge digestion by using biogas production and hydrogen sulphide concentration. *Chem. Eng. J.* **2014**, *250*, 303–311.
94. Khanal, S.K.; Huang, J.-C. Online Oxygen Control for Sulfide Oxidation in Anaerobic Treatment of High-Sulfate Wastewater. *Water Environ. Res.* **2006**, *78*, 397–408.
95. Khanal, S.K.; Huang, J.C. ORP-based oxygenation for sulfide control in anaerobic treatment of high-sulfate wastewater. *Water Res.* **2003**, *37*, 2053–2062.
96. Greer, D. Biogas conditioning and upgrading in action. *Biocycle* **2010**, *51*, 53–56.
97. Lusk, P. Methane Recovery from Animal Manures The Current Opportunities Casebook. *Midwest Res. Inst. U.S. Dep. Energy* **1998**, 150.
98. Libarle, D.L. Barriers to Adoption of Methane Digester Technology on California Dairies, California Polytechnic State University, 2014.
99. Awe, O.W.; Zhao, Y.; Nzihou, A.; Minh, D.P.; Lyczko, N. A Review of Biogas

Utilisation, Purification and Upgrading Technologies. *Waste and Biomass Valorization* **2017**, *8*, 267–283.

100. Ayiania, M.; Carbajal-Gamarra, F.M.; Garcia-Perez, T.; Frear, C.; Suliman, W.; Garcia-Perez, M. Production and characterization of H₂S and PO₄³⁻ carbonaceous adsorbents from anaerobic digested fibers. *Biomass and Bioenergy* **2019**, *120*, 339–349.
101. Thompson, K.A.; Shimabuku, K.K.; Kearns, J.P.; Knappe, D.R.U.; Summers, R.S.; Cook, S.M. Environmental Comparison of Biochar and Activated Carbon for Tertiary Wastewater Treatment. *Environ. Sci. Technol.* **2016**, *50*, 11253–11262.
102. Dalai, A.K.; Cundall, M.T.; De, M. Direct oxidation of hydrogen sulphide to sulphur using impregnated activated carbon catalysts. *Can. J. Chem. Eng.* **2008**, *86*, 768–777.
103. Nguyen-Thanh, D.; Bandosz, T.J. Activated carbons with metal containing bentonite binders as adsorbents of hydrogen sulfide. *Carbon N. Y.* **2005**, *43*, 359–367.
104. Sakanishi, K.; Wu, Z.; Matsumura, A.; Saito, I.; Hanaoka, T.; Minowa, T.; Tada, M.; Iwasaki, T. Simultaneous removal of H₂S and COS using activated carbons and their supported catalysts. *Catal. Today* **2005**, *104*, 94–100.
105. Wallace, R.; Suresh, S.; Fini, E.; Bandosz, T. Efficient Air Desulfurization Catalysts Derived from Pig Manure Liquefaction Char. *C* **2017**, *3*, 37.
106. Rajkovich, S.; Enders, A.; Hanley, K.; Hyland, C.; Zimmerman, A.R.; Lehmann, J. Corn growth and nitrogen nutrition after additions of biochars with varying properties to a temperate soil. *Biol. Fertil. Soils* **2012**, *48*, 271–284.

107. Shang, G.; Li, Q.; Liu, L.; Chen, P.; Huang, X. Adsorption of hydrogen sulfide by biochars derived from pyrolysis of different agricultural/forestry wastes. *J. Air Waste Manag. Assoc.* **2016**, *66*, 8–16.
108. Weber, K.; Quicker, P. Properties of biochar. *Fuel* **2018**, *217*, 240–261.
109. Sitthikhankaew, R.; Chadwick, D.; Assabumrungrat, S.; Laosiripojana, N. Effects of humidity, O₂, and CO₂ on H₂S adsorption onto upgraded and KOH impregnated activated carbons. *Fuel Process. Technol.* **2014**, *124*, 249–257.
110. Boppart, S. Impregnated Carbons for the Adsorption of H₂S and Mercaptans. *Am. Chem. Soc.* **1996**, 389–393.
111. Mireles, S.; Parsons, J.; Trad, T.; Cheng, C.L.; Kang, J. Lead removal from aqueous solutions using biochars derived from corn stover, orange peel, and pistachio shell. *Int. J. Environ. Sci. Technol.* **2019**.
112. Xu, X.; Cao, X.; Zhao, L.; Sun, T. Comparison of sewage sludge- and pig manure-derived biochars for hydrogen sulfide removal. *Chemosphere* **2014**, *111*, 296–303.
113. Zhao, B.; Xu, H.; Zhang, T.; Nan, X.; Ma, F. Effect of pyrolysis temperature on sulfur content, extractable fraction and release of sulfate in corn straw biochar. *RSC Adv.* **2018**, *8*, 35611–35617.
114. Wang, B.; Lehmann, J.; Hanley, K.; Hestrin, R.; Enders, A. Adsorption and desorption of ammonium by maple wood biochar as a function of oxidation and pH. *Chemosphere* **2015**, *138*, 120–126.
115. Ahmed, M.B.; Zhou, J.L.; Ngo, H.H.; Guo, W.; Chen, M. Progress in the preparation and application of modified biochar for improved contaminant removal from water and wastewater. *Bioresour. Technol.* **2016**, *214*, 836–851.

116. Lee, S.; Lee, T.; Kim, D. Adsorption of Hydrogen Sulfide from Gas Streams Using the Amorphous Composite of α -FeOOH and Activated Carbon Powder. *Ind. Eng. Chem. Res.* **2017**, *56*, 3116–3122.
117. Sethupathi, S.; Zhang, M.; Rajapaksha, A.U.; Lee, S.R.; Nor, N.M.; Mohamed, A.R.; Al-Wabel, M.; Lee, S.S.; Ok, Y.S. Biochars as potential adsorbers of CH₄, CO₂ and H₂S. *Sustain.* **2017**, *9*, 1–10.
118. Balsamo, M.; Cimino, S.; de Falco, G.; Erto, A.; Lisi, L. ZnO-CuO supported on activated carbon for H₂S removal at room temperature. *Chem. Eng. J.* **2016**, *304*, 399–407.
119. Sun, Y.; Zhang, J.P.; Wen, C.; Zhang, L. An enhanced approach for biochar preparation using fluidized bed and its application for H₂S removal. *Chem. Eng. Process. Process Intensif.* **2016**, *104*, 1–12.
120. Huang, C.C.; Chen, C.H.; Chu, S.M. Effect of moisture on H₂S adsorption by copper impregnated activated carbon. *J. Hazard. Mater.* **2006**, *136*, 866–873.
121. Ciahotný, K.; Kyselová, V. Hydrogen Sulfide Removal from Biogas Using Carbon Impregnated with Oxidants. *Energy & Fuels* **2019**.
122. Arcibar-Orozco, J.A.; Wallace, R.; Mitchell, J.K.; Bandosz, T.J. Role of surface chemistry and morphology in the reactive adsorption of H₂S on Iron (Hydr)oxide/graphite oxide composites. *Langmuir* **2015**, *31*, 2730–2742.
123. Deublein, D.; Steinhauser, A. *Biogas from waste and renewable resources: an introduction*; John Wiley & Sons, 2011; ISBN 3527643710.
124. Park, J.H.; Kang, H.J.; Park, K.H.; Park, H.D. Direct interspecies electron transfer via conductive materials: A perspective for anaerobic digestion applications.

- Bioresour. Technol.* **2018**, *254*, 300–311.
125. Wang, G.; Li, Q.; Gao, X.; Wang, X.C. Synergetic promotion of syntrophic methane production from anaerobic digestion of complex organic wastes by biochar: Performance and associated mechanisms. *Bioresour. Technol.* **2018**, *250*, 812–820.
 126. Zhao, Z.; Li, Y.; Quan, X.; Zhang, Y. Towards engineering application: Potential mechanism for enhancing anaerobic digestion of complex organic waste with different types of conductive materials. *Water Res.* **2017**, *115*, 266–277.
 127. Wang, C.; Liu, Y.; Gao, X.; Chen, H.; Xu, X.; Zhu, L. Role of biochar in the granulation of anaerobic sludge and improvement of electron transfer characteristics. *Bioresour. Technol.* **2018**, *268*, 28–35.
 128. Cheng, Q.; De Los Reyes, F.L.; Call, D.F. Amending anaerobic bioreactors with pyrogenic carbonaceous materials: the influence of material properties on methane generation. *Environ. Sci. Water Res. Technol.* **2018**, *4*, 1794–1806.
 129. Liu, F.; Rotaru, A.E.; Shrestha, P.M.; Malvankar, N.S.; Nevin, K.P.; Lovley, D.R. Promoting direct interspecies electron transfer with activated carbon. *Energy Environ. Sci.* **2012**, *5*, 8982–8989.
 130. Jang, H.M.; Choi, Y.K.; Kan, E. Effects of dairy manure-derived biochar on psychrophilic, mesophilic and thermophilic anaerobic digestions of dairy manure. *Bioresour. Technol.* **2018**, *250*, 927–931.
 131. Ahmad, M.; Rajapaksha, A.U.; Lim, J.E.; Zhang, M.; Bolan, N.; Mohan, D.; Vithanage, M.; Lee, S.S.; Ok, Y.S. Biochar as a sorbent for contaminant management in soil and water: a review. *Chemosphere* **2014**, *99*, 19–33.

132. APHA-AWWA-WEF *Standard methods for the examination of water and wastewater*; 21st ed.; APHA, AWA, WEF: Washington, DC, 2005;
133. Villar da Gama, B.M.; Elisandra do Nascimento, G.; Silva Sales, D.C.; Rodríguez-Díaz, J.M.; Bezerra de Menezes Barbosa, C.M.; Menezes Bezerra Duarte, M.M. Mono and binary component adsorption of phenol and cadmium using adsorbent derived from peanut shells. *J. Clean. Prod.* **2018**, *201*, 219–228.
134. Kizito, S.; Wu, S.; Kipkemoi Kirui, W.; Lei, M.; Lu, Q.; Bah, H.; Dong, R. Evaluation of slow pyrolyzed wood and rice husks biochar for adsorption of ammonium nitrogen from piggery manure anaerobic digestate slurry. *Sci. Total Environ.* **2015**, *505*, 102–112.
135. Hou, J.; Huang, L.; Yang, Z.; Zhao, Y.; Deng, C.; Chen, Y.; Li, X. Adsorption of ammonium on biochar prepared from giant reed. *Environ. Sci. Pollut. Res.* **2016**, *23*, 19107–19115.
136. Pipíška, M.; Richveisová, B.M.; Frišták, V.; Horník, M.; Remenárová, L.; Stiller, R.; Soja, G. Sorption separation of cobalt and cadmium by straw-derived biochar: a radiometric study. *J. Radioanal. Nucl. Chem.* **2017**, *311*, 85–97.
137. Liu, H.; Dong, Y.; Wang, H.; Liu, Y. Ammonium adsorption from aqueous solutions by strawberry leaf powder: Equilibrium, kinetics and effects of coexisting ions. *Desalination* **2010**, *263*, 70–75.
138. Yin, Q.; Zhang, B.; Wang, R.; Zhao, Z. Biochar as an adsorbent for inorganic nitrogen and phosphorus removal from water: a review. *Environ. Sci. Pollut. Res.* **2017**, *24*, 26297–26309.
139. Fang, C.; Zhang, T.; Li, P.; Jiang, R.F.; Wang, Y.C. Application of magnesium

- modified corn biochar for phosphorus removal and recovery from swine wastewater. *Int. J. Environ. Res. Public Health* **2014**, *11*, 9217–9237.
140. Rotaru, A.-E.; Shrestha, P.M.; Liu, F.; Markovaite, B.; Chen, S.; Nevin, K.P.; Lovley, D.R. Direct Interspecies Electron Transfer between *Geobacter metallireducens* and *Methanosarcina barkeri*. *Appl. Environ. Microbiol.* **2014**, *80*, 4599–4605.
141. Luo, C.; Lü, F.; Shao, L.; He, P. Application of eco-compatible biochar in anaerobic digestion to relieve acid stress and promote the selective colonization of functional microbes. *Water Res.* **2015**, *68*, 710–718.
142. Yu, L.; Yuan, Y.; Tang, J.; Wang, Y.; Zhou, S. Biochar as an electron shuttle for reductive dechlorination of pentachlorophenol by *Geobacter sulfurreducens*. *Sci. Rep.* **2015**, *5*, 1–10.
143. Yuan, Y.; Bolan, N.; PrévotEAU, A.; Vithanage, M.; Biswas, J.K.; Ok, Y.S.; Wang, H. Applications of biochar in redox-mediated reactions. *Bioresour. Technol.* **2017**, *246*, 271–281.
144. Park, C.M.; Novak, J.T. The effect of direct addition of iron(III) on anaerobic digestion efficiency and odor causing compounds. *Water Sci. Technol.* **2013**, *68*, 2391–2396.
145. Van Vinh, N.; Zafar, M.; Behera, S.K.; Park, H.S. Arsenic(III) removal from aqueous solution by raw and zinc-loaded pine cone biochar: equilibrium, kinetics, and thermodynamics studies. *Int. J. Environ. Sci. Technol.* **2015**, *12*, 1283–1294.
146. BOLAN, N.S.; SZOGI, A.A.; CHUASAVATHI, T.; SESHADRI, B.; ROTHROCK, M.J.; PANNEERSELVAM, P. Uses and management of poultry

- litter. *Worlds. Poult. Sci. J.* **2010**, *66*, 673–698.
147. Kelleher, B.P.; Leahy, J.J.; Henihan, A.M.; O’dwyer, T.F.; Sutton, D.; Leahy, M.J. Advances in poultry litter disposal technology—a review. *Bioresour. Technol.* **2002**, *83*, 27–36.
148. Chastain, J.P.; Coloma-del Valle, A.; Moore, K.P. Using broiler litter as an energy source: energy content and ash composition. *Appl. Eng. Agric.* **2012**, *28*, 513–522.
149. De Filippis, P.; Scarsella, M.; Verdone, N.; Zeppieri, M.; de Caprariis, B. Poultry litter valorization to energy. *WIT Trans. State-of-the-art Sci. Eng.* **2014**, *84*, 185–191.
150. Staver, K.W.; Brinsfield, R.B. Agriculture and Water Quality on the Maryland Eastern Shore: Where Do We Go from Here? *Bioscience* **2006**, *51*, 859.
151. Habetz, D.; Echols, R.; Ten, P.; Drive, P. Development of Successful Poultry Litter-to-Energy Furnace. **2006**, *0300*.
152. Chan, K.Y.; Van Zwieten, L.; Meszaros, I.; Downie, A.; Joseph, S. Using poultry litter biochars as soil amendments. *Soil Res.* **2008**, *46*, 437–444.
153. Santos Dalólio, F.; da Silva, J.N.; Carneiro de Oliveira, A.C.; Ferreira Tinôco, I. de F.; Christiam Barbosa, R.; Resende, M. de O.; Teixeira Albino, L.F.; Teixeira Coelho, S. Poultry litter as biomass energy: A review and future perspectives. *Renew. Sustain. Energy Rev.* **2017**, *76*, 941–949.
154. Lynch, D.; Henihan, A.M.; Bowen, B.; Lynch, D.; McDonnell, K.; Kwapinski, W.; Leahy, J.J. Utilisation of poultry litter as an energy feedstock. *Biomass and Bioenergy* **2013**, *49*, 197–204.
155. Cotana, F.; Coccia, V.; Petrozzi, A.; Cavalaglio, G.; Gelosia, M.; Merico, M.C.

- Energy valorization of poultry manure in a thermal power plant: Experimental campaign. *Energy Procedia* **2014**, *45*, 315–322.
156. Billen, P.; Costa, J.; Van Der Aa, L.; Van Caneghem, J.; Vandecasteele, C. Electricity from poultry manure: A cleaner alternative to direct land application. *J. Clean. Prod.* **2015**, *96*, 467–475.
157. Williams, A.G.; Leinonen, I.; Kyriazakis, I. Environmental benefits of using Turkey litter as a fuel instead of a fertiliser. *J. Clean. Prod.* **2016**, *113*, 167–175.
158. Kryzanowski, T. Demonstration Poultry Litter-to-Energy Project Experiencing Growing Pains Available online: <https://www.manuremanager.com/demonstration-project-experiencing-growing-pains-30348/>.
159. Peters, J.; Combs, S.; Hoskins, B.; Jarman, J.; Kovar, J.; Watson, M.; Wolf, A.; Wolf, N. Recommended methods of manure analysis. *Univ. Wisconsin Coop. Ext. Publ. Madison, WI* **2003**.
160. Standardization, I.O. for *Environmental Management: Life Cycle Assessment; Principles and Framework*; ISO, 2006;
161. Guide, I.S.O. 35 (2006) Reference materials—general and statistical principles for certification. *Int. Organ. Stand. (ISO), Geneva* **2006**, *64*.
162. EIA Table C3. *Primary Energy Consumption Estimates, 2017*; 2017; Vol. 2017;.
163. Moore, P.A.; Miles, D.; Burns, R.; Pote, D.; Berg, K.; Choi, I.H. Ammonia Emission Factors from Broiler Litter in Barns, in Storage, and after Land Application. *J. Environ. Qual.* **2011**, *40*, 1395.
164. Reijnders, L.; Huijbregts, M.A.J. Life cycle emissions of greenhouse gases associated with burning animal wastes in countries of the European Union. *J.*

- Clean. Prod.* **2005**, *13*, 51–56.
165. de Graff, L. (CE D.); Odegard, I. (CE D.); Nusselder, S. (CE D. *LCA of thermal conversion of poultry litter at BMC Moerdijk*; Delft, 2017;
 166. Jeswani, H.K.; Whiting, A.; Martin, A.; Azapagic, A. Environmental impacts of poultry litter gasification for power generation. *Energy Procedia* **2019**, *161*, 32–37.
 167. Moore, P.A.; Daniel, T.C.; Sharpley, A.N.; Wood, C.W. Poultry manure management: Environmentally sound options. *J. Soil Water Conserv.* **1995**, *50*, 321–327.
 168. Meisinger, J.; Jokela, W. Ammonia volatilization from dairy and poultry manure. *Manag. Nutr. Pathog. from Anim. Agric.* **2000**, 1–21.
 169. D.C.Wolf; J.T.Gilmour; P.M.Gale Estimating Potential Ground and Surface Water Pollution from Land Application of Poultry Litter - II. **1988**.
 170. Akiyama, H.; McTaggart, I.P.; Ball, B.C.; Scott, A. N₂O, NO, and NH₃ emissions from soil after the application of organic fertilizers, urea and water. *Water. Air. Soil Pollut.* **2004**, *156*, 113–129.
 171. Codling, E.E.; Chaney, R.L.; Sherwell, J. Poultry litter ash as a potential phosphorus source for agricultural crops. *J. Environ. Qual.* **2002**, *31*, 954–961.
 172. Chen, Z.; Jiang, X. Microbiological Safety of Chicken Litter or Chicken Litter-Based Organic Fertilizers: A Review. *Agriculture* **2014**, *4*, 1–29.